

Circulação de Hg e MeHg em Ecossistemas Amazônicos Naturais e Artificiais: Efeitos da Sazonalidade, Físico-química e Matéria Orgânica

INÁCIO ABREU PESTANA

UNIVERSIDADE ESTADUAL DO NORTE FLUMINENSE DARCY RIBEIRO

CAMPOS DOS GOYTACAZES – RJ

OUTUBRO – 2018

FICHA CATALOGRÁFICA

UENF - Bibliotecas

Elaborada com os dados fornecidos pelo autor.

P476

Pestana, Inácio Abreu.

Circulação de Hg e MeHg em ecossistemas amazônicos naturais e artificiais :
efeitos da sazonalidade, físico-química e matéria orgânica / Inácio Abreu Pestana.
-Campos dos Goytacazes, RJ, 2018.

123 f. : il.

Bibliografia: 42 - 48; 68 - 75; 104 - 11; 120 - 123.

Tese (Doutorado em Ecologia e Recursos Naturais) - Universidade Estadual do
Norte Fluminense Darcy Ribeiro, Centro de Biociências e Biotecnologia, 2018.
Orientadora: Cristina Maria Magalhaes de Souza.

1. Ciclo biogeoquímico do mercúrio. 2. Organificação do mercúrio. 3.
hidrelétricas. 4. lagos. 5. isótopos estáveis. I. Universidade Estadual do Norte
Fluminense Darcy Ribeiro. II. Título.

CDD - 577

Circulação de Hg e MeHg em Ecossistemas Amazônicos Naturais e Artificiais: Efeitos da Sazonalidade, Físico-química e Matéria Orgânica

INÁCIO ABREU PESTANA

Tese apresentada ao Centro de Biociências e Biotecnologia da Universidade Estadual do Norte Fluminense Darcy Ribeiro, como parte das exigências para a obtenção do título de doutor em Ecologia e Recursos Naturais.

Orientadora: Prof.^a Dr.^a Cristina Maria Magalhães de Souza
Coorientador: Prof. Dr. Wanderley Rodrigues Bastos

CAMPOS DOS GOYTACAZES – RJ
OUTUBRO – 2018

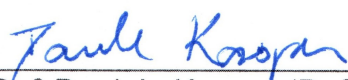
Circulação de Hg e MeHg em Ecossistemas Amazônicos Naturais e Artificiais: Efeitos da Sazonalidade, Físico-química e Matéria Orgânica

INÁCIO ABREU PESTANA

Tese apresentada ao Centro de Biociências e Biotecnologia da Universidade Estadual do Norte Fluminense Darcy Ribeiro, como parte das exigências para a obtenção do título de doutor em Ecologia e Recursos Naturais.

Aprovada em: 29 / 10 / 18

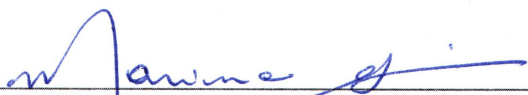
Comissão Examinadora:



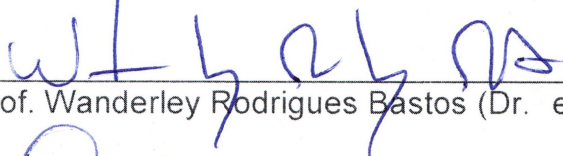
Dr.^a Daniele Kasper (Dr.^a em Ecologia) – UFRJ



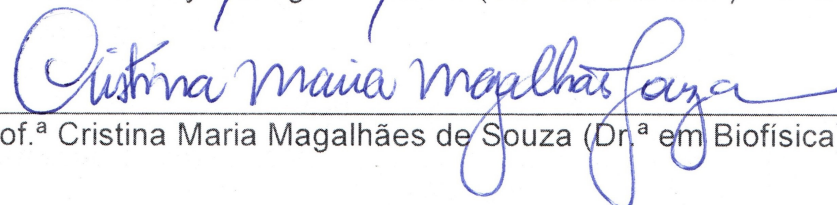
Dr. Dario Pires de Carvalho (Dr. em Biofísica) – Santo Antônio Energia S.A.



Prof.^a Marina Satika Suzuki (Dr.^a em Biociências e Biotecnologia) – UENF



Prof. Wanderley Rodrigues Bastos (Dr. em Biofísica) – UNIR (Coorientador)



Prof.^a Cristina Maria Magalhães de Souza (Dr.^a em Biofísica) – UENF (Orientadora)

[...] Os tipos de rio descritos nem sempre são claramente distintos um do outro. Na natureza, encontramos transições em indefinidos níveis entre águas brancas e águas claras e entre águas claras e águas negras. Além disso, às vezes o mesmo rio pode mudar seu “tipo” periodicamente ou ocasionalmente com as estações ou mesmo a cada chuva. Muito menos que um lago, um rio tem suas características determinadas por suas próprias leis internas, sendo apenas um produto de sua paisagem circundante, principalmente na zona das cabeceiras. Sua água poderia ser descrita como a "urina da paisagem". Dessa forma, podemos concluir que os tipos de rios descritos não são abstrações, “ideias” de rios, mas descrições mais ou menos grosseiras de um conjunto de causas e efeitos do ecossistema que constitui uma paisagem qualquer. [...]

-Dr. Harald Sioli, 1965

Aos meus amados pais, Conceição e Vilmar
A minha irmã-mãe, Bia
Ao meu irmão-pai, Bertrand
Ao meu irmão-gêmeo, Bruno.

AGRADECIMENTOS

Agradeço a todos os professores que tive na minha vida. Vocês me ajudaram a entender o funcionamento da vida em seu amplo sentido e, por extensão, as regras do nosso mundo físico. Tamanho foi o impacto de vocês na minha forma de pensar que decidi, humildemente, seguir a mesma profissão. Se eu conseguir fazer por outra pessoa o que vocês fizeram por mim, todo o investimento público e privado na minha formação terá valido a pena. Tenho alguns professores que gostaria de destacar. Na 8^o série do Ensino Fundamental, minha professora de língua portuguesa Rosangela Pereira me ensinou tanto sobre estrutura linguística que hoje acho o implícito das leituras tão belos quanto o explícito. No Ensino Médio, minha professora de Biologia Maria de Fátima Torquato, carinhosamente Fatinha, detalhou com tanta maestria o funcionamento dos organismos vivos que me inspirou a cursar Ciências Biológicas. No Ensino Superior e Pós-Graduação, minha professora, orientadora e amiga Cristina Maria Magalhães de Souza, carinhosamente Cristal, ressignificou a palavra “profundidade” ao me explicar como a matéria funciona, o que me fez seguir no estudo da geoquímica por quase 10 anos. Mais que isso, me ajudou a entender como as pessoas funcionam e ampliou minha visão de mundo irreversivelmente. Acreditou no meu potencial e, por ter acreditado, me fez chegar até aqui.

Agradeço a meus pais que me deram todo o suporte que eu precisava durante todos esses anos de formação. Ao meu pai, agradeço por ter me ensinado a ter objetividade e foco, o que eu largamente apliquei na minha disciplina de estudos e gerenciamento de tempo. A minha mãe, agradeço por ter me ensinado a ter leveza e inteligência emocional, o que me ajudou a atravessar o ambiente acadêmico sem sofrer com as artimanhas da mente. A minha irmã Bia, agradeço por me ensinar a ajudar o próximo, o que me fez um profissional mais solícito. Ao meu irmão Bertrand, agradeço por ser uma segunda figura paterna e fonte de inspiração. Ao meu irmão Bruno, agradeço pelos treinos na língua inglesa, *anytime, anywhere*, pelo carinho que transborda, por levar a palavra “empatia” a outro nível e por ser uma fonte de amor em um convívio diário de quase 5 anos.

Agradeço ao professor Wanderley Rodrigues Bastos pela orientação, pelas valiosas dicas e pela sempre pronta disponibilidade em todos os momentos que precisei. Em extensão, agradeço ao Laboratório de Biogeoquímica Ambiental (UNIR) pelo suporte logístico e determinações químicas.

Agradeço ao Laboratório de Ciências Ambientais (LCA, UENF) e aos amigos que fiz. Vocês deram leveza a uma jornada que não foi trivial. A vocês, todo meu carinho e amor.

À FAPERJ e ao CNPq pelo fomento para desenvolvimento dessa tese. À CAPES pela concessão da bolsa de estudos.

SUMÁRIO

Lista de Abreviações.....	xi
Lista de Tabelas.....	xii
Lista de Figuras.....	xiii
Resumo.....	xviii
Abstract.....	xix
Sobre a estrutura dessa Tese.....	xx

1. Introdução Geral.....	21
1.1 A problemática do Hg na região amazônica.....	21
1.2 O funcionamento de lagos naturais e artificiais.....	22

Capítulo 1:

“Methylmercury in environmental compartments of a hydroelectric reservoir in the Western Amazon, Brazil”

Abstract.....	26
Graphical Abstract.....	27
1. Introduction.....	28
2. Materials and Methods.....	29
2.1 Study Area.....	29
2.2 Sampling.....	30
2.3 Sample processing.....	31
2.4 MeHg determination.....	31
2.5 Total Fe determination.....	32
2.6 Total Hg, carbon and nitrogen determination.....	32
2.7 Statistical analyzes.....	33
3. Results.....	34
3.1 MeHg in the compartments of Samuel Reservoir.....	34
3.2 Geochemical Supports.....	37
4. Discussion.....	38
4.1 MeHg in aquatic macrophytes tissues.....	38
4.2 Spatial-temporal dynamics of MeHg in SPM.....	40
4.3 Sediment profile and geochemical support.....	41
5. Conclusion.....	42
6. Acknowledgments.....	42
7. References.....	42

Capítulo 2:

“The impact of hydroelectric dams on mercury dynamics in South America: A review”

Abstract.....	50
1. Introduction.....	51
2. Materials and methods.....	51
2.1 Studies included.....	52
2.2 Statistical Analysis.....	52
3. Hg methylation in South American hydroelectric reservoirs.....	52
4. The impact of damming rivers on Hg concentrations in fish and humans.....	55
5. The effect of damming on Hg downstream export from reservoirs.....	61

6. New insights: the temporal and morphological influences of reservoirs on Hg circulation.....	63
7. Suggestions for future studies on Hg dynamics in South American reservoirs and impact mitigation strategies.....	66
8. Acknowledgments.....	67
9. References.....	68
Supplementary Material 1.....	76

Capítulo 3:

“Total Hg and methylmercury dynamics in a river-floodplain system in the Western Amazon: influence of seasonality, organic matter, and physical and chemical parameters”

Abstract.....	78
Graphical Abstract.....	79
1. Introduction.....	80
2. Materials and Methods.....	82
2.1 Study Area.....	82
2.2 Sampling.....	84
2.3 Processing of water, plant and sediment samples.....	85
2.4 Total Hg determination.....	86
2.5 MeHg determination.....	86
2.6 Total Fe determination.....	87
2.7 Anion determinations.....	87
2.8 C and N elemental composition and ¹³ C isotopic signature of organic matter.....	88
2.9 Statistical analyses.....	88
3. Results.....	89
3.1 Physical and chemical parameters of the water column.....	89
3.2 Suspended particulate matter	90
3.3 Dissolved matter.....	94
3.4 Sediment profile.....	97
3.5 Aquatic macrophytes.....	97
4. Discussion.....	98
4.1 The physico-chemical transition from Madeira River to Cuniã Igarapé-lake system.....	98
4.2 Spatial-temporal dynamics of total Hg in SPM and dissolved matter	99
4.3 Methylation in the water column of the river-igarapé-lake system.....	101
4.4 Hg deposition and methylation in the sediment profile.....	102
4.5 Influence of the aquatic macrophyte biotype on the total Hg and MeHg accumulation and translocation.....	103
5. Conclusion.....	103
6. Acknowledgments.....	104
7. References.....	104
Supplementary Material 1.....	112
Supplementary Material 2.....	113
Supplementary Material 3.....	114
Supplementary Material 4.....	115
Supplementary Material 5.....	116
Supplementary Material 6.....	117

2. Discussão Geral.....	118
3. Considerações Finais.....	119
4. Referências.....	120

LISTA DE ABREVIÇÕES

- %MeHg** – Resultado da divisão da concentração de Hg total pela de MeHg * 100
- (C:N)_x** – Razão atômica de carbono e nitrogênio
- ‰** – Partes por mil
- ANCOVA** – Análise de Covariância
- ANOVA** – Análise de Variância
- C₃ metabolism** – Plantas que produzem fosfoglicerato como primeiro composto da fotossíntese
- CG-AFS** – Cromatografia gasosa acoplada a um espectrômetro de fluorescência atômica
- CNPq** – Conselho Nacional de Desenvolvimento Científico e Tecnológico
- dry wt.** – Dried weight
- e** – Número de Euler, base dos logaritmos naturais. Aproximadamente igual à 2,718281828459045235360.
- FAPERJ** – Fundação Carlos Chagas Filho de Amparo à Pesquisa do Estado do Rio de Janeiro
- IAEA** – International Atomic Energy Agency
- ICP-AES** – Espectrometria de Emissão Atômica por Plasma Acoplado Indutivamente
- IRMS** – Espectrometria de massa de razões isotópicas
- LCA** – Laboratório de Ciências Ambientais
- ln** – Logaritmo natural
- MAD** – Mediana dos Desvios Absolutos
- MeHg** – Abreviação para CH₃Hg⁺, metilmercúrio
- MPS** – Material particulado em suspensão (nesse estudo, composto por partículas < 0, 7µm)
- NIST** – National Institute of Standards and Technology
- p** – Probabilidade da hipótese nula (H₀) de um teste estatístico ser verdadeira
- R²_{model} ou R²** – Coeficiente de determinação múltiplo de um modelo geral ou generalizado de regressão
- R²_{partial}** – Coeficiente de determinação parcial de um modelo geral ou generalizado de regressão
- RO** – Rondônia
- SPM** – Suspended particulate matter
- UENF** – Universidade Estadual do Norte Fluminense Darcy Ribeiro
- UNIR** – Universidade Federal de Rondônia
- δ¹³C** – Resultado de (¹³C/¹²C_{amostra} / ¹³C/¹²C_{da formação Pee Dee -1}) * 1000

LISTA DE TABELAS

Introdução Geral

Tabela 1 – Características contrastantes entre lagos e reservatórios de hidrelétricas, adaptada de Straškraba e Tundisi (2000)	24
---	-----------

Capítulo 1

Table 1 – Total Hg and MeHg concentrations and %MeHg in sediment, SPM and roots of aquatic macrophytes of this and previous studies.....	35
---	-----------

Capítulo 3

Supplementary Material 2 – Physical and chemical parameters of sampled points (Figure 1). The centrality and dispersion of data (median \pm median absolute deviations, MAD) were calculated for each variable in each hydrological period. Upper and lowercase letters represent statistical differences among hydrological periods for each median calculated, considering 95% certainty.....	113
Supplementary Material 3 – Major anions concentrations determined in the river-igarapé-lake system for all hydrological periods sampled.....	114
Supplementary Material 6 – Studies of floodplain-river systems in the Amazon region and their concentrations of Hg chemical species.....	117

LISTA DE FIGURAS

Capítulo 1

Graphical Abstract	27
Figure 1 – Location of sampling points within Samuel Reservoir. The map was created with satellite images of the reservoir during the low water period with the emerged islands represented. The direction of water flow is from south to north.....	30
Figure 2 – MeHg/total Hg ratio (%MeHg) in the environmental compartments of Samuel Reservoir. The sediment and macrophyte data are related to the ebb period while for the SPM is a compilation of the three hydrological periods (high water, ebb period and low water). Different letters denote high statistical support for the mean difference ($p < 0.001$). Hollow circles represent outliers (outside 1.5 times the interquartile range above the upper quartile). The y-axis distance between the numbers is in logarithmic scale.....	34
Figure 3 – MeHg concentrations in tissues of aquatic macrophytes sampled during the ebb period (May 2012). The percent values on the bars represent the MeHg/total Hg ratio (%MeHg).....	36
Figure 4 – MeHg concentration in SPM among sampled points and among hydrological periods. The percent values on the bars represent the MeHg/total Hg ratio (%MeHg).....	36
Figure 5 – MeHg concentrations in the sediment profile sampled at the center of the reservoir (<i>Reservoir2</i> , Figure 1) during the ebb period (May 2012). The percent values next to triangles represent MeHg/total Hg ratio (%MeHg).....	36
Figure 6 – Multiple regression of MeHg concentration in the sediment (A) and SPM (B) using as predictors the organic matter quality (C:N ratio) and total Hg concentration. The explanation of the model (R^2_{model}) results from the sum of the partial explanations ($R^2_{partial}$) of each variable. The dashed lines form the multiple regression plane among the variables. The red tones highlight the depth of the points on the graphic.....	37
Figure 7 – (A) Linear regression between MeHg concentrations and organic matter lability (C:N ratio) in the sediment profile (gray squares, dashed line, $R^2 = 0.62$, $p = 0.007$) and quadratic regression between MeHg concentrations and total Hg concentration in the sediment profile (filled circles, solid line, $R^2 = 0.86$, $p < 0.001$). (B) – Linear regression (adjusted to $\frac{1}{MeHg}$) between MeHg concentrations and organic matter lability (C:N ratio) in the SPM (gray squares, dashed line, $R^2 = 0.42$, $p = 0.03$) and quadratic regression between MeHg concentrations and total Hg concentration in the SPM (filled circles, solid line, $R^2 = 0.34$, $p = 0.28$).....	38

Capítulo 2

Figure 1 – South American hydroelectric reservoirs that have been studied regarding Hg dynamics. The miniatures show the morphology of the reservoirs (out of scale) and their corresponding area (km²), depth (m) and age after filling (years). The studies for each reservoir are listed in front of their name. **Guri** (Veiga 1996; 1997; Veiga and Hilton, 2001); **Tucuruí** (Aula et al., 1995; Porvari, 1995; Malm et al., 2004; Kehrig et al., 2008; Palermo, 2008; Kehrig et al., 2009); **Balbina** (Kehrig et al., 1998; Kehrig et al., 2008; Kehrig et al., 2009; Forsberg et al., 2013; Kasper et al., 2014); **Itaipu** (Kerkhoff, 2016); **Samuel** (Brasil et al., 2004a; Brasil et al., 2004b; Nascimento et al., 2009; Almeida, 2012; Kasper et al., 2012; Pestana et al., 2016; 2019). **Manso** (Hylander et al., 2006; Tuomola et al., 2008); **Petit-Saut** (Coquery et al., 2003; Durrieu et al., 2005; Boudou et al., 2005; Peretyazhko et al., 2005; Muresan et al., 2008); **Urrá** (Feria et

al., 2010; Marrugo-Negrete et al., 2013; Ruiz-Guzmán et al., 2014; Marrugo-Negrete et al., 2015); **Ribeirão das Lajes** (Palermo, 2008); **Vigário** (Palermo, 2008; Kasper et al., 2009); **Cabixi 1** (Cebalho et al., 2017); **Cabixi 2** (Cebalho et al., 2017)..... 53

Figure 2 – Relationship between MeHg and dissolved O₂ in the water column of South American reservoirs (N=18). ■ **Petit-Saut** (Coquery et al., 2003 [measured from 0 to 25 cm below surface waters]; Boudou et al., 2005 [measured from 0 to 30 cm below surface waters]); ● **Samuel** (Almeida, 2012 [measured from 0 to 25 cm below surface waters]); ▲ **Balbina** (Kasper et al., 2014 [measured from 0 to 20 cm below surface waters]). The light gray shading identifies the prediction interval of the regression model while the dark gray shading identifies the confidence interval of the model, both calculated with 95% certainty..... 55

Figure 3 – Total Hg concentrations in biotic and abiotic compartments of South American reservoirs. Values inside each box are median ± interquartile range. The distances between the y-axis values were log-transformed to optimize the data visualization. **Superficial sediment** (Aula et al., 1995; Malm et al., 2004; Hylander et al., 2006; Palermo, 2008; Marrugo-Negrete et al., 2015; Pestana et al., 2016; Kerkhoff, 2016); **Aquatic macrophytes** (Aula et al., 1995; Pestana et al., 2016); **Plankton** (Malm et al., 2004; Dominique et al., 2007; Palermo, 2008; Nascimento et al., 2009; Almeida, 2012; Kasper et al., 2012; Kasper et al., 2014); **Suspended particulate matter** (Aula et al., 1995; Coquery et al., 2003; Malm et al., 2004; Dominique et al., 2007; Palermo, 2008; Almeida, 2012; Kasper et al., 2012; Kasper et al., 2014; Pestana et al., 2016); **Top-chain predatory fish** (Porvari, 1995; Veiga, 1996; Kehrig et al., 1998; Brasil et al., 2004a; Malm et al., 2004; Hylander et al., 2006; Kehrig et al., 2008; Palermo, 2008; Tuomola et al., 2008; Kehrig et al., 2009; Kasper et al., 2012; Forsberg et al., 2013; Marrugo-Negrete et al., 2013; Kasper et al., 2014; Ruiz-Guzmán et al., 2014; Marrugo-Negrete et al., 2015; Kerkhoff, 2016; Cebalho et al., 2017). *Data based on wet weight..... 57

Figure 4 – Relationship between the total Hg concentrations observed in top predatory fish and the mean depth of several tropical reservoirs. Fish length from each study is reported after each reference. ■ **Balbina** (Kehrig et al., 1998 - length not reported; Kehrig et al., 2008 - 34.2 ± 24.6 cm; Kehrig et al., 2009 - 27.0 ± 24.4; Forsberg et al., 2013 - length not reported; Kasper et al., 2014 - 27.5 ± 4.9); ● **Cabixi 1** (Cebalho et al., 2017 - 10.5 ± 3.6 cm); ▲ **Cabixi 2** (Cebalho et al., 2017 - 16.14 ± 7.42 cm); ◇ **Urrá** (Ruiz-Guzmán et al., 2014 - 32.2 ± 4.6; Marrugo-Negrete et al., 2013 - 24.1 ± 8.1 cm; Marrugo-Negrete et al., 2015 - 24.6 ± 3.8); □ **Samuel** (Brasil et al., 2004b - length not reported; Kasper et al., 2012 - 31.4 ± 5.6); ○ **Tucuruí** (Porvari, 1995 - 38.1 ± 8.5; Malm et al., 2004 - length not reported; Kehrig et al., 2008 - 27.5 ± 13.4 cm; Kehrig et al., 2009 - 27.6 ± 25.8); △ **Vigário** (Kasper et al., 2009 - 19.5 ± 3.4 cm); × **Guri** (Veiga, 1996 - length not reported). The light gray shading identifies the prediction interval of the regression model while the dark gray shading identifies the confidence interval of the model, both calculated with 95% certainty. The distances between the y-axis values were log-transformed to optimize the data visualization. Bars represents standard error of mean..... 58

Figure 5 – Time series of Hg concentration determined in muscle of top predatory fish in South American reservoirs. Fish length from each study is reported after each reference. ● **Manso** (Hylander et al., 2006 - 33.3 ± 15.9 cm; Tuomola et al., 2008 - 36.4 ± 26.6 cm); ▲ **Balbina** (Kehrig et al., 1998 - length not reported; Kehrig et al., 2008 - 34.2 ± 24.6 cm; Kehrig et al., 2009 - 27.0 ± 24.4 cm; Forsberg et al., 2013 - length not reported; Kasper et al., 2014 - 27.5 ± 4.9 cm); ■ **Tucuruí** (Porvari, 1995 - 38.1 ± 8.5 cm; Malm et al., 2004 - length not reported; Kehrig et al., 2008 - 27.5 ± 13.4 cm; Kehrig et al., 2009 - 27.6 ± 25.8 cm); ◆ **Guri** (Veiga, 1996 - length not reported); ▽ **Urrá** (Ruiz-Guzmán et al., 2014 - 32.2 ± 4.6 cm; Marrugo-Negrete et al., 2013 - 24.1 ± 8.1 cm; Marrugo-Negrete et al., 2015 - 24.6 ± 3.8 cm). The light gray and blue shading identify the prediction interval of the regression model while the dark gray and blue shading identify the confidence interval of the model, both calculated with 95% certainty. The distances between the y-axis values were log-transformed to optimize the data visualization. Bars represents standard error of mean..... 60

Figure 6 – (A) Relationship between Hg concentration in the surface sediments of South American reservoirs in two scenarios: considering up to 35-year reservoirs (dashed line, gray shading, N = 6) and reservoirs up to 110 years (continuous line, blue shading, N = 9). **(B)** Relationship between Hg concentration in surface sediments and mean depth of South America reservoirs (N=9). **(C)** Relation between Hg concentration in surface sediments and the area of tropical reservoirs (N=9). Δ **Ribeirão das Lajes** (Palermo, 2008); \bullet **Manso** (Hylander et al., 2006); \blacklozenge **Tucuruí** (Aula et al., 1995 e Malm et al., 2004); \blacktriangle **Samuel** (Pestana et al., 2016); \blacksquare **Itaipu** (Kerkhoff, 2016). The light gray and light blue shades identify the prediction interval of the model while the dark gray and dark blue shades identify the confidence interval of the model, both calculated with 95% certainty. Bars represent standard error of mean..... 64

Figure 7 – Time series of Hg concentration in the suspended particulate matter in South American reservoirs (N=9). \blacktriangle **Samuel** (Almeida, 2012; Kasper et al., 2012; Pestana et al., 2016); Δ **Tucuruí** (Malm et al., 2004; Aula et al., 1995). The light blue shading identifies the prediction interval of the model while the dark blue shading identifies the confidence interval of the model, both calculated with 95% certainty. Bars represents standard error of mean..... 66

Supplementary Material 1 – Cumulative frequency of published studies on Hg cycling in South American reservoirs by environmental compartment (N=27). Few studies have paired data from biotic and abiotic compartments, which makes it difficult to construct multivariate predictive models..... 76

Capítulo 3

Graphical Abstract..... 79

Figure 1 – Map of the river-igarapé-lake system studied and its location within Brazil (miniature). The filled circles indicate two sampling points along the Madeira River (River1, River2), two sampling points along Cuniã Igarapé (Igarapé1, Igarapé2) and three sampling points in Cuniã Lake (Lake1, Lake2, Lake3). The physical and chemical parameters are detailed in **Supplementary Material 2**. The colors illustrate the mixing of the Madeira River waters in Cuniã Igarapé with progressive sedimentation of particles along its winding path of approximately 37 km. Madeira River water flow is from south to north..... 83

Figure 2 – Variation of the physical and chemical parameters with increasing distance from the Madeira River. **(A)** *River1* and *River2*; **(B)** *Igarapé1*; **(C)** *Igarapé2*; **(D)** *Lake2*; **(E)** *Lake1*; **(F)** *Lake3* sample points (**Figure 1**). Logarithmic regressions explain the process satisfactorily for pH ($r^2 = 0.53$; $p = 0.000001$; $Y = -0.1479\ln(X) + 6.2814$), electrical conductivity ($r^2 = 0.86$; $p < 0.000001$; $Y = -6.352\ln(X) + 36.091$) and dissolved O₂ ($r^2 = 0.24$; $p = 0.005$; $Y = -0.4642\ln(X) + 5.6492$). The temperature did not show variations with increasing distance from the Madeira River ($r^2 = 0.02$, $p = 0.35$) and had median \pm MAD of 27.2 \pm 1.0. 90

Figure 3 (A) – Total Hg concentrations in SPM in the river-igarapé-lake system for each hydrological period sampled. Lowercase letters identify the differences ($p < 0.05$) between ecosystems within the same hydrological period. **(B) –** MeHg concentrations in SPM in the river-igarapé-lake system for each hydrological period sampled. No significant direct effects of seasonality or interaction between seasonality and sampled ecosystems were detected ($p = 0.29$ and $p = 0.96$, respectively). Significant differences were observed in MeHg concentrations in the SPM between the river and the igarapé-lake system in all hydrological periods evaluated ($p < 0.000001$). %MeHg (MeHg/total Hg ratio) is indicated for each ecosystem and hydrological period. **(C) –** Total Hg concentrations in dissolved matter in the river-igarapé-lake system for each hydrological period sampled. Lowercase letters identify the differences ($p < 0.05$) between ecosystems within the same hydrological period while uppercase letters differentiate $p < 0.05$ the hydrological periods within the same ecosystem. The distances between the y-axis values were log-transformed to optimize the data visualization in all panels..... 91

Figure 4 – Carbon and nitrogen elemental composition ((C:N)_a ratio) and carbon-13 (δ¹³C) isotopic signature in the SPM for the three evaluated ecosystems. The internal table represents the percentage of isotopic area overlapped between Ellipse 1 and Ellipse 2, in relation to Ellipse 1 area. The ellipses were constructed considering distance of one standard deviation from the centroids of the respective variables. **(B)** Carbon and nitrogen elemental composition ((C:N)_a ratio) and carbon-13 (δ¹³C) isotopic signature in the dissolved matter for the three evaluated ecosystems. **(C)** Carbon and nitrogen elemental composition ((C:N)_a ratio) and carbon-13 (δ¹³C) isotopic signature reported for the Amazon region (light grey, no borders; Hedges et al., 1986; Meyers, 1994; Martinelli et al., 2003; Kim et al., 2012). The isotopic and elemental area determined for each of the environmental compartments from this study is represented superimposed (in color, with borders)..... 93

Figure 5 – Multivariate regression of MeHg concentration in the SPM with the carbon and nitrogen elemental composition ((C: N)_a ratio) and carbon-13 (δ¹³C) isotopic signature also in SPM. The regression plane is represented by the transparent gray form and was constructed with the following equation: $Z = e^{-0.4130X + 0.5861Y - 16.1855}$ ($r^2 = 0.79$; $p = 0.00000001$). If you are unable to view this graph interactively, [click here](#)..... 94

Figure 6 – **(A)** Multivariate regression of MeHg concentration in the SPM with water column oxygenation (dissolved O₂) and its acidity (pH). The regression plane is represented by the transparent gray form and was constructed with the following equation: $Z = e^{-1.6392X - 0.0771Y + 11.8969}$ ($r^2 = 0.80$; $p = 0.000001$). If you are unable to view this graph interactively, [click here](#). **(B)** Multivariate regression of MeHg concentration in the sediment profile with the carbon and nitrogen elemental composition ((C:N)_a ratio) and carbon-13 (δ¹³C) isotopic signature. The regression plane is represented by the transparent gray form and was constructed with the following equation: $Z = 4.67X - 0.95Y + 157.52$ ($r^2 = 0.93$; $p = 0.004$). If you are unable to view this graph interactively, [click here](#)..... 95

Figure 7 – **(A)** Exponential regression between MeHg concentration in the SPM and SO₄²⁻ concentration in the water column. The regression is indicated by the black solid line and was constructed using the following equation: $Y = 20.38903X^{-0.004945}$ ($r^2 = 0.73$; $p = 0.00000001$). The light blue shaded area represents the prediction interval of the model while the dark blue shaded area represents the confidence interval of the model, both calculated with 95% certainty. The distances between the y-axis values were log-transformed to optimize the data visualization. **(B)** – Quadratic regression between total Hg total and total Fe concentration in the SPM. The regression is indicated by the black solid line and was constructed using the following equation: $\ln(Y) = -0.9057X^2 + 7.3611X - 9.0281$ ($r^2 = 0.57$; $p = 0.0000001$). The distances between the y-axis values were log-transformed to optimize the data visualization..... 96

Figure 8 – Total Hg concentration (white, gray and blue bars) and MeHg concentration (black bars) in the aquatic macrophyte tissues (N=1) sampled during the late falling-water period. The %MeHg (MeHg / total Hg ratio) is indicated for each aquatic macrophyte tissue sample..... 97

Supplementary Material 1 – Rainfall (INMET, 2018) and water level (Schwatke et al., 2015) for the Madeira River during the years that this study was conducted. The sampled months are highlighted in bold on the x-axis and represent the early falling-water (May 2012), rising-water (February 2013) and late falling-water (June 2013) periods. The Madeira River water during the sampled periods is shown in blue, while the accumulated rainfall for the sampled periods is highlighted in black on the graph..... 112

Supplementary Material 4 – Total Hg and MeHg concentrations along a sediment profile sampled in the central part of Cuniã Lake (Lake2; Figure 1) during the late falling-water period. The %MeHg (MeHg/total Hg ratio) is indicated for each depth, next to the MeHg concentrations.. 115

Supplementary Material 5 – SPM concentrations in the river-*igarapé*-lake system for each hydrological period sampled. Lowercase letters identify the differences ($p < 0.05$) between ecosystems within the same hydrological period while uppercase letters differentiate ($p < 0.05$) the hydrological periods within the same ecosystem. The distances between the y-axis values were log-transformed to optimize the data visualization..... **116**

RESUMO

Essa tese teve como objetivo geral avaliar a circulação de Hg e MeHg em ecossistemas amazônicos artificiais (Capítulos 1 e 2) e naturais (Capítulo 3). No Capítulo 1 são apresentados os resultados de um estudo realizado no reservatório da Hidrelétrica de Samuel (Porto Velho, Rondônia, Brasil) cujas concentrações de MeHg foram avaliadas no material particulado em suspensão (MPS) da coluna d'água, macrófitas aquáticas e sedimento. Além disso, as associações do MeHg com a matéria orgânica foram avaliadas no sedimento e MPS. No Capítulo 2 são apresentados os resultados de uma revisão sistemática da literatura acerca dos impactos da construção de hidrelétricas Sul Americanas no ciclo biogeoquímico do Hg. Além da síntese do conhecimento produzido em 27 anos de estudos resgatados, meta-análises foram utilizadas para propor novos *insights* sobre a problemática. No Capítulo 3 são apresentados os resultados de um estudo realizado em um sistema amazônico composto por um rio de águas brancas e um pequeno rio de floresta (chamado localmente de igarapé) que adentra uma planície de inundação e o conecta com um lago distante a 37 km desse rio principal. O rio em questão é o rio Madeira, segundo maior rio da região amazônica enquanto que o sistema igarapé-lago é localizado na reserva extrativista do lago Cuniã. Nesse trabalho, foi avaliada a concentração de Hg total e MeHg em alguns compartimentos do ecossistema como a coluna d'água (MPS e a fração dissolvida), sedimento e macrófitas aquáticas. Além disso, associações do MeHg no MPS, fração dissolvida e sedimento com a matéria orgânica e parâmetros físico-químicos da coluna d'água foram avaliados. Em síntese, podemos dizer que a circulação de Hg nos ecossistemas aquáticos amazônicos artificiais (Capítulos 1 e 2) e naturais (Capítulo 3) está intimamente associada à dinâmica da matéria orgânica nesses ambientes (Capítulos 1 e 3). O estado de degradação da matéria orgânica (Capítulos 1 e 3) e os parâmetros físico-químicos da coluna d'água (Capítulos 2 e 3) são peças-chave para a compreensão do processo de metilação do Hg nesses ecossistemas que, uma vez transformado em MeHg, pode se biomagnificar ao longo da cadeia trófica (Capítulo 2). As macrófitas aquáticas (Capítulos 1 e 3), a coluna d'água (Capítulos 1, 2 e 3) e o sedimento (Capítulos 1 e 3) são compartimentos do ecossistema capazes de metilar o Hg e, por isso, podem ser utilizados como indicadores em estudos de monitoramento em ambientes naturais e artificiais.

ABSTRACT

This thesis had as general aim to evaluate the Hg and MeHg circulation in artificial (Chapters 1 and 2) and natural (Chapter 3) Amazonian ecosystems. Chapter 1 presents the results of a study carried out in the Samuel Hydroelectric Reservoir (Porto Velho, Rondônia, Brazil), where MeHg concentrations were evaluated in the suspended particulate material (SPM) of the water column, aquatic macrophytes and sediment. In addition, MeHg associations with organic matter were evaluated in the sediment and SPM. Chapter 2 presents the results of a systematic review of the literature on the impacts of South American hydroelectric plants construction on the Hg biogeochemical cycle. In addition to the synthesis produced in 27 years of studies, meta-analyzes were used to propose new insights on the problem. Chapter 3 presents the results of a study realized in an Amazon system composed by a white water river and a small forest river (called *igarapé* by locals) that enters a floodplain and connects this river to a lake 37 km far from distance. The river in question is the Madeira River, second largest river in the Amazon region, while the *igarapé*-lake system is located in the extractive reserve of Cuniã Lake. In this work, total Hg and MeHg concentrations were determined in the water column (SPM and the dissolved fraction), sediment and aquatic macrophytes. In addition, MeHg associations with organic matter and with physico-chemical parameters of the water column were evaluated in SPM, dissolved fraction and sediment. In summary, the Hg circulation in artificial (Chapters 1 and 2) and natural (Chapter 3) Amazonian aquatic ecosystems is closely associated with the organic matter dynamics in these environments (Chapters 1 and 3). The degradation state of organic matter (Chapters 1 and 3) and the physico-chemical parameters of the water column (Chapters 2 and 3) are key pieces for the understanding the methylation of Hg in these ecosystems that, once transformed in MeHg, can biomagnify along the trophic chain (Chapter 2). The aquatic macrophytes (Chapters 1 and 3), the water column (Chapters 1, 2 and 3) and the sediment (Chapters 1 and 3) are ecosystem compartments capable of Hg methylation and can therefore be used as indicators in monitoring studies in both natural and artificial environments.

SOBRE A ESTRUTURA DESSA TESE

Essa tese é composta de:

- (1) **Uma introdução geral**, em que é abordada sinteticamente a problemática de Hg na região amazônica e discutida as principais diferenças de funcionamento entre lagos naturais e artificiais;
- (2) **Três artigos científicos**, em que são apresentados dados sobre a dinâmica de Hg e MeHg em lagos naturais e artificiais. Cada um contém seu próprio resumo, introdução, métodos, resultados, discussão e conclusão pertinentes.
- (3) **Uma discussão geral**, em que os resultados dos três artigos são sintetizados em uma perspectiva mais ampla sobre o funcionamento de sistemas amazônicos naturais e artificiais.
- (4) **Considerações finais**, em que são ressaltadas lacunas a serem preenchidas por estudos futuros.

1. Introdução Geral

1.1 A problemática do Hg na região amazônica

A região amazônica foi historicamente assolada pelo uso indiscriminado do Hg durante o que se ficou conhecido como a “corrida do ouro”, visto que o Hg é um dos poucos elementos que consegue amalgamar o ouro e facilitar seu processo de extração de solos e sedimentos aluvionares (Lacerda e Salomons, 1998; Malm, 1998; Lacerda e Malm, 2008). Justamente nesse contexto, os estudos iniciais na região amazônica acerca da dinâmica de Hg partiam do pressuposto que as altas concentrações encontradas em diversas matrizes ambientais seriam devidas ao processo de mineração (Pfeiffer e Lacerda, 1988; Malm et al., 1990; Nriagu et al., 1992). Entretanto, estudos subsequentes indicaram que a circulação e elevadas concentrações de Hg na região amazônica estão relacionadas a processos naturais e que a mineração apenas produz efeitos em uma escala espacial limitada (Roulet e Luccote, 1995; Lechler et al., 2000; Fadini e Jardim, 2001; Wasserman et al., 2003). Essa dispersão do Hg nas matrizes ambientais na região amazônica é atribuída principalmente ao fato do elemento possuir em seu ciclo biogeoquímico uma fase gasosa, o que o torna ubíquo, e a presença de suportes geoquímicos que facilitam seu acúmulo em solos, como oxihidróxidos de Fe e Al (Roulet e Lucotte, 1995; Lechler et al., 2000). Como os solos da Amazônia são muito antigos, variando em 500 mil e 1 milhão de anos (Johnson, 2003), o Hg emitido por fontes naturais ou antrópicas presente na atmosfera já passou por vários ciclos de deposição e volatilização, fazendo com que o sítio de ligação desses oxihidróxidos de Fe e Al ficassem saturados e transformassem a Amazônia em um grande reservatório natural de Hg (Johnson, 2003).

O Hg presente nos solos da região amazônica migra para o ambiente aquático por meio da erosão de partículas as quais ele está associado ou por processos de lixiviação (Lacerda et al., 1989). A Amazônia possui o maior sistema hídrico do mundo (Tollefson, 2011) e o nível d'água dos seus grandes rios aumenta drasticamente durante o período hidrológico caracterizado na região como “enchente”, inundando os solos adjacentes e deslocando o Hg dos solos para o corpo d'água em sua forma particulada ou dissolvida, caracterizando a estação chuvosa da região. Esse evento é periódico e foi descrito por Junk et al. (1989) como “pulso de inundação”, que faz com que a região tenha quatro períodos hidrológicos bem definidos: o já mencionado período de “enchente”; o período de “águas altas”, quando o nível d'água dos grandes rios está em sua máxima amplitude; o período de “vazante”, quando o nível d'água dos rios começa a diminuir, visto a diminuição das chuvas; e o período de “águas baixas”, quando o nível d'água dos rios está na sua menor

amplitude, caracterizando a estação seca da região. Uma vez no corpo d'água, o Hg pode continuar associado ao material particulado em suspensão (MPS), que eventualmente se deposita ao material sedimentar, ou se associar à matéria orgânica dissolvida formando complexos estáveis na coluna d'água (Lacerda e Malm, 2008), com elevado tempo de residência. A floresta amazônica é responsável por 20-25% do estoque de carbono do planeta, o que facilita a liberação de matéria orgânica para o ecossistema aquático, via serapilheira ou decomposição (Bernoux et al., 2002).

Uma vez no ecossistema aquático, o Hg^{2+} inorgânico pode ser metilado e formar o metilmercúrio (CH_3Hg^+ , abreviado como MeHg), forma orgânica e mais tóxica do elemento (WHO, 1990). As bactérias sulfato-redutoras são os principais organismos descritos na literatura capazes de realizar o processo (King et al., 1999; Flemming et al., 2006; Parks et al., 2013) que ocorre majoritariamente em ambientes aquáticos anóxicos, como os sedimentos de rios e lagos. Diferentemente do Hg^{2+} inorgânico, o MeHg é altamente lipofílico e, conseqüentemente, atravessa a membrana celular dos organismos (Lacerda e Malm, 2008) como o fitoplâncton, o que facilita sua absorção diretamente da coluna d'água. Uma vez que esses organismos são ingeridos pelos consumidores, o MeHg é novamente absorvido pelas membranas do trato intestinal dos animais (Wiener et al., 2002) e, assim, tem sua concentração aumentada ao longo da cadeia trófica, processo conhecido como biomagnificação. Os peixes predadores topo de cadeia, portanto, apresentam elevadas concentrações do metal e, ao terem seus tecidos consumidos, expõem a população humana aos efeitos adversos do MeHg, que incluem problemas generalizados do sistema nervoso (Rice et al., 2003; Myers et al., 2004) e cardíacos (Guallar et al., 2002), podendo levar a morte em alguns casos (Dorea et al., 2010).

1.2 O funcionamento de lagos naturais e artificiais

As planícies de inundação ou várzeas fazem parte da fisionomia natural do ecossistema amazônico e são caracterizadas por sua alta conectividade aos grandes rios da região por meio de canais, principalmente durante o período de enchente, no qual recebem grande quantidade de nutrientes, visto o transbordo do canal principal do rio (Sioli, 1967; Junk, 1989). É também durante o período de enchentes que esses ecossistemas recebem a maior carga de Hg, que é majoritariamente transportada pela fração particulada da coluna d'água (Maia et al., 2009; Maia et al., 2017). Durante o período de vazante e águas baixas, a elevada carga de MPS retida nos lagos confinados nas planícies de inundação se sedimenta e possibilita a penetração de luz (Sioli, 1967), fazendo com que a produtividade fitoplanctônica e das macrófitas aquáticas represente 73% de todo carbono

orgânico ali produzido (Junk & Furch, 1985). O crescimento desses organismos aumenta a carga de matéria orgânica nos lagos e seus canais favorecendo a metilação do Hg (Mauro et al., 1999; Guimarães et al., 2000).

Em contraposição às planícies de inundação regidas sazonalmente por seus rios associados, os reservatórios de hidrelétricas são lagos artificiais com níveis d'água controlados pela ação humana e tem sido cada vez mais representantes de uma fisionomia artificial da região (Castello e Macedo, 2016). Dado o enorme potencial hídrico da região e o aumento da demanda de energia elétrica devido à crescente urbanização e globalização (IEA, 2014), o governo brasileiro vem investindo na construção de hidrelétricas, represando a águas de rios de médio e grande porte (Tollefson, 2011; Castello e Macedo, 2016). A área terrestre no entorno do canal dos rios represados é rica em matéria orgânica lábil cuja decomposição fomenta anoxia e, por tanto, favorece os processos de metilação de Hg (Almeida, 2012). Além disso, o alagamento também favorece a remobilização do Hg dos solos inundados para a coluna d'água, dispersando o contaminante ao longo de toda a cadeia trófica (Lacerda e Malm, 2008).

Os lagos naturais e artificiais são ambientes com características contrastantes que podem ser úteis como modelos para a compreensão da circulação de Hg na região amazônica. Por exemplo, a profundidade de um reservatório é naturalmente maior próxima à barragem, de forma a manter um nível d'água adequado para geração de energia elétrica. Isso faz com que a distribuição de Hg associado ao MPS seja heterogênea dentro da área de um reservatório, uma vez que a barragem se torna uma área de sedimentação mais eficiente que a área a montante (Pestana et al., 2016). Como consequência da maior profundidade, há maior produção de MeHg próximo a barragem que, através da drenagem de água pelas turbinas, pode ser ressuspensionado e exportado à jusante da barragem (Almeida, 2012). Por outro lado, a geomorfologia côncava de um lago típico de uma planície de inundação favorece maiores profundidades em sua área central, que recebe o MPS erodido de suas encostas progressivamente (Couto, 2004). Além disso, a elevada produtividade em uma planície de inundação provê um grande aporte de matéria orgânica que pode flexionar a oxiclina do lago para poucos centímetros abaixo da superfície da coluna d'água (Junk & Furch, 1985), favorecendo os processos de metilação. Outras características poderiam ser descritas e discutidas como contrastantes a esses ambientes, tendo impactos diretos ou indiretos na circulação do Hg (Tabela 1).

Tabela 1 – Características contrastantes entre lagos e reservatórios de hidrelétricas, adaptada de [Straškraba e Tundisi \(2000\)](#)

Característica	Lago	Reservatório
Área de drenagem	Menor	Maior
Tempo de residência da água	Mais longo (anos)	Mais curto (dias)
Morfometria	Formato de U	Formato de V
Flutuação do nível d'água	Menor (natural)	Maior (comportas)
Hidrodinâmica	Mais regular (natural)	Variável (comportas)
Pulsação	Natural	Operada pelo homem
Sistema para aproveitamento hídrico	Raros	Comuns
Origem	Natural	Antrópica
Idade	Velho (> Pleistoceno)	Novo (< 100 anos)
Envelhecimento	Lento	Rápido
Local de formação	Depressões	Canal de rios
Formato	Regular (\pm circular)	Dendrítico (triangular)
Profundidade Máxima	Perto do centro	Perto da barragem
Sedimentos de fundo	Autóctones	Alóctones
Profundidade da descarga	Superficial	Profunda

A literatura é controversa sobre os efeitos da construção de lagos artificiais no ciclo biogeoquímico do Hg quando comparado a lagos naturais. Por exemplo, a avaliação de seis lagos canadenses não conseguiu detectar diferenças significativas na concentração de Hg total na coluna d'água entre lagos artificiais e naturais ([Montgomery et al., 1995](#)). Por outro lado, a avaliação de 1008 lagos estadunidenses levou a conclusão de que a concentração de Hg total e MeHg nos sedimentos de fundo em lagos naturais era aproximadamente 4,6 e 2,2 vezes maior quando comparada àquelas observadas em lagos artificiais, respectivamente ([EPA, 2016](#)). Outra controversa é que alguns autores argumentam que o represamento de um ambiente aquático para a construção de hidrelétricas poderia aumentar as concentrações de MeHg nas matrizes ambientais do reservatório, visto a maior disponibilidade de matéria orgânica presente em solos recentemente inundados para fomentar os processos de metilação ([Porvari, 1995](#); [Hylander et al., 2006](#)). Por outro lado, pode se argumentar que a maior disponibilidade de matéria orgânica pode imobilizar o Hg visto que sua degradação gera sulfetos ([Jackson, 1991](#)).

A maioria dessas avaliações e estimativas são feitas em ecossistemas temperados. Essa tese, por outro lado, contém dados sobre a circulação de Hg em ecossistemas tropicais. Nos capítulos subsequentes serão abordados os impactos de reservatórios de hidrelétricas no ciclo biogeoquímico do Hg, além de sua dinâmica em um sistema rio-planície de inundação, todos na região amazônica ocidental.

Capítulo 1:

Methylmercury in environmental compartments of a hydroelectric reservoir in the Western Amazon, Brazil

→ Submetido à Revista **Chemosphere** em **17/07/2018**
Qualis-Capes (Área de Biodiversidade, 2014-2016): **A2**
Fator de Impacto (2017): **4.427**
Status: **Publicado** (<https://doi.org/10.1016/j.chemosphere.2018.10.106>)

Methylmercury in environmental compartments of a hydroelectric reservoir in the Western Amazon, Brazil

Inacio A Pestana^{*a}, Wanderley R Bastos^b, Marcelo G Almeida^a, Marilia H Mussy^c & Cristina MM Souza^a

^aEcology and Natural Resources Postgraduate Program, Laboratory of Environmental Sciences, Biosciences and Biotechnology Center, Norte Fluminense Darcy Ribeiro State University, Av. Alberto Lamego, 2000 – Parque Califórnia – CEP: 28013-602, Campos dos Goytacazes, Rio de Janeiro, Brazil

^bRegional Development and Environment Postgraduate Program, Environmental Biogeochemistry Wolfgang C. Pfeiffer, Rondônia Federal University, Av. Pres. Dutra, 2967 – Olaria – CEP: 76801-059, Porto Velho, Rondônia, Brazil

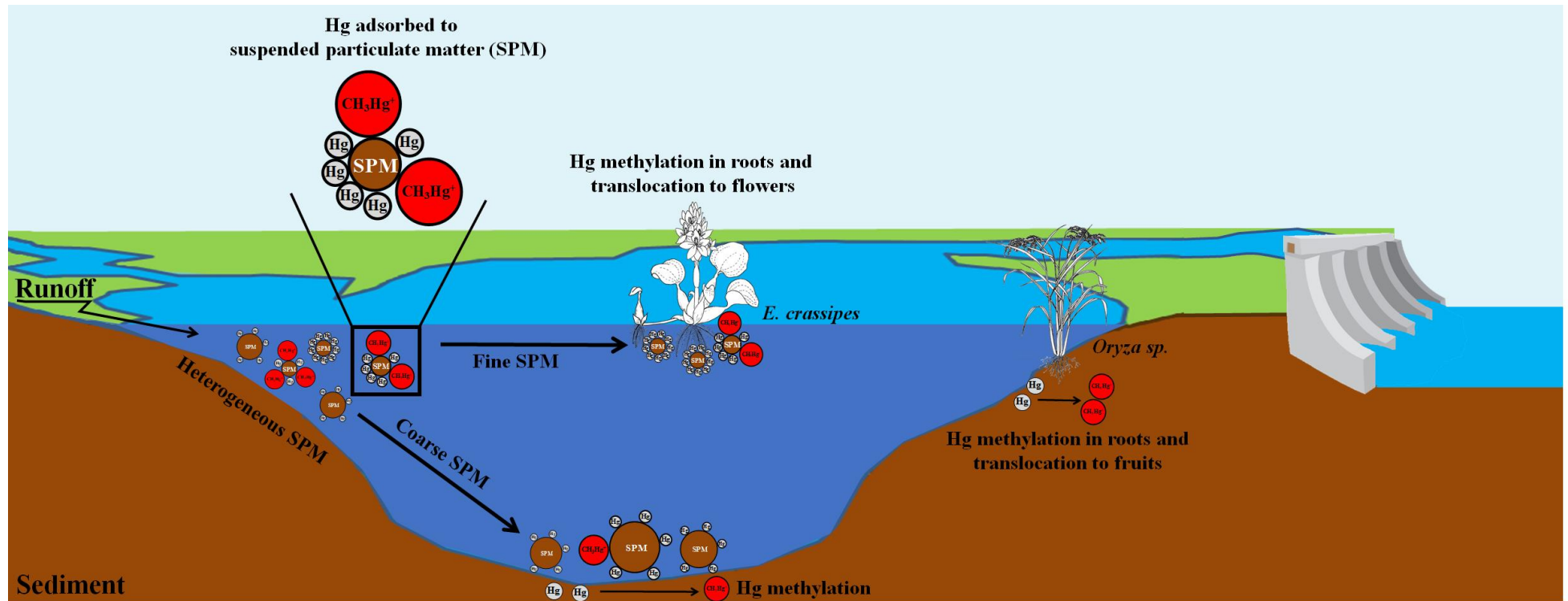
^cBiological Sciences (Biophysics) Postgraduate Program, Carlos Chagas Filho Institute of Biophysics, Rio de Janeiro Federal University, Av. Pedro Calmon, 550 – Cidade Universitária – CEP: 21941-901, Rio de Janeiro, Rio de Janeiro, Brazil

Abstract

Damming rivers to generate electricity creates a lentic environment that favors methylmercury (MeHg) formation. Reservoirs in the Amazon are critical environments for MeHg formation, considering its old soils and the use of Hg in gold mining in the region. The objective of this study was to evaluate MeHg accumulation in three environmental compartments (aquatic macrophytes, suspended particulate matter (SPM) and sediment) of the Samuel reservoir (Western Amazon, Brazil), during the low water, ebb and high water hydrological periods, characterizing the dry season, the end of the rainy season and the rainy season, respectively. MeHg concentrations were determined through GC-AFS. The aquatic macrophytes presented higher %MeHg in their roots (up to 12%) compared to their other tissues. This ratio was 1.7 and 5.9 times higher than those observed for SPM and the sediment, but MeHg concentrations were the lowest (0.5 to 4.5 ng g⁻¹) among the three environmental compartments. Contrary, the highest MeHg concentration was observed in SPM (104 ng g⁻¹) during the low water period. The MeHg concentration in the sediment profile decreased with increasing depth (0.93 to 0.48 ng g⁻¹) and with decreasing organic matter lability (increasing C:N ratio). In the SPM, on the other hand, MeHg concentration showed a positive association with increasing C:N ratio. We conclude that MeHg dynamics in the SPM are associated with the hydrological periods, with peaks during the low water period. The organic matter lability of the sediments is more limiting to the production of MeHg than the total Hg concentrations.

Keywords: Mercury methylation; Aquatic macrophytes; Amazon hydroelectric reservoir; Suspended particulate matter; Sediment profile

Graphical Abstract



1. Introduction

The presence of river dams to generate electricity causes several impacts on the Hg biogeochemical cycle. The transformation of a lotic environment into a lentic one, associated with the flooding of the land area, favors the remobilization of the bottom sediment, which in turn releases Hg, organic matter and other chemical species to the water column (Forsberg & Kemenes, 2006; Kasper et al., 2014). The organic matter decomposition generates physical and chemical stratification in the water column, creating favorable conditions for Hg transformation into its most toxic chemical species, methylmercury (MeHg) (Coquery et al., 2003; Boudou et al., 2005; Hylander et al., 2006).

The production of MeHg in bottom sediments is mainly mediated by sulfate-reducing bacteria (Benoit et al., 2002) or iron-reducing bacteria (Kerin et al., 2006), whereas in exposed soils there is evidence that this production can also be mediated by some fungi (Fischer et al., 1995; Miranda, 2010). Comparatively, Hg methylation in roots of aquatic macrophytes is more efficient than in sediment and soil, given the high availability of organic matter for microbial growth (Guimarães et al., 1998). Mercury methylation is favored by anoxic conditions, although there is evidence of

this process occurring in aerobic environments (Gionfriddo et al., 2016).

MeHg sources to the water column of a reservoir may be associated with: (1) the drainage of forest soils adjacent to the reservoir, rich in organic matter and Hg (allochthonous methylation, followed by erosion) (Malm, 2008; Miranda, 2010; Pestana et al., 2016); (2) the bottom sediment (autochthonous methylation, followed by resuspension) (Miranda, 2010); (3) the roots of aquatic macrophytes (autochthonous methylation, with subsequent release to the water column) (Mauro et al., 1999; Mauro et al., 2001); and/or (4) methylation occurring in the reservoir's own water column (autochthonous methylation, possibly associated with the microbial loop) (Nascimento et al., 2009; Almeida, 2012).

Amazonian reservoirs are particularly susceptible to high MeHg concentrations in their environmental compartments, since the old soils of the region contain naturally high Hg concentrations, as a consequence of several cycles of evaporation, wet and dry deposition and accumulation, which is strongly associated with organic matter and Al- and Fe-oxyhydroxides (Lechler et al. 2000; Roulet et al. 2000; Lacerda & Malm, 2008; Selin, 2009; Fearnside, 2014). Besides this, the gold rush in the 1990s left an estimated 168 metric tons of Hg⁰ in the Amazon, used in the amalgamation and

separation of gold in mining processes (Lacerda and Salomons, 1992; Bastos et al., 2006).

Since the Amazon has the largest river system in the world (Tollefson, 2011), the captation of its underexploited water resources for electric power generation is one of the priority strategies of the Brazilian government, which plans to build at least 221 hydroelectric dams in the region, of which 20% will be located in the Madeira river sub-basin (Castello e Macedo, 2016). Among the consequences of mass impoundment of watercourses (Forsberg et al., 2017), Hg accumulation and methylation in the reservoir compartments can compromise the entire food chain and human contamination can reach critical levels, as already observed in populations that rely on fish consumption from reservoirs as a primary protein source (Leino and Lodenius, 1995; Kehrig et al., 1998).

Studies evaluating MeHg circulation in reservoirs have broadly addressed the concentration of this contaminant in carnivorous and piscivorous fish, since they are the most often consumed by people (Porvari, 1995; Kehrig et al., 1998; Brasil et al., 2004; Kasper et al., 2014). On the other hand, studies of the dispersion and production of MeHg among other biotic and abiotic compartments of reservoirs are less frequent (Coquery et al., 2003; Muresan et al., 2008), but necessary to

understand the contamination of the food chain and, in a larger context, the MeHg dynamics in these artificial ecosystems. Also, studies on the Hg dynamics in tropical reservoirs are still scarce in literature (Kasper et al., 2012; Kasper et al., 2014) compared to temperate reservoirs (Larssen, 2009; Hsu-Kim et al., 2018).

This work aimed to broaden the understanding of MeHg circulation in tropical reservoirs and to provide data that can support adequate management of these ecosystems. In this study, three environmental compartments (aquatic macrophytes, suspended particulate matter (SPM) and sediment) were evaluated to understand the critical accumulation sites of MeHg in the Samuel Reservoir. Specifically, (1) through the SPM we evaluated the spatial-temporal dynamics of MeHg; (2) through the sediment profile we evaluated the deposition and MeHg accumulation; (3) through aquatic macrophytes we evaluated MeHg accumulation by the roots and the translocation to other plant tissues; and (4) through the associations of MeHg with geochemical supports (Fe, C, N) in the SPM and sediment we evaluated the transport and limitations of Hg methylation in these environment compartments.

2. Materials and methods

2.1 Study Area

Samuel Reservoir (**Figure 1**), located in the city of Porto Velho (Rondônia, Brazil), was created in 1988 by damming the Jamari River, one of the tributaries of the Madeira River. The reservoir has a surface area of 580 km² during the high water period and 140 km² during the low water period and it is influenced by small adjacent streams and forest rivers, known as *igarapés* in the region (SEDAM, 2002). The minimum and maximum depth recorded were 8 m (*Jamari*, **Figure 1**) and 33 m (*Reservoir2*, **Figure 1**), respectively.

2.2 Sampling

The sampling was carried out in three hydrological periods: high water (February 2013), ebb (May 2012) and low water period (October 2011), characterizing the rainy season, the end of the rainy season and the dry season, respectively. These hydrological periods are characteristic of the Amazon region and indicate the height fluctuation of the water column observed in the reservoir. The ebb period is an intermediate period in which the height of the water column observed during the high water progressively decreases until reaching the

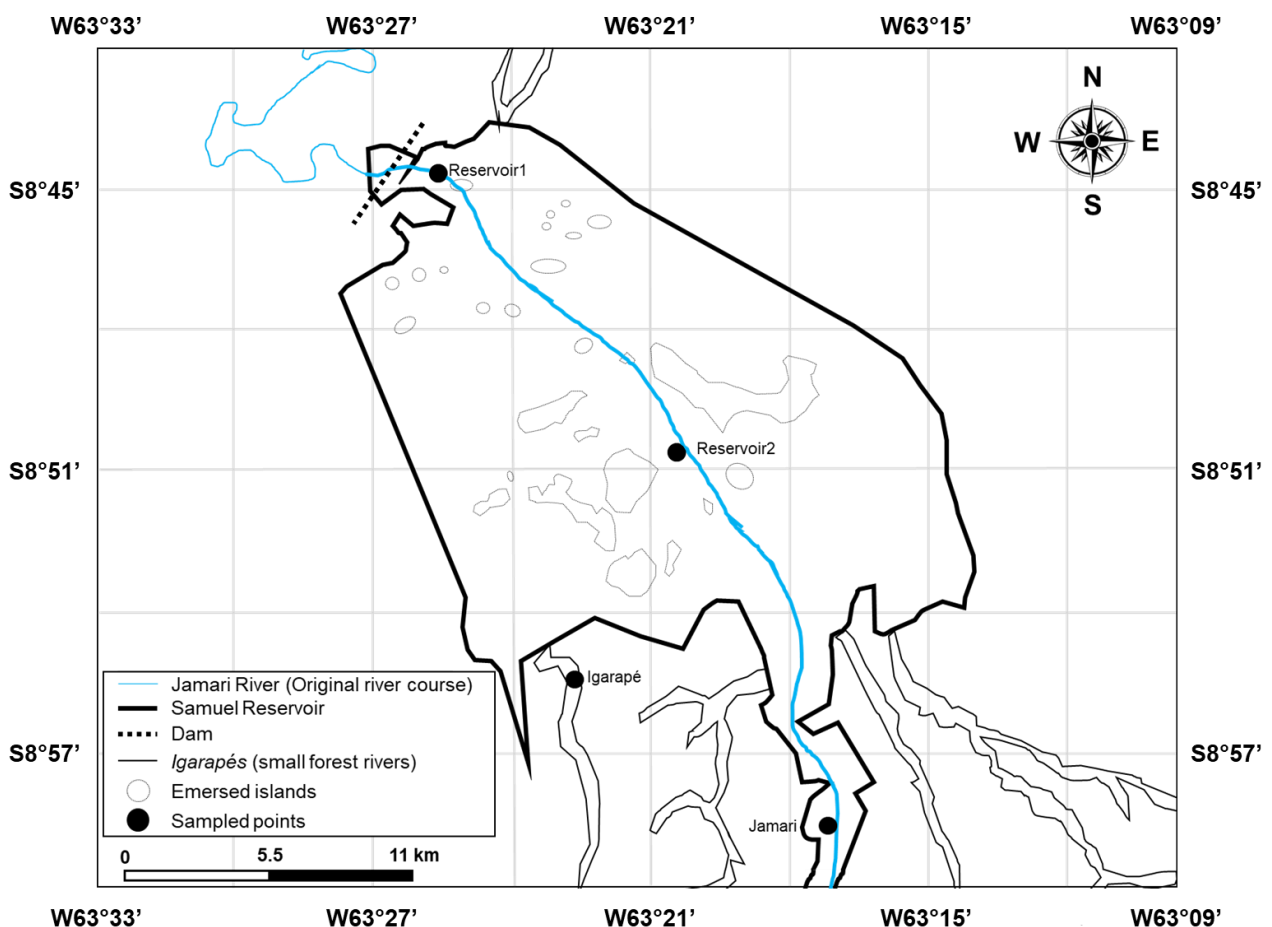


Figure 1 – Location of sampling points within Samuel Reservoir. The map was created with satellite images of the reservoir during the low water period with the emerged islands represented. The direction of water flow is from south to north.

lowest level observed in the low water period.

The sampled points within the reservoir (**Figure 1**) form a transect from the Jamari River (*Jamari*, **Figure 1**) to the dam (*Reservoir1*, **Figure 1**). All points were georeferenced using a GPS receiver (Trimble GeoExplorer XT 500).

Water was sampled at a depth of 0.3 m, separating particles larger than 63 μm using a sieve, and placed in pre-rinsed 2 L polyethylene flasks. Samples were protected from light and processed at the Wolfgang C. Pfeiffer Environmental Biochemical Laboratory at Rondônia Federal University.

During the ebb period, a sediment profile was sampled at the center of the reservoir using a polyethylene tube (*Reservoir2*, **Figure 1**), as well as two aquatic macrophytes species (*Eichhornia crassipes* and *Oryza sp.*).

2.3 Sample processing

Suspended particulate material (SPM) was obtained after filtration using Whatman® GF/F paper (0.7 μm porosity). The sediment profile was sectioned every 2 cm until 20cm depth and fractionated using a 63 μm sieve.

Aquatic macrophytes were separated into roots, leaves, stalks, flowers and fruits, when present, and washed with deionized water to remove associated coarse material. The roots were washed

until they could be visually separated (observing a homogeneous color), suggesting the removal of the coarse adsorbed elements. All samples (SPM, sediment profile and macrophyte tissues) were dried by lyophilization and homogenized using a mortar and pestle.

2.4 MeHg determination

MeHg in biotic (aquatic macrophyte tissues) and abiotic matrices (SPM and sediment) were solubilized following the protocol described by [Liang et al. \(1994\)](#) for biotic samples and validated by [Almeida \(2012\)](#) and [Beldowski et al. \(2014\)](#) for abiotic samples. Then, solubilized samples were ethylated following the protocol described by [EPA 1630 \(2001\)](#). Briefly, aliquots of 0.5 g (aquatic macrophyte tissues, sediment and SPM) were weighed in Teflon® tubes in which 5 mL of a 25% KOH/methanol solution was added to extract and solubilize MeHg. These samples were kept in an oven for 6 h at 70 °C, and were shaken every hour. At the end of 6 h, the samples were allowed to rest for 48 h in the dark to avoid MeHg photodegradation ([Liang et al., 1994](#)).

At the end of 48 h, MeHg determination was carried out. Amber vials received 30 μL of the solubilized sample, 200 μL of a 2 mol L⁻¹ acetic acid/sodium acetate solution (CH₃COOH/CH₃COONa) and 50 μL of 1% sodium tetraethylborate

(NaBEt₄) and were filled with ultrapure water (Milipore Mili-Q, model Integral A10, Molsheim, France) to 40 mL (EPA 1630, 2001).

The determination was carried out using a gas chromatograph coupled to a cold vapor atomic fluorescence spectrophotometer (GC-CVAFS, MERX-M Automated Methyl Mercury Analytical System, Brooks Rand Labs, Seattle, WA, USA). The detection limit was 0.0017 ng g⁻¹ dry wt. and accuracy was checked by analyzing matrix spikes (90 ± 13%, N=6). Recovery was 91%±9% (N=6) and 96±10% (N=6), using IAEA-140 (Sea Weed, *Fucus sp.*) and IAEA-356 (Polluted marine sediment) reference material, respectively.

2.5 Total Fe determination

The method for total Fe determination in abiotic matrices (SPM, sediment) followed the protocol described by Pozebon et al. (2005). Briefly, aliquots of 0.5 g (sediment and SPM) were transferred to a Teflon[®] bomb filled with 7mL of HNO₃ 65%, 6mL of HF 48% and 3 mL of HCl 35%. The bomb was capped and allowed to rest for 24 h and, then, placed in a digester block system at 160 °C for 9h. After 9h, 10mL of H₃BO₃ 4% were added to the digestion to neutralize the HF. After cooling, the final extract was filtered using Whatman[®] 40 paper and completed to 30

mL with ultrapure water (Milipore Mili-Q model, Integral A10, Molsheim, France) in a volumetric flask.

Fe determination was carried out using inductively coupled plasma atomic emission spectroscopy (ICP-AES, Liberty Series II, Varian, Australia), with detection limit of 0.2 µg g⁻¹ dry wt. The accuracy of the method using certified samples (NIST 2702 and 1646A) was 93% and analytical reproducibility was at least 90%.

2.6 Total Hg, carbon and nitrogen determination

Total Hg, carbon and nitrogen concentrations used in this study were obtained from Pestana et al. (2016). For total Hg determination, the authors used a protocol adapted from Bastos et al. (1998) that consist in solubilize abiotic samples (0.3 g of SPM and 0.5 g of sediment) using 8 mL of aqua regia (3 HCl 37 %:1 HNO₃ 65 %) and biotic samples (0.2 g of the macrophyte tissues) using 4 mL of ultrapure water (Milipore Mili-Q model, Integral A10, Molsheim, France) + 2 mL of H₂O₂ 30 % + 3 mL of H₂SO₄ 97 % + 3 mL of HNO₃ 65 % in Teflon[®] tubes. The tubes were capped and digestion were carried out in a microwave oven (Mars Express, CEM, Model 907501, USA) during 25 minutes (10 min until it reached 95 °C, and 15 min with constant temperature of 95 °C and power of 1600 W, as described by Santos et al., 2005). The final extract was

filtered using Whatman® 40 paper and completed to 50 mL with ultrapure water (Milipore Mili-Q model, Integral A10, Molsheim, France) in a volumetric flask. The total Hg concentration was determined using an Hg Analyzer (QuickTrace, M-75000, CETAC, Nebraska, USA). The recovery of Hg in the SPM and sediment samples (NIST 2702) was 93 %, and the recovery in the macrophytes samples (NIST 1515) was 90 %. The limit of detection for Hg in the SPM and sediment was 0.4 ng g⁻¹ and the limit of detection for Hg in the plant samples was 1 ng g⁻¹.

For the carbon and nitrogen elemental composition of organic matter, [Pestana et al. \(2016\)](#) used 1 mg of SPM and 10 mg of sediment samples placed in tin (Sn) capsules. The determinations were carried out in an elemental analyzer (Flash 2000, Organic Elemental Analyzer, Thermo Scientific, Milan, Italy) and the atomic ratios of carbon and nitrogen (abbreviated by C:N) were calculated to infer the organic matter lability. High C:N ratios indicate a recalcitrant organic matter while small C:N ratios indicate a labile organic matter ([Meyers 1994](#); [Cloern et al. 2002](#); [Kennedy et al. 2005](#)). The level of analytical reproducibility for the same samples was at least 95 %

2.7 Statistical analyses

The statistical analyses were carried out with the R software ([R Core Team,](#)

[2018](#)). The descriptive statistics used were the median and interquartile range (abbreviated by IQR), due to the asymmetry of most of the data. If the mean (average values) has been used as a measure of centrality and the standard deviation as a measure of dispersion, representation of the data would be biased (mean and standard deviation are strongly affected by asymmetry and outliers). The differences of mean MeHg concentrations among environmental compartments were evaluated by ANOVA (*aov*, base package, [R Core Team, 2018](#)) followed by a multiple comparison test (*TukeyHSD*, base package, [R Core Team, 2018](#)), assuming a 95% confidence level. The data were transformed to meet the assumptions ANOVA using a maximum likelihood function (*boxcox*, MASS package, [Venables and Ripley, 2002](#)) so that the asymmetry and the outliers did not interfere with the test.

Multiple, linear and quadratic regression models were proposed to explain the associations of MeHg and geochemical supports (*lm*, base package, [R Core Team, 2018](#)). Multiple regression models were plotted using 3D graphics (*scatterplot3d*, *scatterplot3d* package, [Ligges and Mächler, 2003](#)) and decomposition of sum of squares of each independent variable (R^2_{partial}) of these models was performed through an ANOVA table (*summary.aov*, base package, [R](#)

Core Team, 2018). The data were transformed, when necessary, to meet the assumptions of each model using a maximum likelihood function (*boxcox*, MASS package, Venables and Ripley, 2002).

3. Results

3.1 MeHg in the compartments of Samuel Reservoir

MeHg formation and accumulation in the environmental compartments was evaluated through MeHg/total Hg ratio (%MeHg, **Figure 2**). The highest %MeHg was observed in the roots of aquatic macrophytes ($8.9\% \pm 6.6$, **Figure 2**), followed by SPM ($5.1\% \pm 7.0$, **Figure 2**)

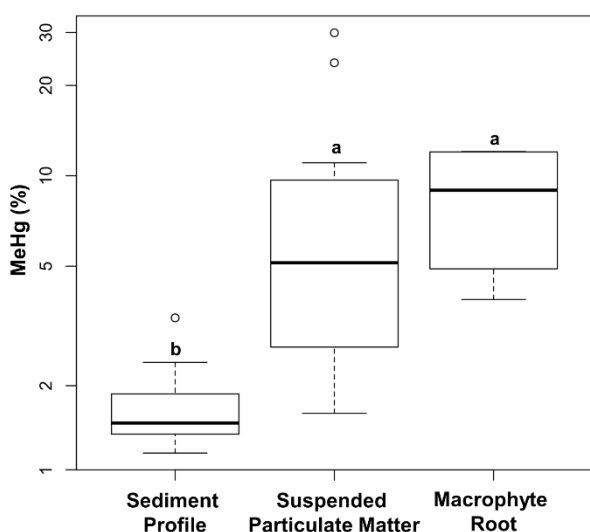


Figure 2 – MeHg/total Hg ratio (%MeHg) in the environmental compartments of Samuel Reservoir. The sediment and macrophyte data are related to the ebb period while for the SPM is a compilation of the three hydrological periods (high water, ebb period and low water). Different letters denote high statistical support for the mean difference ($p < 0.001$). Hollow circles represent outliers (outside 1.5 times the interquartile range above the upper quartile). The y-axis distance between the numbers is in logarithmic scale.

and sediment ($1.5\% \pm 0.5$, **Figure 2**). On the other hand, MeHg concentration in SPM was 12.5 times higher than observed in the roots of aquatic macrophytes and 50.6 times higher than observed in sediment (**Table 1**).

The %MeHg in the roots of the aquatic macrophytes was 1.7 times higher than observed in the SPM ($p = 0.61$) and 5.9 times higher than observed in the sediment ($p = 0.0004$; **Figure 2**). Between the sampled aquatic macrophytes, the roots and leaves of *Eichhornia crassipes* presented lower MeHg concentrations and %MeHg compared to the same tissues of *Oryza sp.* (**Figure 3**). On the other hand, the stalks of both macrophytes showed similar MeHg concentrations and %MeHg (**Figure 3**). Similar %MeHg were observed between the roots and fruits of *Oryza sp.* and similar MeHg concentrations were observed between the roots and flowers of *Eichhornia crassipes* (**Figure 3**). The %MeHg in the roots of these macrophytes was similar to previous studies carried out in the Brazilian Pantanal and in the Tapajós River, a tributary of the Amazon River (Guimarães et al., 1998; 2000; **Table 1**).

The %MeHg in the SPM was 1.7 times lower than observed in the roots of aquatic macrophytes and 3.4 times higher than observed in the sediment (**Figure 2**). The %MeHg in the SPM showed a wide range (2% – 30%) among the hydrological periods (**Figure 4**). Temporally, MeHg

Table 1 –Total Hg and MeHg concentrations and %MeHg in sediment, SPM and roots of aquatic macrophytes of this and previous studies.

Environmental compartment	Site	Hydrological Period	Total Hg (ng g ⁻¹) dry wt.	MeHg (ng g ⁻¹) dry wt.	%MeHg	Reference
Sediment	Samuel Reservoir		40.61 ± 7.57	0.69 ± 0.16	1.5 ± 0.5	*This Study
	Samuel Reservoir				0.69 ± 0.07	Guimarães et al., 1995
	Petit-Saut reservoir		220.65 ± 80.24	25.87 ± 10.78	11 ± 16	Muresan et al., 2008
	Jamari River				0.66 ± 0.48	Guimarães et al., 1995
	Lake (Tapajós)		214.50 ± 31.82	0.28 ± 0.29	0.16 ± 0.11	Roulet et al., 2001
	Lake (Tapajós)				0.60 ± 0.11	Guimarães et al., 2000
	Lake (Pantanal)				1.16 ± 0.08	Guimarães et al., 1998
Suspended Particulate Matter	Samuel Reservoir	Low water	316.02 ± 22.30	58.35 ± 40.90	18 ± 14	*This Study
		High water	389.63 ± 249.46	11.53 ± 4.09	4 ± 3	*This Study
	Petit-Saut Reservoir	Low water	69.08 ± 6.09	21.43 ± 7.09	32 ± 14	Muresan et al., 2008
		High water	41.49 ± 7.99	6.77 ± 5.29	21 ± 12	Muresan et al., 2008
Macrophyte roots	Samuel Reservoir		3.45 ± 1.82	2.79 ± 2.13	8.9 ± 6.6	*This Study
	Lake (Tapajós)				13.8 ± 24.55	Guimarães et al., 2000
	Lake (Pantanal)				8.42 ± 2.63	Guimarães et al., 1998

*Data from this study is represented by the median ± interquartile range (IQR) due to high asymmetry of the data compared to the Normal distribution and the presence of outliers

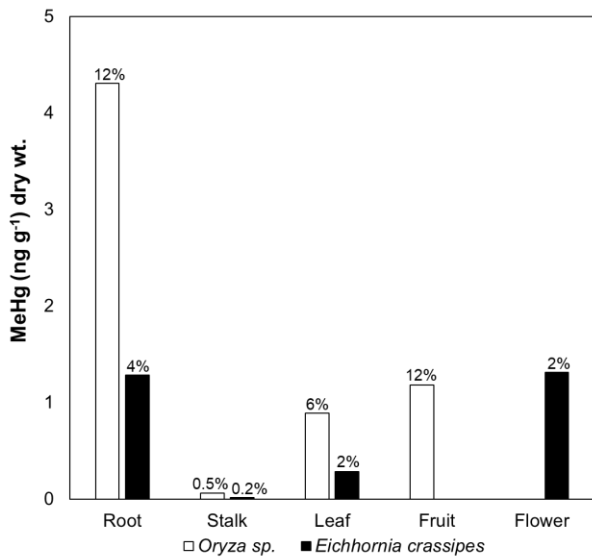


Figure 3 – MeHg concentrations in tissues of aquatic macrophytes sampled during the ebb period (May 2012). The percent values on the bars represent the MeHg/total Hg ratio (%MeHg).

concentrations and %MeHg were higher during the low water period, followed by the ebb and high water periods (**Figure 4**, **Table 1**). Spatially, MeHg concentration and %MeHg were higher in the central part of the reservoir and in the *igarape* during the low water period (*Reservoir2* and *Igarape*; **Figure 4**). Median values of %MeHg in the SPM during the low water period was 4.5 times higher compared to the high water period (**Table 1**). A difference in %MeHg between these two hydrological periods was also observed, with lower variation, in the Petit-Saut Reservoir (%MeHg was 1.5 times higher in the low water period compared to the high water period; [Muresan et al., 2008](#)).

The highest MeHg concentration and %MeHg in the sediment profile were observed in the subsurface (4 cm: 0.88 ng g⁻¹, corresponding to 3% of MeHg),

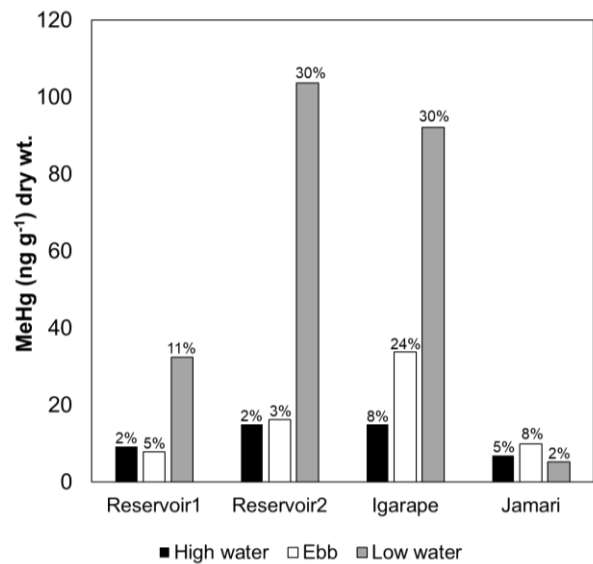


Figure 4 – MeHg concentration in SPM among sampled points and among hydrological periods. The percent values on the bars represent the MeHg/total Hg ratio (%MeHg).

decreasing with depth and reaching the lowest value at 18 cm (0.44 ng g⁻¹; 1% MeHg; **Figure 5**). The %MeHg found in the

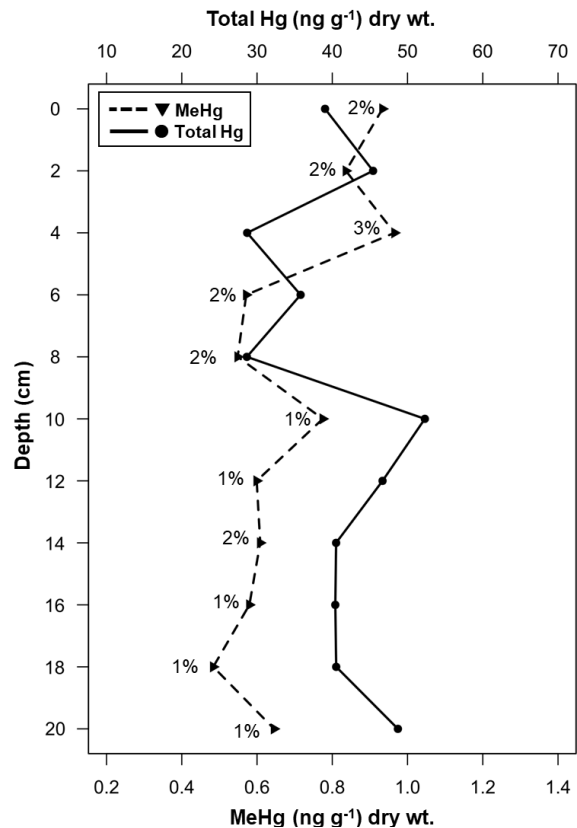


Figure 5 – MeHg concentrations in the sediment profile sampled at the center of the reservoir (*Reservoir2*, **Figure 1**) during the ebb period (May 2012). The percent values next to triangles represent MeHg/total Hg ratio (%MeHg).

sediment of this study was twice that reported by [Guimarães et al. \(1995\)](#), who also studied the Samuel Reservoir 17 years prior to this study, and 7 times smaller compared to Petit-Saut Reservoir ([Muresan et al., 2008](#); **Table 1**). Besides this, the %MeHg found in the sediment of this study was 3 and 9 times higher than those found in floodplains of the Tapajós River, reported by [Guimarães et al. \(2000\)](#) and [Roulet et al. \(2001\)](#), respectively (**Table 1**), and similar to that found in the Brazilian Pantanal ([Guimarães et al., 1998](#); **Table 1**).

3.2 Geochemical Supports

There were no associations between total Fe concentrations and total Hg or MeHg concentrations in either of the two abiotic compartments evaluated (SPM and sediment), as also observed by

[Guimarães et al. \(2000\)](#) studying the Tapajós River. On the other hand, MeHg concentrations were associated with the organic matter lability (C:N ratio) and total Hg concentrations in these two compartments. Multivariate models were used to explain the influence of each of these variables on MeHg concentrations (**Figure 6, A and B**).

Both models indicated a strong influence of the organic matter lability (C:N ratio) on MeHg concentrations in both sediment and SPM ($R^2_{\text{partial}} = 0.54$ for both matrices, **Figure 6, A and B**). On the other hand, total Hg concentrations had a greater influence on MeHg concentrations in the sediment ($R^2_{\text{partial}} = 0.29$, **Figure 6A**) compared to the SPM ($R^2_{\text{partial}} = 0.03$, **Figure 6B**). The relationship between MeHg and total Hg concentrations was quadratic for both compartments while the

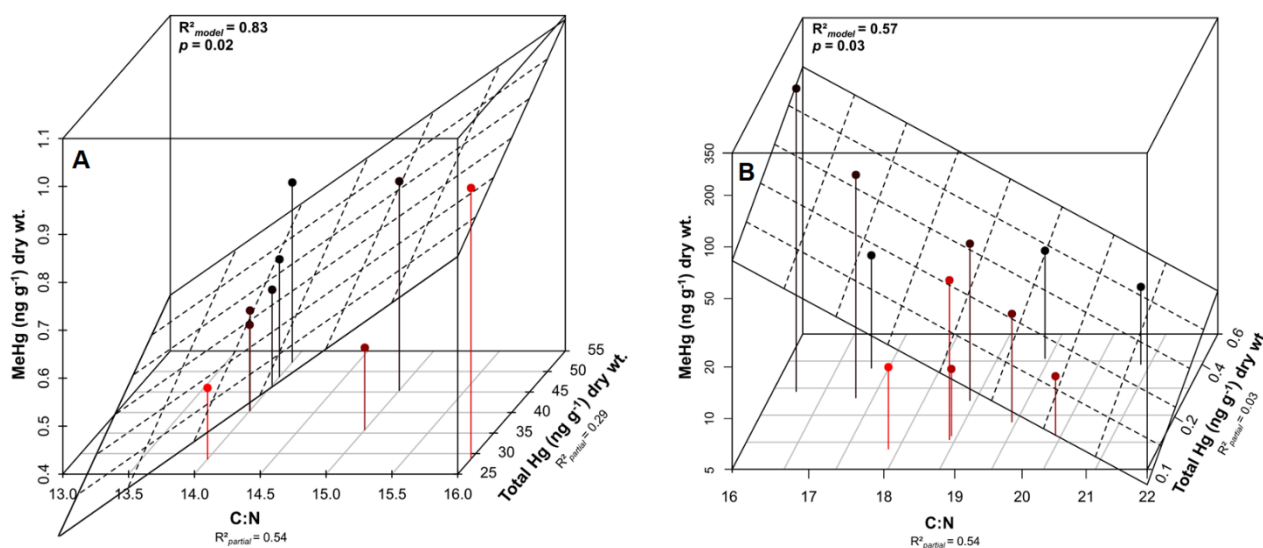


Figure 6 – Multiple regression of MeHg concentration in the sediment (**A**) and SPM (**B**) using as predictors the organic matter quality (C:N ratio) and total Hg concentration. The explanation of the model (R^2_{model}) results from the sum of the partial explanations (R^2_{partial}) of each variable. The dashed lines form the multiple regression plane among the variables. The red tones highlight the depth of the points on the graphic.

relationship between MeHg concentrations and the C:N ratio was linear and positive for the sediment and linear and negative for SPM (Figure 7, A and B).

4. Discussion

4.1 MeHg in aquatic macrophytes tissues

The highest %MeHg observed in the roots of the aquatic macrophytes (Figure 2) is probably associated with the highest retention of organic matter by this compartment, compared to sediment and SPM (Mauro et al., 1999), since this is the principal substrate for microbial activity and source of methyl radical ($-CH_3$) that it is transferred to Hg^{2+} during Hg methylation (King et al., 2001; Flemming et al., 2006; Parks et al., 2013). In addition, the production of organic matter by the

photosynthetic organisms associated with the roots of aquatic macrophytes can feedback Hg methylation in this microenvironment (Mauro et al., 1999; Mauro, 2001).

The rooted aquatic macrophyte *Oryza sp.* presented higher MeHg in its roots (12%, Figure 3) compared to *Eichhornia crassipes* (4%, Figure 3), a floating aquatic macrophyte. The roots of floating aquatic macrophytes (e.g., *Eichhornia crassipes*) extend a few centimeters into the water column (Guimarães et al., 1998), where SPM available for adsorption is of fine granulometry with a high surface area, and consequently high Hg concentrations (Bengtsson and Picado, 2008). The SPM availability in these surface waters depends on particle resuspension from

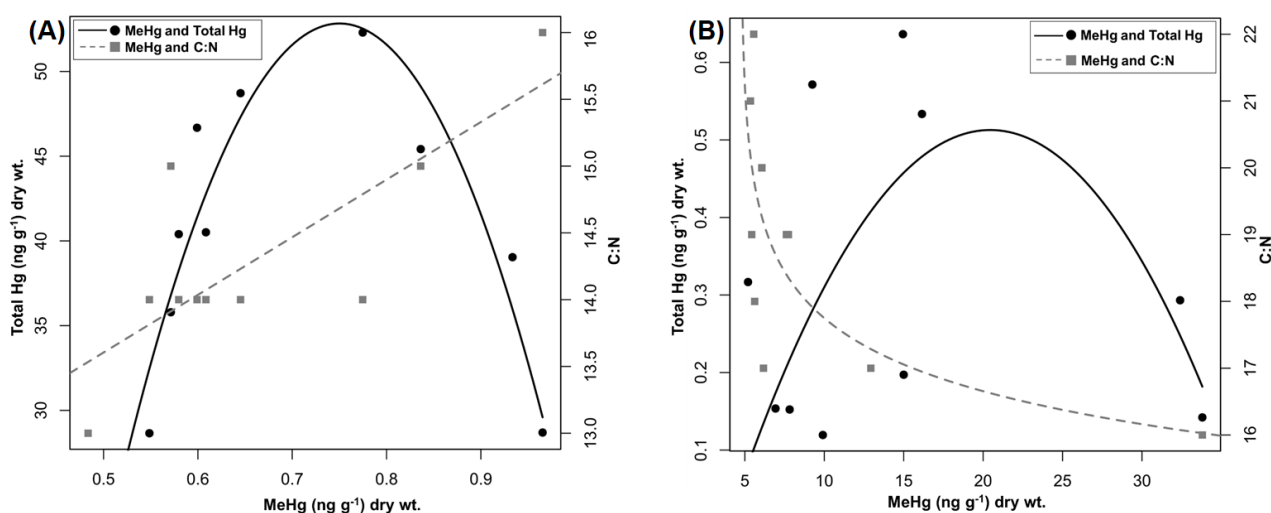


Figure 7 – (A) Linear regression between MeHg concentrations and organic matter lability (C:N ratio) in the sediment profile (gray squares, dashed line, $R^2 = 0.62$, $p = 0.007$) and quadratic regression between MeHg concentrations and total Hg concentration in the sediment profile (filled circles, solid line, $R^2 = 0.86$, $p < 0.001$). **(B)** – Linear regression (adjusted to $\frac{1}{MeHg}$) between MeHg concentrations and organic matter lability (C:N ratio) in the SPM (gray squares, dashed line, $R^2 = 0.42$, $p = 0.03$) and quadratic regression between MeHg concentrations and total Hg concentration in the SPM (filled circles, solid line, $R^2 = 0.34$, $p = 0.28$).

sediments or soil erosion events adjacent to the water body. On the other hand, rooted aquatic macrophytes (e.g., *Oryza sp.*) are continuously exposed to the Hg present in the sediments. Also, the sediment of this reservoir has organic matter more labile (low C:N ratio) compared to SPM (**Figure 6, A and B**), which partially explains this difference. Finally, the anoxia of sediments probably contributed to this difference, since it is one of the main conditions necessary for methylation to occur (Mauro et al., 1999).

In order to complement a gap in the studies of MeHg dynamics in reservoirs, other tissues from the aquatic macrophytes were considered besides the roots. The MeHg in leaves and fruits of *Oryza sp.* can easily be transferred to the trophic chain of the reservoir through herbivory, since the stands of aquatic macrophytes harbor a diverse biota (Mauro et al., 2001; Sánchez-Botero et al., 2003).

The %MeHg ratios observed between the roots of the aquatic macrophytes and the sediment (*Oryza sp.* = 8.0; *Eichornia crassipes* = 2.7) were in the same order of magnitude to those found by Guimarães et al. (1998), studying *Eichornia azuera* and *Salvinia sp.* (5.6 and 9.0, respectively) in a floodplain in the Brazilian Pantanal. While the highest %MeHg observed in this study were in a sediment-rooted macrophyte (*Oryza sp.*), Guimarães et al. (1998) observed it in a

floating aquatic macrophyte (*Salvinia sp.*). The thickness of the roots may be an important aspect to explain these differences, since the root surface area is closely associated with the Hg adsorption capacity in this microenvironment, as well as background Hg concentration in sediment (Guimarães et al., 1998; 2000). The dense macrophyte stands present in reservoirs act as sink of Hg and enhance the ability of these ecosystems to retain contaminants (Molisani et al. 2006). Further studies must be carried out to evaluate the influence of root thickness and the growth form of aquatic macrophytes on the retention of contaminants.

The aquatic macrophytes represent a critical environmental compartment for Hg methylation and accumulation, as demonstrated in this and other studies (Guimarães et al., 1998; 2000; Cesário et al., 2017; Cabrita et al., 2019). Further studies are required which include mass balance of the global production of MeHg by the macrophytes within reservoirs to understand the contribution from each compartment to Hg circulation and export. Also, the methylation and demethylation processes should be further studied in the aquatic macrophytes tissues to understand the role of these processes in the MeHg budget for reservoirs and how this contribute to the global Hg biogeochemical cycle.

4.2 Spatial-temporal dynamics of MeHg in SPM

The MeHg concentrations and %MeHg observed in the SPM were highest during the low water period for *Reservoir1*, *Reservoir2* and *Igarape* sampling sites (**Figure 1**) compared to other hydrological periods (**Figure 4**). On the other hand, for the *Jamari* sampling site, the MeHg concentrations and %MeHg observed in the SPM were highest during the ebb period compared to other hydrological periods (**Figure 4**).

Temporally, the SPM undergoes selective sedimentation starting at the end of the high water period and peaks during the low water period (Malm et al., 2004; Pestana et al., 2016): in the high water period, SPM is heterogeneous in size and mass, since rainfall favors erosion of particles from adjacent soils into the water body (Carvalho, 1983). At the end of the high water period and the beginning of the ebb period the sedimentation of larger and heavier particles is favored while small and light particles remain suspended. Since smaller particles have higher surface area per unit of weight (Bengtsson and Picado, 2008), they have higher MeHg concentrations, which may explain the greater concentrations observed during the low water period (**Figure 4**). Also, resuspension of the sediment is favored when the water column is lower. Higher MeHg concentrations were also observed

in the Petit-Saut Reservoir during low water period compared to high water period (Muresan et al., 2008; **Table 1**). The selective sedimentation process occurs in lentic waters, such as the sampling points within Samuel reservoir area (*Reservoir1*, *Reservoir2*; **Figure 1**) and in small forest rivers, such as the *Igarape* sampling point (**Figure 1**). On the other hand, the process is less intense in lotic waters, which explains the similarity of MeHg concentrations and %MeHg among the hydrological periods for the *Jamari* sampling point (**Figure 1**).

Spatially, the center of the reservoir (*Reservoir2*, **Figure 4**) showed the highest MeHg concentration and %MeHg. During the low water period, several islands emerge around this sample point (**Figure 1**), with a dense plant community, which probably contributed to these high concentrations. Hg methylation at surface water is inefficient, since oxygenation and hydrodynamics are not suitable for methylation to occur (Guimarães et al., 2004). Therefore, the high MeHg concentrations are probably the result of the allochthonous Hg methylation in soils of emerged islands, rich in litter, during the low water period, followed by erosion. Two observations support this hypothesis: (1) the stable isotope carbon signature (^{13}C) indicates that the major source of total Hg in this reservoir is the adjacent forest-covered soils (Pestana et al., 2016); and

(2) %MeHg in seasonally flooded Amazonian soils, such as those in the emerged islands of the reservoir, was in a similar range of this study ($4.00\% \pm 0.39$; Roulet et al., 2001) as well as experiments with Amazonian soils ($3.98\% \pm 1.12$; Miranda, 2010). Both *in situ* and *in vitro* studies had %MeHg similar to the median found in this study for SPM (Figure 2).

4.3 Sediment profile and geochemical support

The highest %MeHg was observed in the sub-surface layer of the sediment profile (4 cm; Figure 5). In this layer, there is probably a balance between oxygenation and the availability of organic matter that is more favorable to Hg methylation compared to the surface layer of the sediment, which although it accumulates more organic matter, is also more oxygenated, limiting the activity of anaerobic organisms (Postgate, 1984). This pattern of higher %MeHg in sub-surface sediment layers was also observed by Guimarães et al., (2000), studying a floodplain lake in the Tapajós River (Table 1).

The organic matter lability (C:N ratio) was a determinant for prediction of MeHg concentrations, both in the sediment (Figure 6A) and in the SPM (Figure 6B). The positive association between MeHg and C:N ratio in the sediment is indicative of Hg methylation (Figure 6A): the more

degraded organic matter (higher C:N ratio) indicates higher microbial activity in the sediments (Kim et al., 2011) and, as a consequence, higher MeHg concentrations are observed. The negative association between MeHg and C:N ratio in the SPM suggests the opposite (Figure 6B). This association also suggests that most MeHg is probably associated with the organic fraction of SPM (e.g., phytoplankton), since (1) this compartment has as characteristic low C:N ratio values; and (2) the sampling was carried out in the superficial water of the reservoir, where phytoplankton abundance is high.

The highest contribution of the C:N ratio to the total explanation of the multivariate models (Figure 6, A and B) indicates that the organic matter lability limits Hg methylation in this reservoir, as opposed to total Hg concentrations. In fact, the relationship between MeHg and total Hg concentrations was quadratic in both compartments, indicating that high total Hg concentrations do not generate an increase in MeHg concentrations (Figure 7, A and B). In contrast, high total Hg concentrations favor the binding of this contaminant to sulfhydryl groups of intracellular proteins of the microorganisms that mediate the methylation process, leading to the loss of enzymatic function, an increase in reactive oxygen species that can interfere with cell redox homeostasis and impairment of all the biochemical machinery (Nascimento

and Chartone-Souza, 2003). These factors may lead to a selection of microorganisms with improved Hg methylation capacity (as already reported by Vishnivetskaya et al., 2011), which can, in turn, enhanced MeHg bioaccumulation in the trophic chain of reservoirs in the long run.

5. Conclusion

The roots of the macrophytes of this reservoir showed higher %MeHg while SPM showed higher MeHg concentration, compared to other environmental compartments. Both the roots of the macrophytes and the fruits of the species *Oryza sp.* are critical tissues for transfer of MeHg to other organisms from this trophic chain.

MeHg dynamics in the SPM are associated with the hydrological periods, with peaks during the low water period. The organic matter lability of the sediments is more limiting to the production of MeHg than the total Hg concentrations.

6. Acknowledgments

We thank the Wolfgang C. Pfeiffer Environmental Biochemical Laboratory at Rondônia Federal University for field logistics and MeHg determinations and the Environmental Sciences Laboratory of Norte Fluminense Darcy Ribeiro State University for total Fe concentrations determinations. C.M.M. Souza received a grant from the Carlos Chagas Filho

Research Support Foundation of the State of Rio de Janeiro (FAPERJ; C-26/111.368/2012) for the purchase of reagents to enable the chemical analysis of this work. Wanderley R. Bastos received grant support from the National Council for Scientific and Technological Development (CNPq-Universal-11, N° 476560/2011-0) for studies of Hg cycling in Samuel Reservoir. We also thank the reviewer for significantly improving the quality and accuracy of this paper through the valuable comments.

7. References

- Almeida R (2012) Estudo da Origem, Mobilização e Organificação do Mercúrio no Reservatório da UHE-Samuel, RO. PhD Thesis, in Portuguese. Instituto de Biofísica Carlos Chagas Filho UFRJ/IBCCF, Rio de Janeiro. 117p.
- Bastos WR, Malm O, Pfeiffer WC, Cleary D (1998) Establishment and analytical quality control of laboratories for Hg determination in biological and geological samples in the Amazon Brazil. *Ciência e Cultura* 50:255–260.
- Bastos WR, Gomes JP, Oliveira RC, Almeida R, Nascimento EL, Bernardi JVE, Lacerda LD, Silveira EG, Pfeiffer WC (2006) Mercury in the environment and Riverside population in the Rio Madeira Basin, Amazon, Brazil. *Science of The Total Environment*, 368(1):344-351. <https://dx.doi.org/10.1016/j.scitotenv.2005.09.048>
- Beldowski J, Miotk M, Beldowska M, Pempkowiak J (2014) Total, methyl and organic mercury in sediments of the Southern Baltic Sea. *Marine*

- Pollution Bulletin, 87(1-2):388-395.
<https://doi.org/10.1016/j.marpolbul.2014.07.001>
- Bengtsson G, Picado F (2008) Mercury sorption to sediments: Dependence on grain size, dissolved organic carbon, and suspended bacteria. *Chemosphere*, 73(4):526-531.
<https://doi.org/10.1016/j.chemosphere.2008.06.017>
- Benoit JM, Gilmour CC, Heyes A, Mason RP, Miller CL (2002) Geochemical and biological controls over mercury production and degradation in aquatic systems. *Biogeochemistry of Environmentally Important Trace Elements. ACS Symposium Series 835*, 262–297.
<https://dx.doi.org/10.1021/bk-2003-0835.ch019>
- Boudou A, Maury-Brachet R, Coquery M, Durrieu G, Cossa D (2005) Synergic Effect of Gold Mining and Damming on Mercury Contamination in Fish. *Environmental Science & Technology*, 39(8):2448-2454.
<https://dx.doi.org/10.1021/es049149r>
- Brasil DB, Almeida R, Nascimento EL, Oliveira RC, Miyai R, Bastos WR, Silveira EG (2004) Mercury in Ictiofauna of Smauel Hydroelectric Reservoir, Amazon – Brazil. *RMZ - Materials and Geoenvironment*, 51(1):865-868.
- Cabrita MT, Duarte B, Cesário R, Mendes R, Hintelmann H, Eckey K, Dimock B, Caçador I, Canário J (2019) Mercury mobility and effects in the salt-marsh plant *Halimione portulacoides*: Uptake, transport, and toxicity and tolerance mechanisms. *Science of The Total Environment*, 650(1):111-120.
<https://doi.org/10.1016/j.scitotenv.2018.08.335>
- Carvalho ML (1983) Efeito da flutuação do nível da água sobre a densidade e composição do zooplâncton em lago de várzea da Amazônia, Brasil. *Acta Amazônica*, 13(5-6):715 -724.
<http://dx.doi.org/10.1590/1809-439219831356715>
- Castello L, Macedo MN (2016) Large-scale degradation of the Amazon freshwater ecosystem. *Global Change Biology*, 22(3):990–1007.
<https://dx.doi.org/10.1111/gcb.13173>
- Cesário R, Hintelmann H, Mendes R, Eckey K, Dimock B, Araújo B, Mota AM, Canário J (2017) Evaluation of mercury methylation and methylmercury demethylation rates in vegetated and non-vegetated saltmarsh sediments from two Portuguese estuaries. *Environmental Pollution*, 226:297-307.
<https://doi.org/10.1016/j.envpol.2017.03.075>
- Cloern JE, Canuel EA, Harris D (2002) Stable carbon and nitrogen isotopes composition of aquatic and terrestrial plants of the San Francisco Bay estuarine system. *Limnology and Oceanography*, 47(3):713–729.
<https://dx.doi.org/10.4319/lo.2002.47.3.0713>
- Coquery M, Cossa D, Peretyazhko T, Azemard S, Charlet L (2003) Methylmercury formation in the anoxic waters of the Petit-Saut reservoir (French Guiana) and its spreading in the adjacent Sinnamary river. *J.Phys. IV France*, 107(1):327-331.
<https://dx.doi.org/10.1051/jp4:20030308>
- EPA. USA Environmental Protection Agency 1630 (2001) Methylmercury in water by distillation, aqueous ethylation, purge and trap, and CVAFS. EPA 821-R-01-020.
- Fearnside PM (2014) Impacts of Brazil's Madeira River dams: Unlearned lessons for hydroelectric

- development in Amazonia. *Environmental Science & Policy*, 38:164-172. <https://doi.org/10.1016/j.envsci.2013.11.004>
- Fischer RG, Rapsomanikis S, Andreae MO, Baldi F (1995) Bioaccumulation of Methylmercury and Transformation of Inorganic Mercury by Macrofungi. *Environ. Sci. Technol.*, 29(4):993–999. <http://dx.doi.org/10.1021/es00004a020>
- Fleming EJ, Mack EE, Green PG, Nelson DC (2006) Mercury methylation from unexpected sources: molybdate-inhibited freshwater sediments and an iron-reducing bacterium. *Applied Environmental Microbiology*, 72(1):457-464. <http://dx.doi.org/10.1128/AEM.72.1.457-464.2006>
- Forsberg BR, Kemenes A (2006) Technical report about hydrobiogeochemical studies with specific attention to mercury dynamics (Hg) In: *Pareceres Técnicos dos Especialistas Setoriais—Aspectos Físicos/Bióticos. Relatório de Análise do Conteúdo dos Estudos de Impacto Ambiental (EIA) e do Relatório de Impacto Ambiental (RIMA) dos Aproveitamentos Hidrelétricos de Santo Antônio e Jirau no, Rio Madeira, Estado de Rondônia. Ministério Público do Estado de Rondônia, Porto Velho, Rondônia, Brazil. 2 Volumes. Part B, Vol. I, Parecer 2. pp. 1–32 (Technical report, In Portuguese).*
- Forsberg BR, Melack JM, Dunne T, Barthem RB, Goulding M, Paiva RCD, Sorribas MV, Silva Jr UL, Weisser S (2017) The potential impact of new Andean dams on Amazon fluvial ecosystems. *PLoS ONE* 12(8): e0182254. <https://dx.doi.org/10.1371/journal.pone.0182254>
- Gionfriddo CM, Tate MT, Wick RR, Schultz MB, Zemla A, Thelen MP, Schofield R, Krabbenhoft DP, Holt KE, Moreau JW (2016). Microbial mercury methylation in Antarctic sea ice. *Nature microbiology* 1:16127. <https://doi.org/10.1038/nmicrobiol.2016.127>
- Guimarães JRD, Malm, O, Pfeiffer, WC (1995) A simplified radiochemical technique for measurements of net mercury methylation rates in aquatic systems near goldmining areas, Amazon, Brazil. *Science of The Total Environment*, 175(2):151-162. [https://doi.org/10.1016/0048-9697\(95\)04911-8](https://doi.org/10.1016/0048-9697(95)04911-8)
- Guimarães JRD, Meili M, Malm O, Brito EMS (1998) Hg methylation in sediments and floating meadows of a tropical lake in the Pantanal floodplain, Brazil. *Sci. Total Environ.*, 213(1):165-175. [https://doi.org/10.1016/S0048-9697\(98\)00089-8](https://doi.org/10.1016/S0048-9697(98)00089-8)
- Guimarães JRD, Meili IM, Hylander LD, Silva EC, Roulet M, Mauro JBN, Lemos RA (2000) Mercury net methylation in five tropical floodplain regions of Brazil: high in the root zone of floating macrophyte mats but low in surface sediments and flooded soils. *The Science of the Total Environment*, 261(1-3):99-107. [https://doi.org/10.1016/S0048-9697\(00\)00628-8](https://doi.org/10.1016/S0048-9697(00)00628-8)
- Guimarães JRD, Mauro JBN, Coelho-Souza SA, Poirier H (2004) Study of methylation sites and factors in contaminated aquatic systems in the Amazon using an optimized radiochemical technique, pp 17-27. In: *Health impact of mercury cycling in contaminated environments studied by nuclear techniques. United Nations IAEA.*
- Hylander LD, Gröhn J, Tropp M, Vikström A, Wolpher H, Silva EC, Meili M,

- Oliveira LJ (2006) Fish mercury increase in Lago Manso, a new hydroelectric reservoir in tropical Brazil. *Journal of Environmental Management*, 81(2):155-166. <https://dx.doi.org/10.1016/j.jenvman.2005.09.025>
- Kasper D, Palermo EFA, Branco CWC, Malm O (2012) Evidence of elevated mercury levels in carnivorous and omnivorous fishes downstream from an Amazon reservoir. *Hydrobiologia*, 694(1):87-98. <https://dx.doi.org/10.1007/s10750-012-1133-x>
- Kasper D, Forsberg BR, Amaral, JHF, Leitão, RP, Py-Daniel SS, Bastos WR, Malm O (2014) Reservoir Stratification Affects Methylmercury Levels in River Water, Plankton, and Fish Downstream from Balbina Hydroelectric Dam, Amazonas, Brazil. *Environ. Sci. Technol*, 48(2):1032–1040. <http://dx.doi.org/10.1021/es4042644>
- Kehrig HA, Malm O, Akagi H, Guimarães JRD, Torres JPM (1998) Methylmercury in Fish and Hair Samples from the Balbina Reservoir, Brazilian Amazon. *Environmental Research*, 77(2):84-90. <https://dx.doi.org/10.1006/enrs.1998.3836>
- Kennedy P, Kennedy H, Papadimitriou S (2005) The effect of acidification on the determination of organic carbon, total nitrogen and their stable isotopic composition in algae and marine sediment. *Rapid Communications In Mass Spectrometry*, 19(8):1063–1068. <https://dx.doi.org/10.1002/rcm.1889>
- Kerin EJ, Gilmour CC, Roden E, Suzuki MT, Coates JD, Mason RP (2006) Mercury Methylation by Dissimilatory Iron-Reducing Bacteria. *Applied and Environmental Microbiology*, 72(12):7919–7921. <https://dx.doi.org/10.1128%2FAEM.01602-06>
- Kim M, Han S, Gieskes J, Deheyn DD (2011) Importance of organic matter lability for monomethylmercury production in sulfate-rich marine sediments. *Science of The Total Environment*, 409(4):778-784. <https://doi.org/10.1016/j.scitotenv.2010.10.050>
- King JK, Kostka JE, Frischer ME, Saunders FM, Jahnke RA (2001) A quantitative relationship that demonstrates mercury methylation rates in marine sediments are based on the community composition and activity of sulfate-reducing bacteria. *Environmental Science and Technology*, 35(12):2491-2496. <http://dx.doi.org/10.1021/es001813q>
- Hsu-Kim H, Eckley CS, Achá D, Feng X, Gilmour CC, Jonsson S, Mitchell CPJ (2018) Challenges and opportunities for managing aquatic mercury pollution in altered landscapes. *Ambio*, 47(2):141-169. <http://dx.doi.org/10.1007/s13280-017-1006-7>
- Lacerda LD, Malm O (2008) Contaminação por mercúrio em ecossistemas aquáticos: uma análise das áreas críticas. *Estudos Avançados*, 22(63):173-190. <http://dx.doi.org/10.1590/S0103-40142008000200011>
- Lacerda LD, Solomons W (1992) Mercúrio na Amazônia: uma bomba relógio química? Rio de Janeiro. CETEM/CNPq 78p.
- Larsen, T (2009) Mercury in Chinese reservoirs. *Environmental Pollution*, 158(1):24-25. <http://dx.doi.org/10.1016/j.envpol.2009.07.026>
- Lechler PJ, Miller JR, Lacerda LD, Vinson D, Bonzongo JC, Lyons WB, Warwick

- JJ (2000) Elevated mercury concentrations in soils, sediments, water and fish of the Madeira River Basin, Brazilian Amazon: a function of natural enrichments? *Sci Tot Environ.* 260(1):87-96.
[https://doi.org/10.1016/S0048-9697\(00\)00543-X](https://doi.org/10.1016/S0048-9697(00)00543-X)
- Leino T, Lodenius M (1995) Human hair mercury levels in Tucuruí Area, State of Para, Brazil. *Science of The Total Environment*, 175(2):119–125.
[https://dx.doi.org/10.1016/0048-9697\(95\)04908-J](https://dx.doi.org/10.1016/0048-9697(95)04908-J)
- Liang L, Bloom, NS, Horvat, M (1994) Simultaneous determination of mercury speciation in biological materials by GC/CVAFS after ethylation and room-temperature precollection. *Chinical Chemistry*, 40(4):602-607.
<http://clinchem.aaccjnls.org/content/40/4/602>
- Ligges U and Mächler M (2003). scatterplot3d - An R Package for Visualizing Multivariate Data. *Journal of Statistical Software* 8(11):1-20.
<http://dx.doi.org/10.18637/jss.v008.i11>
- Malm O, Palermo EFA, Santos HSB, Rebelo MF, Kehrig HA, Oliveira RB, Meire RO, Pinto FN, Moreira LPA, Guimarães JRD, Torres JPM, Pfeiffer WC (2004) Transport and cycling of mercury in Tucuruí reservoir, Amazon, Brazil: 20 years after fulfillment. *RMZ - Materials and Geoenvironment*, 51(1):1195-1198.
- Malm O (2008) Evaluation of the environmental quality and human exposure to contaminants in the drainage basin of the Jamari River (tributary of the Madeira River with various types of anthropic impact. Programa Piloto para Proteção das Florestas Tropicais do Brasil, Phase 2 (PPG-7). Technical Report, in Portuguese.
- Mauro JBM, Guimarães JRD, Melamed R (1999) Aguapé agrava contaminação por mercúrio. *Ciência Hoje*, 25(150):68-71 (In Portuguese).
- Mauro JBN, Guimarães JRD, Melamed R (2001) Mercury Methylation in macrophyte roots of a tropical lake. *Water, Air and Soil Pollution*, 127(1-4):271-280.
<https://doi.org/10.1023/A:1005222902966>
- Meyers PA (1994) Preservation of elemental and isotopic source identification of sedimentary organic matter. *Chemical Geology*, 114(3-4):289–302.
[https://doi.org/10.1016/0009-2541\(94\)90059-0](https://doi.org/10.1016/0009-2541(94)90059-0)
- Miranda MR (2010) Formação de metilmercúrio na bacia do rio Madeira, Rondônia. Rio de Janeiro. PhD Thesis, in Portuguese. Universidade Federal do Rio de Janeiro, Instituto de Biofísica Carlos Chagas Filho UFRJ/IBCCF, 138 p.
- Molisani MM, Rocha R, Machado W, Barreto RC, Lacerda LD (2006). Mercury contents in aquatic macrophytes from two reservoirs in the Paraíba do Sul: Guandú river system, SE Brazil. *Brazilian Journal of Biology*, 66(1):101-107.
<http://dx.doi.org/10.1590/S1519-69842006000100013>
- Muresan B, Cossa D, Richard S, Dominique Y (2008) Monomethylmercury sources in a tropical artificial reservoir. *Applied Geochemistry*, 23(5):1101-1126.
<https://dx.doi.org/10.1016/j.apgeochem.2007.11.006>
- Nascimento AMA, Chartone-Souza E (2003) Operon *mer*: Bacterial resistance to mercury and potential for bioremediation of contaminated environments. *Genetics and Molecular Research*, 2(1):92-101.

- Nascimento EL, Gomes JPO, Carvalho DP, Almeida R, Bastos WR, Miyai KR (2009) Mercúrio na comunidade planctônica do Reservatório da Usina Hidrelétrica de Samuel (RO), Amazônia ocidental. *Geochimica Brasiliensis*, 23(1):101-116 (in portuguese).
- Parks JM, Johns A, Podar M, Bridou R, Hurt RA Jr, Smith SD, Tomanicek SJ, Qian Y, Brown SD, Brandt CC, Palumbo AV, Smith JC, Wall JD, Elias DA, Liang L (2013) The Genetic Basis for Bacterial Mercury Methylation. *Science*, 339(6125):1332-1335. <https://doi.org/10.1126/science.1230667>
- Pestana IA, Bastos WR, Almeida MG, Carvalho DP de, Resende CER, Souza, CMM (2016) Spatial-temporal dynamics and sources of total Hg in a hydroelectric reservoir in the Western Amazon, Brazil. *Environmental Science and Pollution Research*, 23(10):9640-9648. <https://doi.org/10.1007/s11356-016-6185-4>
- Porvari P (1995) Mercury levels of fish in Tucuruí hydroelectric reservoir and in River Mojú in Amazonia, in the state of Pará, Brazil. *Science of The Total Environment*, 175(2):109-117. [https://dx.doi.org/10.1016/0048-9697\(95\)04907-X](https://dx.doi.org/10.1016/0048-9697(95)04907-X)
- Postgate JR (1984) *The sulfate-reducing bacteria*. Cambridge: Cambridge University Press. 224 p.
- Pozebon D, Lima EC, Maia SM, Fachel JMG (2005) Heavy metals contribution of non-aqueous fluids used in offshore oil drilling. *Fuel*, 84(1):53-61. <https://doi.org/10.1016/j.fuel.2004.08.002>
- R Core Team (2018) *R: A language and environment for statistical computing*. R Foundation for Statistical Computing, Vienna, Austria. URL <https://www.R-project.org/>.
- Roulet M, Lucotte M, Canuel R, Farella N, Courcelles M, Guimaraes J, Mergler D, Amorim M (2000) Increase in mercury contamination recorded in lacustrine sediments following deforestation in central Amazon. *Chemical Geology*, 165(3):243-266. [https://doi.org/10.1016/S0009-2541\(99\)00172-2](https://doi.org/10.1016/S0009-2541(99)00172-2)
- Roulet M, Guimarães JRD, Lucotte M (2001) Methylmercury Production and Accumulation in Sediments and Soils of an Amazonian Floodplain – Effect of Seasonal Inundation. *Water, Air, & Soil Pollution*, 128(1-2):41-60. <https://doi.org/10.1023/A:1010379103335>
- Sánchez-Botero JI, Farias ML, Piedade MT, Garcez DS (2003) Ictiofauna associada às macrófitas aquáticas *Eichhornia azurea* (SW.) Kunth. e *Eichhornia crassipes* (Mart.) Solms. no lago Camaleão, Amazônia Central, Brasil. *Acta Scientiarum. Biological Sciences*, 25(2):369-375. <http://dx.doi.org/10.4025/actascibiols.v25i2.2026>
- Santos EJ, Herrmann AB, Frescura VLA, Curtius AJ (2005) Simultaneous determination of As, Hg, Sb, Se and Sn in sediments by slurry sampling axial view inductively coupled plasma optical emission spectrometry using on-line chemical vapor generation with internal standardization. *Journal of Analytical Atomic Spectrometry*, 20(6):538–543. <https://dx.doi.org/10.1039/B502964C>
- SEDAM. Secretaria do Estado de Desenvolvimento Ambiental (2002) *Atlas Geoambiental de Rondônia*. Secretaria de Desenvolvimento Ambiental, Porto Velho (In Portuguese).

- Selin, NE (2009) Global biogeochemical cycling of mercury: A review. *Annual Review of Environment and Resources* 34:43–63. <https://doi.org/10.1146/annurev.enviro.051308.084314>
- Tollefson J (2011) A struggle for power. *Nature*, 479:160-161. <https://dx.doi.org/10.1038/479160a>
- Venables WN, Ripley BD (2002) *Modern Applied Statistics with S*. Fourth Edition. Springer, New York. <https://doi.org/10.1007/978-0-387-21706-2>
- Vishnivetskaya TA, Mosher JJ, Palumbo AV, Yang ZK, Podar M, Brown SD, Brooks SC, Gu B, Southworth GR, Drake MM, Brandt CC, Elias DA (2011). Mercury and Other Heavy Metals Influence Bacterial Community Structure in Contaminated Tennessee Streams. *Applied and Environmental Microbiology*, 77(1):302-311. <https://dx.doi.org/10.1128/AEM.01715-10>

Capítulo 2:

The impact of hydroelectric dams on mercury dynamics in South America: A review

→ Submetido à Revista **Chemosphere** em **17/08/2018**
Qualis-Capes (Área de Biodiversidade, 2014-2016): **A2**
Fator de Impacto (2017): **4.427**
Status: **Publicado** (<https://doi.org/10.1016/j.chemosphere.2018.12.035>)

The impact of hydroelectric dams on mercury dynamics in South America: A review

Inácio Abreu Pestana^{*a}, Lucas Silva Azevedo^a, Wanderley Rodrigues Bastos^b, Cristina Maria Magalhães de Souza^a

^aPrograma de Pós-Graduação em Ecologia e Recursos Naturais, Laboratório de Ciências Ambientais, Centro de Biociências e Biotecnologia, Universidade Estadual do Norte Fluminense Darcy Ribeiro, Av. Alberto Lamego, 2000 – Parque Califórnia – CEP: 28013-602, Campos dos Goytacazes, Rio de Janeiro, Brasil

^bPrograma de Pós-Graduação em Desenvolvimento Regional e Meio Ambiente, Laboratório de Biogeoquímica Ambiental Wolfgang C. Pfeiffer, Universidade Federal de Rondônia, Av. Pres. Dutra, 2967 – Olaria – CEP: 76801-059, Porto Velho, Rondônia, Brasil

Abstract

The increase in global demand for electric energy is reflected in plans to construct numerous hydroelectric dams in South America that can cause chronic ecological impacts if not built and managed correctly. One of the main impacts generated by hydropower dams is the accumulation of Hg chemical species in their reservoir compartments and the downstream transport of these contaminants. Hg circulation in these environments has been studied for 27 years and this review brings a synthesis of the dynamics that are now well established, so that future studies can focus on gaps and inconsistent results in the literature. The topics cover the methylation process of Hg, its transfer along the trophic chain and the impacts downstream from dams. In addition, meta-analyses are used to propose regression models that explain Hg dispersion in environmental compartments of reservoirs, using as predictors morphological, spatial and temporal aspects of these environments.

Keywords: Mercury; Hydroelectric; Methylation; Impacts; Sediment; Fish

1. Introduction

The construction of hydroelectric dams triggers a series of environmental and social impacts, such as loss of native habitat for endemic species and biodiversity (Castello & Macedo, 2016), impaired fish migration (Fearnside, 2001; Hylander et al., 2006), changes in aquatic ecosystems' functioning (Castello & Macedo, 2016), greenhouse gas production (Kemenes et al., 2011), retention of suspended particulate matter (Finer & Jenkins, 2012; Forsberg et al., 2017), and relocation of native communities (Fearnside, 2014a; Fearnside, 2014b).

Hydroelectric dams also modify complex biogeochemical cycles such as those of mercury (Hg), the third-leading pollutant on the priority list of the American Agency for Toxic Substances and Disease Registry (ATSDR, 2017), given its impact on human health. The flooding of areas previously covered with vegetation creates conditions that favor Hg conversion to its most toxic chemical species, methylmercury (MeHg). This Hg methylation associated with biomagnification in the trophic chain is the main reason environmental and health researchers have studied hydroelectric dams, since MeHg exposure causes loss of attention and memory (Rice et al., 2003), cardiovascular problems (Guallar

et al., 2002) and dysfunctions throughout the sympathetic and parasympathetic nervous system (Myers et al., 2004).

The impacts in Hg cycling caused by South American hydroelectric dams have been studied for 27 years, with the first publications dating from the 1990s (Aula et al., 1995; Porvari, 1995). Since then, several approaches have been used to understand Hg dynamics and fate in these environments. Considering the existence of plans to construct 277 new hydroelectric dams in the Amazon basin (Castello & Macedo, 2016) and 10 new hydroelectric dams in Colombia (UPME, 2010), it is necessary to review the knowledge produced over the years so that the outlines and questions of future studies can focus on the divergences and gaps in the literature.

This review presents a synthesis of well-established processes of Hg cycling in South American hydroelectric reservoirs in its first three topics. The fourth topic presents the results of meta-analysis, to propose regression models that explain Hg dispersion in reservoir compartments, using as predictors the morphological, spatial and temporal aspects of these environments. The fifth topic presents suggestions for future studies and alternatives to mitigate the impacts of hydroelectric construction on Hg cycling.

2. Materials and methods

2.1 Studies included

The articles used in this review were selected from the Google Scholar and ScienceDirect databases. The search was conducted in each database using the terms ["mercury" + "reservoir"], ["mercury" + "dam"] and ["mercury" + "hydroelectric"]. In the next step, only articles that contained data on Hg circulation in reservoirs located in South American countries were selected. An additional search was carried out in the reference list of the articles selected in the first step to locate other works, such as theses and articles not indexed in the mentioned databases that could be relevant for this review. All studies used in this review are from 12 different reservoirs, as indicated in **Figure 1**.

2.2 Statistical Analysis

Statistical analyses were performed with the R software (R Core Team, 2018). The regressions in **Figures 2, 4, 5, 6 and 7** were carried out with the mean Hg concentration contained in each selected article. When the data from selected articles were plotted on scatterplots, they were extracted using the *digitize* package (Poisot, 2011). The standard error of each mean, determination coefficient (R^2), p values, and the 95% confidence and prediction intervals (*predict* function, R Core Team, 2018) are indicated in the graphs. The data were transformed, when

necessary, to meet the assumptions of each regression using a maximum likelihood function (*boxcox*, MASS package; Venables and Ripley, 2002).

Figure 3 was constructed combining the mean and standard deviation extracted from each article (Monte Carlo method, Kroese et al., 2014), assuming normal distribution of data reported by the authors and using the *rnorm* function (R Core Team, 2018).

3. Hg methylation in South American hydroelectric reservoirs

The water column of South American hydroelectric reservoirs has been studied by several authors to understand the relationship between depth, oxygenation and MeHg formation (Coquery et al., 2003; Boudou et al., 2005; Muresan et al., 2008; Almeida, 2012; Kasper et al., 2014; Pestana et al., 2019). Among these authors, there is a consensus that Hg methylation is more pronounced at greater depths, mainly due to a decrease in dissolved oxygen, which generates anoxic and reducing conditions in the hypolimnion, basic conditions for microorganisms in the bottom sediment to transfer a methyl group ($-CH_3$) from decomposed organic matter to Hg^{2+} . Sulfate-reducing and iron-reducing bacteria are recognized in the literature as the main microorganisms capable of Hg methylation (King et al., 1999; Benoit et al.,

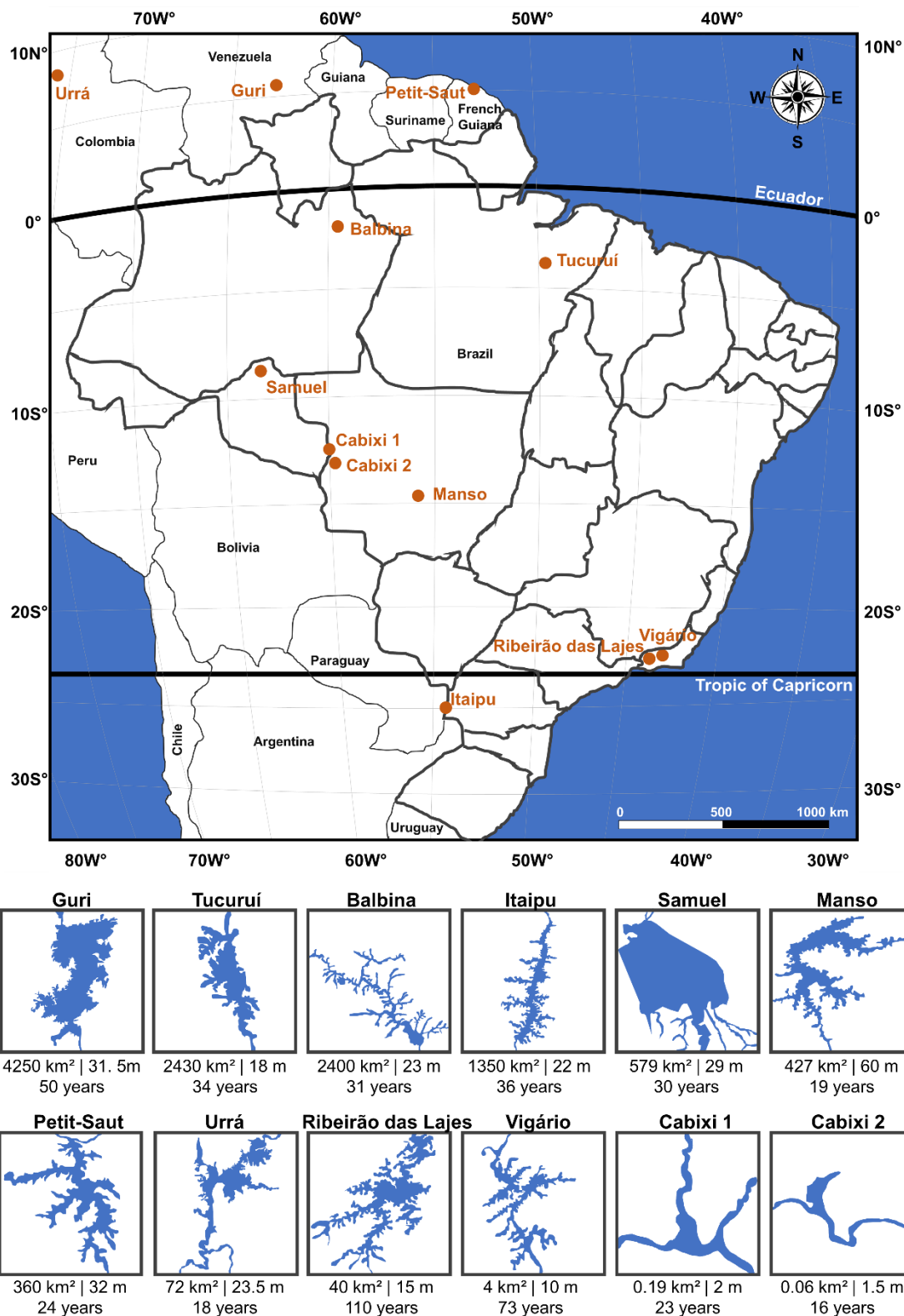


Figure 1 – South American hydroelectric reservoirs that have been studied regarding Hg dynamics. The miniatures show the morphology of the reservoirs (out of scale) and their corresponding area (km²), depth (m) and age after filling (years). The studies for each reservoir are listed in front of their name. **Guri** (Veiga 1996; 1997; Veiga and Hilton, 2001); **Tucuruí** (Aula et al., 1995; Porvari, 1995; Malm et al., 2004; Kehrig et al., 2008; Palermo, 2008; Kehrig et al., 2009); **Balbina** (Kehrig et al., 1998; Kehrig et al., 2008; Kehrig et al., 2009; Forsberg et al., 2013; Kasper et al., 2014); **Itaipu** (Kerkhoff, 2016); **Samuel** (Brasil et al., 2004a; Brasil et al., 2004b; Nascimento et al., 2009; Almeida, 2012; Kasper et al., 2012; Pestana et al., 2016; 2019). **Manso** (Hylander et al., 2006; Tuomola et al., 2008); **Petit-Saut** (Coquery et al., 2003; Durrieu et al., 2005; Boudou et al., 2005; Peretyazhko et al., 2005; Muresan et al., 2008); **Urrá** (Feria et al., 2010; Marrugo-Negrete et al., 2013; Ruiz-Guzmán et al., 2014; Marrugo-Negrete et al., 2015); **Ribeirão das Lajes** (Palermo, 2008); **Vigário** (Palermo, 2008; Kasper et al., 2009); **Cabixi 1** (Cebalho et al., 2017); **Cabixi 2** (Cebalho et al., 2017).

2002; Parks et al., 2013; Si et al., 2015). Muresan et al. (2008), studying the Petit-Saut reservoir (**Figure 1**), observed an increase in H₂S concentrations, a product of sulfate-reduction, just below the oxycline of the water column, confirming the presence and intense activity of these microorganisms in anoxic layers of the lacustrine zone.

Thermal stratification in hydroelectric reservoirs favors Hg methylation and is generally more pronounced during the dry season, particularly in deep reservoirs, since the lack of rainfall associated with thermal stratification limits the water column stirring. Consequently, the oxygenation of hypolimnetic waters is also compromised during this period, which promotes high Hg methylation rates. During the rainy season, the hypolimnion exports the MeHg produced in the bottom sediment to the epilimnion, homogenizing MeHg concentrations in the water column vertically. Consequently, planktonic microorganisms are more exposed to MeHg and this dynamic between dry and rainy seasons favors MeHg circulation between these two environmental compartments (Coquery et al., 2003; Muresan et al., 2008; Nascimento et al., 2009; Kasper et al., 2014).

Oxyclines from Samuel (RO, Brazil), Petit-Saut (French Guiana) and

Balbina (AM, Brazil) reservoirs (**Figure 1**), determined during the dry season, were found at 5, 10 and 15 meters below the water surface (18, 31 and 65% of the mean depth), respectively, showing (1) high biochemical oxygen demand of microorganisms in the bottom sediments and (2) heterogeneity among the reservoirs with respect to the intensity of decomposition of organic matter in sediments (Coquery et al., 2003; Almeida, 2012; Kasper et al., 2014).

Dissolved oxygen and MeHg concentrations in the water column of these three reservoirs could be fitted by a single regression curve, suggesting that the same process occurs in these environments (**Figure 2**). The MeHg concentration ratio between hypolimnion and epilimnion ranged from 10 (Petit-Saut; Coquery et al., 2003) to 15 (Balbina; Kasper et al., 2014).

Almeida (2012), studying the Samuel reservoir (**Figure 1**), observed that in addition to the vertical variation, the MeHg concentration ratio between hypolimnion and epilimnion also varied spatially within the reservoir area. The lowest vertical differences were observed near the dam, due to the recirculation effect of superficial and deep water masses promoted by the turbines, while the largest differences were observed in

the central part of the reservoir, due to the low hydrodynamics.

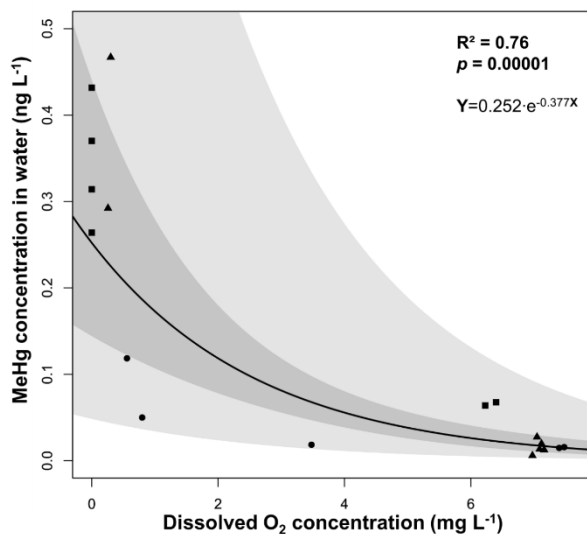


Figure 2 – Relationship between MeHg and dissolved O₂ in the water column of South American reservoirs (N=18). ■ **Petit-Saut** (Coquery et al., 2003 [measured from 0 to 25 cm below surface waters]; Boudou et al., 2005 [measured from 0 to 30 cm below surface waters]); ● **Samuel** (Almeida, 2012 [measured from 0 to 25 cm below surface waters]); ▲ **Balbina** (Kasper et al., 2014 [measured from 0 to 20 cm below surface waters]). The light gray shading identifies the prediction interval of the regression model while the dark gray shading identifies the confidence interval of the model, both calculated with 95% certainty.

Muresan et al. (2008) observed a reasonable positive correlation between chlorophyll *a* and MeHg concentrations in epilimnetic waters of the Petit-Saut reservoir ($R^2 = 0.44$, $p < 0.05$). Although it is frequently reported that this indicates only MeHg accumulation in phytoplankton, this relationship could also be an indication that bacteria from the microbial loop play a role in Hg methylation. Epilimnetic physico-chemical conditions are distant from the deep-water anoxia and reducing characteristics observed in South

American reservoirs, but the close correlation between chlorophyll *a* and MeHg observed at different depths (Muresan et al., 2008) near the water surface could be investigated further to evaluate the possible occurrence of Hg methylation in this oxidizing environment.

4. The impact of damming rivers on Hg concentrations in fish and humans

The effect of damming rivers on the concentration of Hg chemical species in fish is the main question involved in the study of Hg circulation in hydroelectric reservoirs. The frequent examination of this theme is justified by the risk that the ingestion of Hg chemical species poses to human health, especially people living in communities that depend on fish as a primary source of protein, such as those living around Balbina (Kehrig et al., 1998; Forberg et al., 2013; Kasper et al., 2014) and Petit-Saut reservoirs (Boudou et al., 2005).

Hg biomagnification along the trophic chain in South American reservoirs has been extensively investigated by several authors (Porvari, 1995; Kehrig et al., 1998; Malm et al., 2004; Brasil et al., 2004b; Durrieu et al., 2005; Boudou et al., 2005; Kerkhoff, 2016; Hylander et al., 2006; Tuomola et al., 2008; Kasper et al., 2009; Kehrig et al., 2009; Kasper et al., 2012; Cebalho et al., 2017), and there is no divergence in the literature about the

process. The effect of biomagnification on fish depends on the Hg chemical species involved and the feeding habit. Inorganic Hg is absorbed from 10 to 27% in the digestive tract of fish. It has rapid excretion (half-life < 7 months, [Wiener et al., 2002](#)) and generally inorganic Hg concentrations decrease with growth, being diluted by the larger mass of these animals at higher levels of the trophic chain ([Wang & Wong, 2003](#)). On the other hand, MeHg has high absorption rates in the digestive tract (> 90%, [Wiener et al., 2002](#)), its excretion is slow (half-life > 2 years and 9 months; [Wiener et al., 2002](#)) and it is mainly accumulated in the muscles ([Dominique et al., 2007](#); [Kasper et al., 2009](#)), so that biomagnification of MeHg is more prominent compared to inorganic Hg.

Differences in fish feeding habits, widely studied in South American reservoirs ([Porvari, 1995](#); [Kehrig et al., 1998](#); [Malm et al., 2004](#); [Brasil et al., 2004a](#); [Brasil et al., 2004b](#); [Durrieu et al., 2005](#); [Boudou et al., 2005](#); [Kerkhoff, 2016](#); [Hylander et al., 2006](#); [Dominique et al., 2007](#); [Tuomola et al., 2008](#); [Kasper et al., 2009](#); [Kehrig et al., 2009](#); [Kasper et al., 2012](#); [Forberg et al., 2013](#); [Kasper et al., 2014](#); [Cebalho et al., 2017](#)) causes top predatory fish species (carnivorous and piscivorous) to have higher Hg concentrations than the primary consumers, creating a pattern of

increasing concentration: herbivores, detritivores, omnivores, carnivores and piscivores. Some specific studies ([Malm et al., 2004](#); [Kerkhoff, 2016](#)) diverge in this respect: these authors argue that the construction of reservoirs promotes changes in the feeding habits of various species and that this may generate patterns different from those frequently reported. For example, the elevation of the water level caused by the dam may cause a decrease in competition for food among fish species, due to an increase in the foraging area, which in turn may cause the feeding habits of each species to be confined to its central food preferences. In this situation of consumption of specific dietary sources (i.e., non-generalist habits), the Hg concentrations in fish tissues tend to be at more restricted intervals, which may affect the pattern of Hg concentrations among trophic guilds.

[Boudou et al. \(2005\)](#), studying the Petit-Saut reservoir, found similar Hg concentrations in specimens of the same fish species among sample points within the reservoir area and attributed this to the high mobility of these animals. An opposite result was observed by [Porvari \(1995\)](#), studying the Tucuruí reservoir, which suggested that the spatial heterogeneity of Hg concentrations in fish was a consequence of cutting native vegetation at specific points within the reservoir area

during the pre-filling period. In that sense, points where native vegetation clearance did not occur had higher amounts of organic matter and anoxia and promoted Hg methylation and availability more efficiently. It should be noted that the Tucuruí reservoir's surface area is 75% greater than that of Petit-Saut (**Figure 1**), which naturally increases the probability of *in situ* heterogeneity.

The MeHg concentration limit in fish for human consumption (0.5 mg kg^{-1} fresh weight, FAO/WHO, 1991) was exceeded in approximately 80% of the evaluated reservoirs in this review in at least one species of top predatory fish (carnivorous or piscivorous) reported by the authors (Porvari, 1995; Kehrig et al., 1998; Veiga and Hinton, 2001; Malm et al., 2004; Brasil et al., 2004a; Brasil et al., 2004b; Durrieu et al., 2005; Boudou et al., 2005; Hylander et al., 2006; Dominique et al., 2007; Tuomola et al., 2008; Kehrig et al., 2009; Kasper et al., 2012; Forberg et al., 2013; Kasper et al., 2014; Marrugo-Negrete et al., 2015). The mean Hg concentration for top predatory fish from South American reservoirs was also slightly above FAO/WHO (1991) limit (0.53 ± 0.65 ; **Figure 3**). Only two small reservoirs contained fish with MeHg concentrations below the FAO/WHO (1991) limit: Cabixi (Cebalho et al., 2017; 54 specimens, divided into 5 species with 4 distinct eating

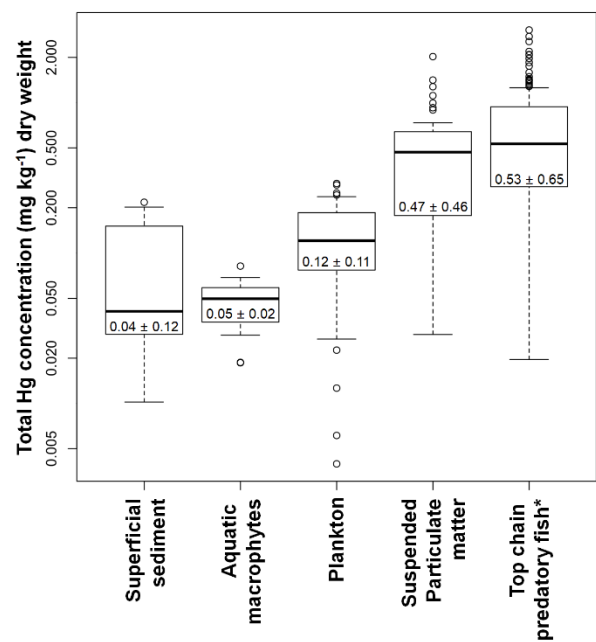


Figure 3 – Total Hg concentrations in biotic and abiotic compartments of South American reservoirs. Values inside each box are median \pm interquartile range. The distances between the y-axis values were log-transformed to optimize the data visualization. **Superficial sediment** (Aula et al., 1995; Malm et al., 2004; Hylander et al., 2006; Palermo, 2008; Marrugo-Negrete et al., 2015; Pestana et al., 2016; Kerkhoff, 2016); **Aquatic macrophytes** (Aula et al., 1995; Pestana et al., 2016); **Plankton** (Malm et al., 2004; Dominique et al., 2007; Palermo, 2008; Nascimento et al., 2009; Almeida, 2012; Kasper et al., 2012; Kasper et al., 2014); **Suspended particulate matter** (Aula et al., 1995; Coquery et al., 2003; Malm et al., 2004; Dominique et al., 2007; Palermo, 2008; Almeida, 2012; Kasper et al., 2012; Kasper et al., 2014; Pestana et al., 2016); **Top-chain predatory fish** (Porvari, 1995; Veiga, 1996; Kehrig et al., 1998; Brasil et al., 2004a; Malm et al., 2004; Hylander et al., 2006; Kehrig et al., 2008; Palermo, 2008; Tuomola et al., 2008; Kehrig et al., 2009; Kasper et al., 2012; Forsberg et al., 2013; Marrugo-Negrete et al., 2013; Kasper et al., 2014; Ruiz-Guzmán et al., 2014; Marrugo-Negrete et al., 2015; Kerkhoff, 2016; Cebalho et al., 2017). *Data based on wet weight.

habits, including carnivore) and Vigário (Kasper et al., 2009; 54 specimens, divided into 12 species with 4 distinct eating habits, including carnivore). This

relationship between reservoir area and Hg accumulation in fish was hypothesized by Kasper et al. (2014) and Cebalho et al. (2017), suggesting that shallower reservoirs have less complex trophic chains (Post et al., 2000), and as a consequence there is lower potential for MeHg biomagnification compared to large hydroelectric reservoirs. In addition, the photodecomposition of MeHg can significantly reduce its bioavailability to biota in shallow reservoirs when compared to large ones (Hammerschmidt & Fitzgerald, 2006). Although a direct relationship between reservoir area and Hg concentration in fish was not observed ($R^2=0.07$; $p=0.17$; Porvari 1995; Kehrig et al., 1998; Brasil et al., 2004b; Malm et al., 2004; Kerkhoff, 2016; Kehrig et al., 2008; Kehrig et al., 2009; Kasper et al., 2009; Kasper et al., 2012; Forsberg et al., 2013; Kasper et al., 2014; Cebalho et al., 2017), the relationship between the mean depth of the reservoir and Hg concentration in top predatory fish (carnivorous or piscivorous) showed a consistent pattern (Figure 4), supporting the hypothesis of Kasper et al. (2014) and Cebalho et al. (2017).

The distribution of Hg chemical species in fish organs has been studied by several researchers (Dominique et al., 2007; Kasper et al., 2009) with the objective of evaluating Hg dynamics

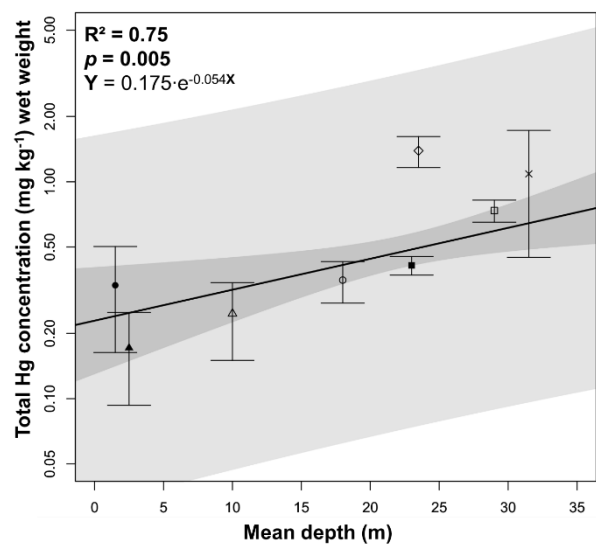


Figure 4 – Relationship between the total Hg concentrations observed in top predatory fish and the mean depth of several tropical reservoirs. Fish length from each study is reported after each reference. ■ **Balbina** (Kehrig et al., 1998 - length not reported; Kehrig et al., 2008 - 34.2 ± 24.6 cm; Kehrig et al., 2009 - 27.0 ± 24.4 ; Forsberg et al., 2013 - length not reported; Kasper et al., 2014 - 27.5 ± 4.9); ● **Cabixi 1** (Cebalho et al., 2017 - 10.5 ± 3.6 cm); ▲ **Cabixi 2** (Cebalho et al., 2017 - 16.14 ± 7.42 cm); ◇ **Urrá** (Ruiz-Guzmán et al., 2014 - 32.2 ± 4.6 ; Marrugo-Negrete et al., 2013 - 24.1 ± 8.1 cm; Marrugo-Negrete et al., 2015 - 24.6 ± 3.8); □ **Samuel** (Brasil et al., 2004b - length not reported; Kasper et al., 2012 - 31.4 ± 5.6); ○ **Tucuruí** (Porvari, 1995 - 38.1 ± 8.5 ; Malm et al., 2004 - length not reported; Kehrig et al., 2008 - 27.5 ± 13.4 cm; Kehrig et al., 2009 - 27.6 ± 25.8); △ **Vigário** (Kasper et al., 2009 - 19.5 ± 3.4 cm); × **Guri** (Veiga, 1996 - length not reported). The light gray shading identifies the prediction interval of the regression model while the dark gray shading identifies the confidence interval of the model, both calculated with 95% certainty. The distances between the y-axis values were log-transformed to optimize the data visualization. Bars represents standard error of mean.

among species with distinct feeding habits in South American reservoirs. The liver and kidneys are the organs with the highest Hg accumulation, although the percentage of MeHg is low due to the

involvement of these organs in detoxification, including MeHg demethylation (Elia et al., 2003). The affinity of gonads with teratogenic compounds, such as MeHg, may negatively influence the offspring and population dynamics of these animals, compromising the integrity of the entire trophic chain of reservoirs (Coquery et al., 2003; Boudou et al., 2005).

A few studies (Leino and Lodenius, 1995; Kehrig et al., 1998; Forsberg et al., 2013) have assessed the final consequence (human physiological responses) of MeHg intake via fish consumption from reservoirs. Leino and Lodenius (1995) correlated MeHg concentrations in the hair of people living near Tucuruí reservoir with the amount of carnivorous fish consumed by them ($R^2 = 0.75$; $p < 0.05$), based on the Hg concentrations reported by Porvari (1995). On the other hand, Kehrig et al. (1998) did not detect a significant correlation between MeHg concentrations present in the hair of Balbina residents with the amount of fish consumed ($R^2 = 0.01$; $p = 0.50$). Kehrig et al. (1998) also did not observe a temporal pattern in the longitudinal Hg determinations in hair.

Forsberg et al. (2013; 2017), also studying Balbina reservoir, showed that the MeHg concentrations in hair samples collected over 20 years after the

construction of the reservoir increased during the first 12 years after filling and then declined, suggesting that MeHg concentration in fish (and consequently in humans that consume them) returns to the pre-filling values in 15 to 20 years. This decrease of MeHg concentrations in fish could be associated with a decrease in Hg methylation rates due to organic matter depletion caused by the microbial community of the bottom sediments, which self-limit the process (Verdon et al., 1991). However, this finding disagrees with our meta-analysis, which evaluated Hg concentration in top predatory fish (carnivorous or piscivorous) from South American reservoirs over time (**Figure 5**), and does not indicate a marked downward trend. Hg concentrations in fish from all reservoirs were adjusted to a regression with slope of 0.169 (gray shading, **Figure 5**), except for Urrá reservoir (Colombia), which was adjusted to a regression with a slope 3.3-fold higher compared to the former (blue shading, **Figure 5**). Fish size is comparable among reservoirs (**Figure 5 caption**), so this does not explain the difference between slopes. On the other hand, there is gold mining in a watershed nearby Urrá reservoir (Marrugo-Negrete et al., 2015) that is associated with high atmospheric Hg concentrations in the area (Marrugo-Negrete et al., 2014), due to the use of Hg in gold mining (Lacerda and Salomons, 1998; Lacerda and Malm,

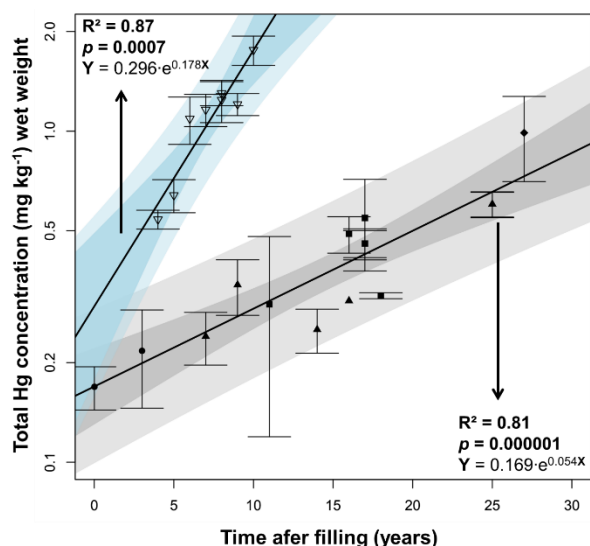


Figure 5 – Time series of Hg concentration determined in muscle of top predatory fish in South American reservoirs. Fish length from each study is reported after each reference. ● **Manso** (Hylander et al., 2006 - 33.3 ± 15.9 cm; Tuomola et al., 2008 - 36.4 ± 26.6 cm); ▲ **Balbina** (Kehrig et al., 1998 - length not reported; Kehrig et al., 2008 - 34.2 ± 24.6 cm; Kehrig et al., 2009 - 27.0 ± 24.4 cm; Forsberg et al., 2013 - length not reported; Kasper et al., 2014 - 27.5 ± 4.9 cm); ■ **Tucuruí** (Porvari, 1995 - 38.1 ± 8.5 cm; Malm et al., 2004 - length not reported; Kehrig et al., 2008 - 27.5 ± 13.4 cm; Kehrig et al., 2009 - 27.6 ± 25.8 cm); ◆ **Guri** (Veiga, 1996 - length not reported); ▽ **Urrá** (Ruiz-Guzmán et al., 2014 - 32.2 ± 4.6 cm; Marrugo-Negrete et al., 2013 - 24.1 ± 8.1 cm; Marrugo-Negrete et al., 2015 - 24.6 ± 3.8 cm). The light gray and blue shading identify the prediction interval of the regression model while the dark gray and blue shading identify the confidence interval of the model, both calculated with 95% certainty. The distances between the y-axis values were log-transformed to optimize the data visualization. Bars represents standard error of mean.

2008), which could explain the differences between the regression slopes. Interestingly, Hg concentrations in fish from Balbina and Tucuruí reservoirs, located in the Amazon region, were adjusted together with the other reservoirs in the lower slope regression (gray shading, **Figure 5**). This is unexpected,

since the Amazon region was historically devastated by the indiscriminate use of Hg in gold mining (Pfeiffer and Lacerda, 1988; Malm et al., 1990; Nriagu et al., 1992), leaving a legacy of 168 tons of Hg⁰ in the region (Lacerda and Salomons, 1998). Also, Amazonian soils are very old (between 500,000 and 1 million years; Johnson, 2003), and this causes the region to have naturally high Hg background concentrations due to the numerous cycles of Hg deposition and evaporation over the years that saturate the soil particles rich in Fe and Al-oxyhydroxides with Hg. (Roulet and Luccote, 1995; Lechler et al., 2000; Fadini and Jardim, 2001; Wasserman et al., 2003). This means that although gold mining partially explains this difference between slopes, other factors such as removal of forest cover through slash-and-burn, conversion the forest cover to pasture and agricultural purposes (Lacerda et al., 2004; Almeida et al., 2005) and the degree of urbanization surrounding these reservoirs must also play a role in Hg circulation between these regions.

It is worth mentioning, however, that the oldest reservoir with a time-series on Hg concentration in top predatory fish (carnivorous or piscivorous) in the literature only goes back 27 years (Veiga, 1996), so new data can modify this

regression line to a curve. In any of these situations, these data (**Figure 5**) reinforce the need for monitoring studies in this environmental compartment with strong impact on human health.

5. The effect of damming on Hg downstream export from reservoirs

In addition to changes reported in Hg circulation and accumulation within hydroelectric reservoir areas, many researchers have reported equally severe impacts downstream from dams over the years (Veiga, 1997; Veiga and Hinton, 2001; Coquery et al., 2003; Malm et al., 2004; Boudou et al., 2005; Hylander et al., 2006; Dominique et al., 2007; Tuomola et al., 2008; Muresan et al., 2008; Feria et al., 2010; Kasper et al., 2012; Kasper et al., 2014; Marrugo-Negrete et al., 2015; Cebalho et al., 2017).

The lacustrine zone near the dam is generally the deepest area of reservoir, due to the need for water retention at a suitable height for the operation of turbines, so this zone is particularly prone to particle sedimentation. Hg concentrations in surface sediments sampled in a transect upstream from the dam were found to be higher near the dam and then to decline abruptly immediately downstream (Malm et al., 2004; Hylander et al., 2006, Palermo, 2008). Correspondingly, there is an increase in Hg concentration in suspended particulate

matter (SPM) downstream, since waters drained by traditional turbines (vertical) to generate electricity come from the hypolimnion of the reservoirs (Malm et al., 2004). Several authors (Coquery et al., 2003; Malm et al., 2004; Boudou et al., 2005; Dominique et al., 2007; Tuomola et al., 2008; Kasper et al., 2012; Kasper et al., 2014) agree that this is the main cause of downstream impacts: the hypolimnion of reservoirs is where the conditions for Hg methylation are favored, causing waters exported downstream to be enriched in MeHg. This can also modify the physio-chemistry of the post-dam watercourse, promoting methylation in these locations. The resuspended particles of the bottom sediment caused by the turbines are responsible for approximately 80% of the total Hg transport downstream from the dam (Coquery et al., 2003; Boudou et al., 2005), and the impacts are higher during the dry season due to water column stratification (Kasper et al., 2014). It is interesting to note that this pattern is not frequent in temperate reservoirs, since the stratification is absent or very small in these regions (Porvari, 1998).

In the dissolved fraction of the water column, Boudou et al. (2005) and Dominique et al. (2007) reported a 10-fold increase in MeHg concentrations downstream from the Petit-Saut reservoir. In both studies the authors argued that the

impact of MeHg on fish occurs indirectly, since the gill absorption of MeHg is negligible (Wiener et al., 2002), so food is the main route of MeHg absorption (Hall et al., 1997). In this sense, the link for MeHg contamination and biomagnification in trophic chains downstream is phytoplankton. These organisms absorb MeHg from the water column and make it bioavailable for fish absorption via feeding. Malm et al. (2004) observed a shift in Hg partitioning from detrital SPM to plankton in an upstream-dam transect sampled within Tucuruí reservoir: while there was a 3-fold increase in Hg concentration in the plankton, there also was a 3-fold decrease associated with detrital SPM.

Increasing Hg concentration in the muscle tissue of fish caught downstream from dams has been reported by several authors, with magnitudes of 3-fold (Petit-Saut, Boudou et al., 2005), 1.5-fold (Manoso, Hylander et al., 2006 and Tuomola et al., 2008), 2.5-fold (Samuel, Malm et al., 2004 and Kasper et al., 2012) and 3.8-fold (Balbina, Kasper et al., 2014) higher compared to Hg concentration in the muscle of fish caught within the respective reservoirs. Highlight should be given to Dominique et al. (2007), studying the Petit-Saut reservoir, who determined Hg concentrations in the top predatory fish downstream and upstream of $3.40 \pm 0.20 \text{ mg kg}^{-1}$ and $0.32 \pm 0.05 \text{ mg kg}^{-1}$ (fresh

weight), representing a 10-fold increase in Hg concentration. In addition to the muscle tissue, downstream enrichment factors were also observed in other fish organs: 2.6-fold for the liver, 6.3-fold for the gills, 9.8-fold for the kidneys (Dominique et al., 2007) and 1.6-fold for the gut (Kasper et al., 2012). Dominique et al. (2007) hypothesized that the increase of Hg concentration in fish tissues downstream can be also a consequence of higher consumption of food by these animals, given the higher need to replace spent energy in swimming in this lotic environment compared to the lentic environment of reservoirs.

Kasper et al. (2014), studying Balbina reservoir, were able to detect Hg concentrations in zooplankton up to 260 km downstream during the rainy season, and observed high concentrations in the zooplankton up to 35 km after the dam during the dry season, compared to the upstream reach. In addition, they also observed an increase of Hg concentration in tissues of top-chain predatory fish up to 180 km downstream from the dam. The authors argued that the flood pulse, characteristic of Amazonian environments during the rainy season, carries organic matter from floodplains adjacent to the reservoir, which favors Hg methylation both upstream and downstream. In this same work, a decrease of dissolved MeHg

concentrations in the surface waters downstream was only observed after 200 km, when oxygenation increased compared to the values determined immediately after the dam. The authors hypothesized that this decrease, besides being influenced by the local reoxygenation (physical O₂ diffusion caused by turbulent flow), is also a result of the dilution effect promoted by the water discharges from the tributaries of the river downstream from the dam.

Cebalho et al. (2017) provided another perspective for impacts observed downstream. Studying Cabixi 1 and 2 reservoirs (**Figure 1**), they observed higher Hg concentrations in fish within the reservoir areas compared to fish downstream. In this sense, they argued that all downstream impacts frequently reported in the literature are strictly for large and deep reservoirs where stratification is recurrent and seasonal, whereas for shallow reservoirs (these two reservoirs have an average depth of 2 m, **Figure 1**), the pattern may be just the opposite.

6. New insights: the temporal and morphological influences of reservoirs on Hg circulation

Evaluations of the influence of morphological parameters of South American reservoirs on Hg dynamics among environmental compartments were

not found in the literature reviewed, probably because of the economic and logistical difficulty of coordinating sampling campaigns in places so distant from each other (**Figure 1**). In addition, time-series assessments are extremely scarce and restricted to fish (Marrugo-Negrete et al., 2015; Forsberg et al., 2017). In this review, we have tried to fill some gaps using meta-analyses in order to provide new insights about the processes that control Hg circulation in these particular environments.

Some authors argue that the time required for Hg concentrations in the environmental compartments of reservoirs to return to pre-filling values is 15 to 20 years (Verdon et al., 1991; Porvari, 1995; Forsberg et al., 2013) or even 30 years (Hylander et al., 2006). These estimates were obtained by studying reservoirs with up to 35 years of filling, and in fact the data collected for the surface sediment over time well fit a quadratic function, indicating a decline in Hg concentrations in approximately 38 years for the expected background value (**Figure 6A**, dashed line in grey; $R^2 = 0.88$, $p = 0.005$). However, by introducing in the analysis data from a reservoir three times older than the average of the previous ones (Ribeirão das Lajes; Palermo, 2008), the assessment changed, so that no decline perspective of Hg concentration in the

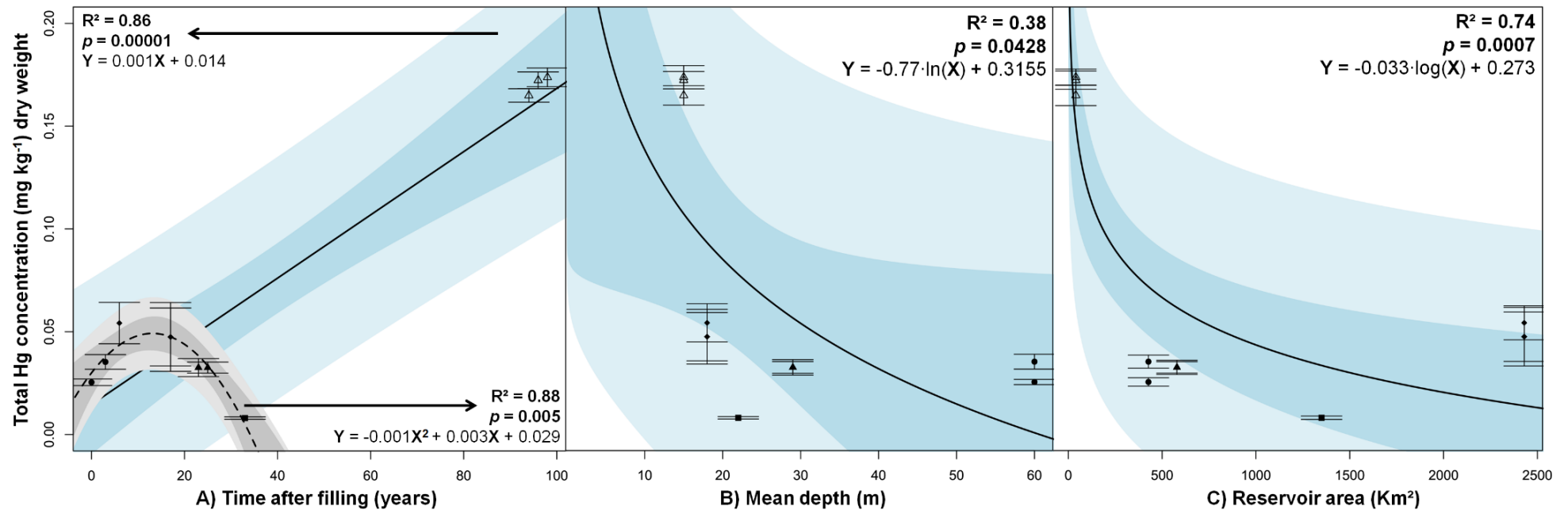


Figure 6 – (A) Relationship between Hg concentration in the surface sediments of South American reservoirs in two scenarios: considering up to 35-year reservoirs (dashed line, gray shading, N = 6) and reservoirs up to 110 years (continuous line, blue shading, N = 9). **(B)** Relationship between Hg concentration in surface sediments and mean depth of South America reservoirs (N=9). **(C)** Relation between Hg concentration in surface sediments and the area of tropical reservoirs (N=9). Δ **Ribeirão das Lajes** (Palermo, 2008); \bullet **Manso** (Hylander et al., 2006); \blacklozenge **Tucuruí** (Aula et al., 1995 e Malm et al., 2004); \blacktriangle **Samuel** (Pestana et al., 2016); \blacksquare **Itaipu** (Kerkhoff, 2016). The light gray and light blue shades identify the prediction interval of the model while the dark gray and dark blue shades identify the confidence interval of the model, both calculated with 95% certainty. Bars represent standard error of mean.

sediments could be noted (**Figure 6A**, solid line in blue, $R^2 = 0.86$, $p = 0.00001$). [Palermo \(2008\)](#) did not report any point sources of Hg contamination in this reservoir, so that we assume the values reported are the result of continuous sedimentation of particles with natural Hg over more than 100 years. This evaluation raises questions about the temporal projections previously made that indicate decline of Hg concentrations in reservoirs and reinforces the need to examine the data carefully to distinguish the noise from the effect in statistical analyses.

We also propose two more regression models to explain Hg accumulation in sediments, considering the mean depth (**Figure 6B**) and reservoir area (**Figure 6C**). These regression models suggest that reservoirs with greater depths (**Figure 6B**) and areas (**Figure 6C**) accumulate less Hg in sediments compared to shallower and smaller reservoirs. Assuming similar Hg concentrations in the SPM for these reservoirs as a source, we expected larger reservoirs to have lower Hg concentrations in sediments due to the larger area for particle deposition in these situations (Hg spatial dilution). Likewise, deeper reservoirs should tend to have lower Hg concentrations in the sediments since the sedimentation of coarse particles (which have low adsorbed Hg) is favored

in detriment to fine particles (with higher adsorbed Hg), which stay suspended in the upper layers of the water column ([Malm et al., 2004](#); [Bengtsson and Picado, 2008](#); [Pestana et al., 2016](#)). Indeed, Hg accumulation in the sediments is mostly a consequence of the retention of the SPM by the lentic environment of the reservoirs: [Forsberg et al. \(2017\)](#) estimated that the construction of the six largest reservoirs planned for the Amazon region in the coming years would be able to retain 64% of all the SPM from the Andean region in its lacustrine region, which would cause severe impacts on benthic organisms.

An exponential increase of Hg concentration in SPM over the years after reservoir filling was observed with no expectation of observable decline (**Figure 7**, $R^2 = 0.40$, $p = 0.06$). The marginal significance of the relationship ($p = 0.06$) is probably associated with the fast cycling characteristic of this environmental compartment, easily influenced by point events that may have occurred during sampling campaigns (**Figure 7**), which increases the regression model's residuals, decreasing the explanatory power (R^2) and significance (p). This increase in Hg concentration in the SPM over time is probably related to the increasing in autochthonous contributions of particles to the water column (resuspension of Hg-rich particles present

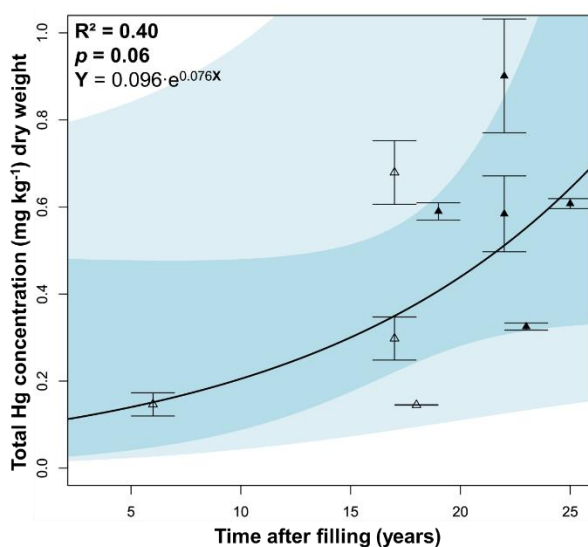


Figure 7 – Time series of Hg concentration in the suspended particulate matter in South American reservoirs ($N=9$). ▲ **Samuel** (Almeida, 2012; Kasper et al., 2012; Pestana et al., 2016); △ **Tucuruí** (Malm et al., 2004; Aula et al., 1995). The light blue shading identifies the prediction interval of the model while the dark blue shading identifies the confidence interval of the model, both calculated with 95% certainty. Bars represents standard error of mean.

in the sediments) rather than the allochthonous contributions (increase of the concentration of Hg in eroded particles of the soils adjacent to the reservoirs), considering the cumulative character of the sediments.

7. Suggestions for future studies on Hg dynamics in South American reservoirs and impact mitigation strategies

The great difficulty of establishing general mechanisms of Hg circulation in South American reservoirs is associated with the lack of representativeness of the various environmental compartments of these ecosystems in the specialized literature (**Supplementary Material 1**). In

order to construct multivariate predictive models, it is necessary to have paired data from the same area of study (e.g., Hg in various environmental compartments of the same reservoir: sediment, fish, SPM, macrophytes), which was not contemplated in the experimental design of most studies reviewed (**Supplementary Material 1**). The basic understanding of Hg dynamics and partitioning among environmental compartments and the seasonal, temporal and morphological circumstances that influence these dynamics is central to assessing risk situations and proposing changes in the way hydroelectric dams are managed in order to avoid long-term ecological damage. In this sense, there should be an effort to reduce the window of approximately 5 ± 3 years between the sampling campaigns and the respective scientific publication, so that the evaluations can be known before the more severe impacts occur in the reservoirs and the communities that depend on this environment economically, including for their subsistence.

In addition, more studies are needed to improve understanding of some points about Hg circulation in tropical reservoirs: (1) the roots of aquatic macrophytes have already been described as microenvironments capable of Hg methylation (Guimarães et al., 2000) with

MeHg/total Hg ratio up to 5.9-fold higher than sediments (Pestana et al., 2019). However, few published studies have evaluated this environmental compartment (Aula et al., 1995; Pestana et al., 2016; Pestana et al., 2019), so little is known about the role played by these aquatic plants in the accumulation and cycling of Hg chemical species in South American reservoirs in terms of mass balance. Besides this, (2) there is an open discussion in the literature (Kehrig et al., 2009; Verburg, 2014; Cebalho et al., 2017) about the influence of the trophic state of a reservoir on the Hg accumulation in the plankton and its impacts on the fish. The most accepted argument is that eutrophic reservoirs promote greater phytoplankton growth, which in turn have lower Hg concentrations due to dilution, considering the greater biomass of phytoplankton. On the other hand, more recent studies (Verburg, 2014; Cebalho et al., 2017) have shown that the evidence for the mentioned process is weak, so more studies of this theme are necessary to improve understanding of the real effects of eutrophication on Hg biomagnification.

As alternatives to mitigate the impacts of hydroelectric on Hg cycling, (1) a greater effort should be made to evaluate the effects of using bulb turbines (horizontal turbines) on Hg mobilization in South American reservoirs. These

horizontal turbines take advantage of the high flow of the rivers and do not require large reservoirs for power generation, which theoretically would reduce thermal and oxygenation stratification of the reservoirs, and as a consequence, Hg methylation. The Santo Antônio and Jirau hydroelectric plants, built on the Madeira River, could be good subjects to evaluate these effects since they use this technology (Carvalho, 2016; Mussy, 2018); (2) the removal of native vegetation before the flooding of a land area decreases the soil organic matter content and, with this, also the Hg methylation rate in sediments and may drastically decrease MeHg biomagnification in these areas (Mailman et al., 2006); (3) In already built hydroelectric dams, aeration of the bottom sediment can be promoted to reduce the abundance of sulfate and iron-reducing bacteria and, therefore, the Hg methylation rates (Mailman et al., 2006).

8. Acknowledgments

Inácio A. Pestana thanks the faculty of the Programa de Pós-Graduação em Ecologia e Recursos Naturais (Laboratório de Ciências Ambientais, Centro de Biociências e Biotecnologia, Universidade Estadual do Norte Fluminense Darcy Ribeiro) for assistance, specifically Prof. Cristina Maria Magalhães de Souza for the comprehensive explanations throughout years on the Hg geochemistry in natural

environments. Wanderley R. Bastos received a grant from Conselho Nacional de Desenvolvimento Científico e Tecnológico (CNPq-Universal-11, no. 476560/2011-0) for studies on Hg cycling in the Samuel reservoir (Porto Velho, RO). This study was also financed in part by Coordenação de Aperfeiçoamento de Pessoa de Nível Superior – Brazil (CAPES) – Finance Code 001. We also thank the reviewers for significantly improving the quality and accuracy of this paper through the valuable comments.

9. References

- Almeida, M.D., Lacerda, L.D., Bastos, W.R., Herrmann, J.C., 2005. Mercury loss from soils following conversion from forest to pasture in Rondônia, Western Amazon, Brazil. *Environmental Pollution* 137, 179-186. <https://doi.org/10.1016/j.envpol.2005.02.026>
- Almeida, R., 2012. Estudo da origem, mobilização e organificação do mercúrio no reservatório da UHE – Samuel, RO. PhD thesis, Universidade Federal do Rio de Janeiro, Centro de Ciências da Saúde Instituto de Biofísica Carlos Chagas Filho, Rio de Janeiro, 117p. (in portuguese)
- ATSDR. Agency for Toxic Substances and Disease Registry, 2017. Substance Priority List, <https://www.atsdr.cdc.gov/spl/index.html>
- Aula, I., Braunschweiler, H., Malin, I., 1995. The watershed flux of mercury examined with indicators in the Tucuruí reservoir in Pará, Brazil. *Science of The Total Environment*, 175(2):97-107. [https://dx.doi.org/10.1016/0048-9697\(95\)04906-1](https://dx.doi.org/10.1016/0048-9697(95)04906-1)
- Bengtsson G., Picado F., 2008. Mercury sorption to sediments: Dependence on grain size, dissolved organic carbon, and suspended bacteria. *Chemosphere*, 73(4):526-531. <https://doi.org/10.1016/j.chemosphere.2008.06.017>
- Benoit, J.M., Gilmour, C.C., Heyes, A., Mason, R.P., Miller, C.L., 2002. Geochemical and biological controls over mercury production and degradation in aquatic systems. *Biogeochemistry of Environmentally Important Trace Elements. ACS Symposium Series 835*, 262–297. <https://dx.doi.org/10.1021/bk-2003-0835.ch019>
- Boudou, A., Maury-Brachet, R., Coquery, M., Durrieu, G., Cossa, D., 2005. Synergic Effect of Gold Mining and Damming on Mercury Contamination in Fish. *Environmental Science & Technology*, 39(8):2448-2454. <https://dx.doi.org/10.1021/es049149r>
- Brasil, D.B., Almeida, R., Nascimento, E.L., Oliveira, R.C., Miyai, R., Bastos, W.R., Silveira, E.G., 2004b. Mercury in Ictiofauna of Smauel Hydroelectric Reservoir, Amazon – Brazil. *RMZ - Materials and Geoenvironment*, 51(1):865-868.
- Brasil, D.B., Oliveira, R.C., Almeida, R., Nascimento, E.L., Miyai, R., Bastos, W.R., Silveira, E.G., 2004a. Historical of Mercury in *Serrasalmus Sp.* Of Samuel Hydroelectric Reservoir, RO – Amazon. *RMZ - Materials and Geoenvironment*, 51(1):864-864.
- Carvalho, D.P. Dinâmica e especiação de mercúrio em compartimentos abióticos na formação do

- reservatório da hidrelétrica Santo Antônio do rio Madeira, RO. 2016. PhD thesis (Instituto de Biofísica Carlos Chagas Filho) Universidade Federal do Rio de Janeiro. Rio de Janeiro. 99p. (in portuguese)
- Castello, L., Macedo, M.N., 2016. Large-scale degradation of the Amazon freshwater ecosystem. *Global Change Biology*, 22(3):990–1007. <https://dx.doi.org/10.1111/gcb.13173>
- Cebalho, E.C., Díez, S., Filho, M.S., Muniz, C.C., Lázaro, W., Malm, O., Ignácio, A.R.A., 2017. Effects of small hydropower plants on Mercury concentrations in fish. *Environmental Science and Pollution Research*, 24(28):22709-22716. <https://dx.doi.org/10.1007/s11356-017-9747-1>
- Coquery, M., Cossa, D., Peretyazhko, T., Azemard, S., Charlet, L., 2003. Methylmercury formation in the anoxic waters of the Petit-Saut reservoir (French Guiana) and its spreading in the adjacent Sinnamary river. *J.Phys. IV France*, 107(1):327-331. <https://dx.doi.org/10.1051/jp4:20030308>
- Dominique, Y., Maury-Brachet, R., Muresan, B., Vigouroux, R., Richard, S., Cossa, D., Mariotti, A., Boudou, A., 2007. Biofilm and mercury availability as key factors for mercury accumulation in fish (*Curimata cyprinoides*) from a disturbed amazonian freshwater system. *Environmental Toxicology and Chemistry*, 26(1):45-52. <https://dx.doi.org/10.1897/05-649R.1>
- Durrieu, G., Maury-Brachet, R., Boudou, A., 2005. Goldmining and mercury contamination of the piscivorous fish *Hoplias aimara* in French Guiana (Amazon basin). *Ecotoxicology and Environmental Safety*, 60(3):351-323. <https://dx.doi.org/10.1016/j.ecoenv.2004.05.004>
- Elia, A. C., Galarini, R., Taticchi, M.I., Dörr, A. J. M., Mantilacci, L., 2003. Antioxidant responses and bioaccumulation in *Ictalurus melas* under mercury exposure. *Ecotoxicology and Environmental Safety*, 55(2):162–167. [https://dx.doi.org/10.1016/S0147-6513\(02\)00123-9](https://dx.doi.org/10.1016/S0147-6513(02)00123-9)
- Fadini PS, Jardim WF. 2001. Is the Negro River Basin (Amazon) impacted by naturally occurring mercury? *Science of The Total Environment*, 275(1-3):71-82. [https://doi.org/10.1016/S0048-9697\(00\)00855-X](https://doi.org/10.1016/S0048-9697(00)00855-X)
- FAO/WHO, 1991. Codex Alimentarius: Guideline Levels for Mercury in Fish (CAC/GL 7-1991). Commission at its Nineteenth Session in Italy 1–10-1991.
- Fearnside, M.P. 2014b. Brazil's Madeira River dams: A setback for environmental policy in Amazonian development. *Water Alternatives* 7(1):256-269.
- Fearnside, P., 2001. Environmental Impacts of Brazil's Tucuruí Dam: Unlearned Lessons for Hydroelectric Development in Amazonia. *Environmental Management*, 27(3):377-396. <https://dx.doi.org/10.1007/s002670010156>
- Fearnside, P., 2014a. Impacts of Brazil's Madeira River Dams: Unlearned lessons for hydroelectric development in Amazonia. *Environmental Science & Policy*, 38(1):164-172. <https://dx.doi.org/10.1016/j.envsci.2013.11.004>
- Feria, J.J., Marrugo, J.L., González, H., 2010. Heavy metals in Sinú river,

- department of Córdoba, Colombia, South America. *Revista Facultad de Ingeniería*, 55:35-44. <http://aprendeenlinea.udea.edu.co/revistas/index.php/ingenieria/article/view/14679>
- Finer, M., Jenkins, C.N., 2012. Proliferation of Hydroelectric Dams in the Andean Amazon and Implications for Andes-Amazon Connectivity. *PLoS ONE*, 7(4):e35126. <https://dx.doi.org/10.1371/journal.pone.0035126>
- Forsberg, B.R., Kasper, D., Peleja, J.R.P., Weisser, S.C., Marshall, B.G., Torres, S.S., 2013. History of mercury contamination in Balbina Reservoir, Central Amazon, Brazil. In: *The 11th International Conference on Mercury as a Global Pollutant*, Edimburgo.
- Forsberg, B.R., Melack, J.M., Dunne, T., Barthem, R.B., Goulding, M., Paiva, R.C.D., Sorribas, M.V., Silva Jr., U.L., Weisser, S., 2017. The potential impact of new Andean dams on Amazon fluvial ecosystems. *PLoS ONE* 12(8): e0182254. <https://dx.doi.org/10.1371/journal.pone.0182254>
- Guallar, E., Sanz-Gallardo, M.I., van't Veer, P., Bode, P., Aro, A., Gomez-Aracena, J., Kark, J.D., Riemersma, R.A., Martin-Moreno, J.M., Kok, F.J., 2002. Mercury, Fish Oils, and the Risk of Myocardial Infarction. *The New England Journal of Medicine*, 347(23):1747-1754. <https://dx.doi.org/10.1056/NEJMoa020157>
- Guimarães, J.R.D., Meil, I. M., Hylander, L.D., Silva, E.C., Roulet, M., Mauro, J.B.N., Lemos, R.A., 2000. Mercury net methylation in five tropical floodplain regions of Brazil: high in the root zone of floating macrophyte mats but low in surface sediments and flooded soils. *The Science of the Total Environment*, 261(1):99-107. [https://dx.doi.org/10.1016/S0048-9697\(00\)00628-8](https://dx.doi.org/10.1016/S0048-9697(00)00628-8)
- Hall, B.D., Bodaly, R.A., Fudge, R.J.P., Rudd, J.W.M., Rosenberg, D.M., 1997. Food as the dominant pathway of methylmercury uptake by fish. *Water, Air, and Soil Pollution*, 100(1):13-24. <https://dx.doi.org/10.1023/A:1018071406537>
- Hammerschmidt, C.R., Fitzgerald, W.F., 2006. Photodecomposition of methylmercury in an arctic Alaskan lake. *Environmental Science & Technology*, 40(4):1212-1216. <https://dx.doi.org/10.1021/es0513234>
- Hylander, L.D., Gröhn, J., Tropp, M., Vikström, A., Wolpher, H., Silva, E.C., Meili, M., Oliveira, L.J., 2006. Fish mercury increase in Lago Manso, a new hydroelectric reservoir in tropical Brazil. *Journal of Environmental Management*, 81(2):155-166. <https://dx.doi.org/10.1016/j.jenvman.2005.09.025>
- Johnson M. 2003. Case Study: Mercury Contamination in the Amazon. Reducing soil erosion may provide a lasting solution. International Development Research Centre. <https://idl-bnc-idrc.dspacedirect.org/handle/10625/52893>
- Kasper, D., Forsberg, B.R., Amaral, J.H.F., Leitão, R.P., Py-Daniel, S.S., Bastos, W.R., Malm, O., 2014. Reservoir Stratification Affects Methylmercury Levels in River Water, Plankton, and Fish Downstream from Balbina Hydroelectric Dam, Amazonas, Brazil. *Environmental Science & Technology*, 48(2):1032-1040. <https://dx.doi.org/10.1021/es4042644>

- Kasper, D., Palermo, E.F.A., Branco, C.W.C., Malm, O., 2012. Evidence of elevated mercury levels in carnivorous and omnivorous fishes downstream from an Amazon reservoir. *Hydrobiologia*, 694(1):87-98.
<https://dx.doi.org/10.1007/s10750-012-1133-x>
- Kasper, D., Palermo, E.F.A., Dias, A.C.M.I., Ferreira, G.L., Leitão, R.P., Branco, C.W.C., Malm, O., 2009. Mercury distribution in different tissues and trophic levels of fish from a tropical reservoir, Brazil. *Neotropical Ichthyology*, 7(4): 751-758.
<http://dx.doi.org/10.1590/S1679-62252009000400025>
- Kehrig, H.A., Howard, B.M., Malm, O., 2008. Methylmercury in a predatory fish (*Cichla* spp.) inhabiting the Brazilian Amazon. *Environmental Pollution*, 154(1):68-76.
<https://dx.doi.org/10.1016/j.envpol.2007.12.038>
- Kehrig, H.A., Malm, O., Akagi, H., Guimarães, J.R.D., Torres, J.P.M., 1998. Methylmercury in Fish and Hair Samples from the Balbina Reservoir, Brazilian Amazon. *Environmental Research*, 77(2):84-90.
<https://dx.doi.org/10.1006/enrs.1998.3836>
- Kehrig, H.A., Palermo, E.F.A., Seixas, T.G., Santos, H.S.B., Malm, O., Akagi, H., 2009. Methyl and total mercury found in two man-made Amazonian Reservoirs. *Journal of the Brazilian Chemical Society*, 20(6):1142-1152.
<http://dx.doi.org/10.1590/S0103-50532009000600021>
- Kemenes, A., Forsberg, B.R., Melack, J.M., 2011. CO₂ emissions from a tropical hydroelectric reservoir (Balbina, Brazil). *Journal of Geophysical Research*, 116(G3):004,
<https://dx.doi.org/10.1029/2010JG001465>
- Kerkhoff, S., 2016. Dinâmica do mercúrio na estrutura do ecossistema do Reservatório da Usina Hidrelétrica de Itaipu. Master's dissertation. Universidade Estadual do Oeste do Paraná, Campos de Toledo, Centro de Engenharias e Ciências Exatas. 85p. (in Portuguese)
- King, J.K., Saunders, F.M., Lee, R.F., Jahnke, R.A., 1999. Coupling mercury methylation rates to sulfate reduction rates in marine sediments. *Environmental Toxicology Chemistry*, 18(7):1362–1369.
<https://dx.doi.org/10.1002/etc.5620180704>
- Kroese, D.P., Brereton, T., Taimre, T., Botev, Z. I., 2014. Why the Monte Carlo method is so important today". *WIREs Comput Stat.* 6, 386–392.
<https://doi.org/10.1002/wics.1314>.
- Lacerda LD, Malm O. 2008. Mercury contamination in aquatic ecosystems: an analysis of the critical areas. *Estudos Avançados*, 22(63): 173-190.
<http://dx.doi.org/10.1590/S0103-40142008000200011>
- Lacerda LD, Salomons W. 1998. Mercury from gold and silver mining. A chemical time bomb? Springer-Verlag Berlin Heidelberg. 147pp.
<https://doi.org/10.1007/978-3-642-58793-1>
- Lacerda, L.D., Souza, M., Ribeiro, M.G., 2004. The effects of land use change on mercury distribution in soils of Alta Floresta, Southern Amazon. *Environmental Pollution* 129, 247-255.
<https://doi.org/10.1016/j.envpol.2003.10.013>

- Lechler, P.J., Miller, J.R., Lacerda, L.D., Vinson, D., Bonzongo, J.C., Lyons, W.B., Warwick, J.J., 2000. Elevated mercury concentrations in soils, sediments, water, and fish of the Madeira River basin, Brazilian Amazon: A function of natural enrichments? *Science of the Total Environment* 260, 87–96. [https://doi.org/10.1016/S0048-9697\(00\)00543-X](https://doi.org/10.1016/S0048-9697(00)00543-X)
- Leino, T., Lodenius, M., 1995. Human hair mercury levels in Tucuruí Area, State of Para, Brazil. *Science of The Total Environment*, 175(2):119–125. [https://dx.doi.org/10.1016/0048-9697\(95\)04908-J](https://dx.doi.org/10.1016/0048-9697(95)04908-J)
- Mailman, M., Stepnuk, L., Cicek, N., Bodaly, R.A.D., 2006. Strategies to lower methyl mercury concentrations in hydroelectric reservoirs and lakes: A review. *Science of The Total Environment* 368, 224-235. <https://doi.org/10.1016/j.scitotenv.2005.09.041>
- Malm O, Pfeiffer WC, Souza CMM, Reuther R. 1990. Mercury pollution due to gold mining in the Madeira river Basin, Amazon/Brazil. *Ambio*, 19(1):11-15.
- Malm, O., Palermo, E.F.A., Santos, H.S.B., Rebelo, M.F., Kehrig, H.A., Oliveira, R.B., Meire, R.O., Pinto, F.N., Moreira, L.P.A., Guimarães, J.R.D., Torres, J.P.M., Pfeiffer, W.C., 2004. Transport and cycling of mercury in Tucuruí reservoir, Amazon, Brazil: 20 years after fulfillment. *RMZ - Materials and Geoenvironment*, 51(1):1195-1198.
- Marrugo-Negrete, J., Navarro-Frómata, A., Ruiz-Guzmán, J., 2015. Total mercury concentrations in fish from Urrá reservoir (Sinú river, Colombia). Six years of monitoring. *Revista MVZ Córdoba*, 20(3):4754-4765. http://www.scielo.org.co/scielo.php?script=sci_arttext&pid=S0122-02682015000300009
- Marrugo-Negrete, J.L., Ruiz-Guzmán, J.A., Díez, S., 2013. Relationship Between Mercury Levels in Hair and Fish Consumption in a Population Living Near a Hydroelectric Tropical Dam. *Biological Trace Element Research*, 151(2):187-194. <https://doi.org/10.1007/s12011-012-9561-z>
- Marrugo-Negrete, J.L., Urango-Cardenas, I.D., Núñez, S.M.B., Díez, S., 2014. Atmospheric deposition of heavy metals in the mining area of the San Jorge river basin, Colombia. *Air Quality, Atmosphere & Health* 7, 577-588. <https://doi.org/10.1007/s11869-014-0260-0>
- Muresan, B., Cossa, D., Richard, S., Dominique, Y., 2008. Methylmercury sources in a tropical artificial reservoir. *Applied Geochemistry*, 23(5): 1101-1126. <https://dx.doi.org/10.1016/j.apgeochem.2007.11.006>
- Mussy, M.H., 2018. Mercúrio em peixes na área de influência da hidrelétrica – Santo Antônio no rio Madeira no pré e pós enchimento. PhD thesis, Universidade Federal do Rio de Janeiro, Centro de Ciências da Saúde Instituto de Biofísica Carlos Chagas Filho, Rio de Janeiro, 129p. (in portuguese).
- Myers, G.J., Davidson, P.W., Weiss, B., 2004. Methyl mercury exposure and poisoning at Niigata, Japan. *Seychelles Medical and Dental Journal*, 7(1):132-133.
- Nascimento, E.L., Gomes, J.P.O., Carvalho, D.P., Ameida, R., Bastos, W.R., Miyai, K.R., 2009. Mercúrio na comunidade planctônica do Reservatório da Usina Hidrelétrica de Samuel (RO), Amazônia

- ocidental. *Geochimica Brasiliensis*, 23(1):101-116. (in portuguese).
- Nriagu JO, Pfeiffer WC, Malm O, Souza CMM, Mierle G. 1992. Mercury pollution in Brazil. *Nature*, 356:389. <https://doi.org/10.1038/356389a0>
- Palermo, E.F.A., 2008. Acúmulo e transporte de mercúrio em reservatórios tropicais. PhD thesis, Universidade Federal do Rio de Janeiro, Centro de Ciências da Saúde Instituto de Biofísica Carlos Chagas Filho, Rio de Janeiro, 96p. (in portuguese).
- Parks, J.M., Johs, A., Podar, M., Bridou, R., Hurt Jr., R.A., Smith, S.D., Tomanicek, S.J., Qian, Y., Brown, S.D., Brandt, C.C., Palumbo, A.V., Smith, J.C., Wall, J.D., Elias, D.A., Liang, L., 2013. The genetic basis for bacterial mercury methylation. *Science* 339 (6125), 1332e1335. <https://doi.org/10.1126/science.1230667>
- Peretyazhko, T., Van Cappellen, P., Meile, C., Coquery, M., Musso, M., Regnier, P., Charlet, L., 2005. Biogeochemistry of Major Redox Elements and Mercury in a Tropical Reservoir Lake (Petit Saut, French Guiana). *Aquatic Geochemistry*, 11(1):33-55. <https://doi.org/10.1007/s10498-004-0752-x>
- Pestana, I.A., Bastos, W.R., Almeida, M.G., Carvalho, D.P., Rezende, C.E., Souza, C.M.M., 2016. Spatial-temporal dynamics and sources of total Hg in a hydroelectric reservoir in the Western Amazon, Brazil. *Environmental Science and Pollution Research*, 23(10):9640-9648. <https://dx.doi.org/10.1007/s11356-016-6185-4>
- Pestana, I.A., Bastos, W.R., Almeida, M.G., Mussy, M.H., Souza, C.M.M., 2019. Methylmercury in environmental compartments of a hydroelectric reservoir in the Western Amazon, Brazil. *Chemosphere* 215, 758–765. <https://doi.org/10.1016/j.chemosphere.2018.10.106>
- Pfeiffer WC, Lacerda LD. 1988. Mercury inputs into the Amazon region, Brazil. *Environmental Technology Letters*, 9(4):325-330. <https://doi.org/10.1080/09593338809384573>
- Poisot, T., 2011. The digitize package: extracting numerical data from scatterplots. *The R Journal* 3, 25–26.
- Porvari, P., 1995. Mercury levels of fish in Tucuruí hydroelectric reservoir and in River Mojú in Amazonia, in the state of Pará, Brazil. *Science of The Total Environment*, 175(2):109-117. [https://dx.doi.org/10.1016/0048-9697\(95\)04907-X](https://dx.doi.org/10.1016/0048-9697(95)04907-X)
- Porvari, P., 1998. Development of fish mercury concentrations in Finnish reservoirs from 1979 to 1994. *Science of The Total Environment*, 213(1): 279–290. [https://dx.doi.org/10.1016/S0048-9697\(98\)00101-6](https://dx.doi.org/10.1016/S0048-9697(98)00101-6)
- Post, D.M, Pace, M.L., Hairston Jr, N.G. 2000. Ecosystem size determines food-chain length in lakes. *Nature*, 405:1047-1049. <https://doi.org/10.1038/35016565>
- R Core Team, 2018. R: A language and environment for statistical computing. R Foundation for Statistical Computing, Vienna, Austria. URL <http://www.R-project.org/>.
- Rice, D.C., Schoeny, R., Mahaffey, K., 2003. Methods and Rationale for Derivation of a Reference Dose for Methylmercury by the U.S. EPA. *Risk Analysis: An International Journal*, 23(1):107-115.

<https://dx.doi.org/10.1111/1539-6924.00294>

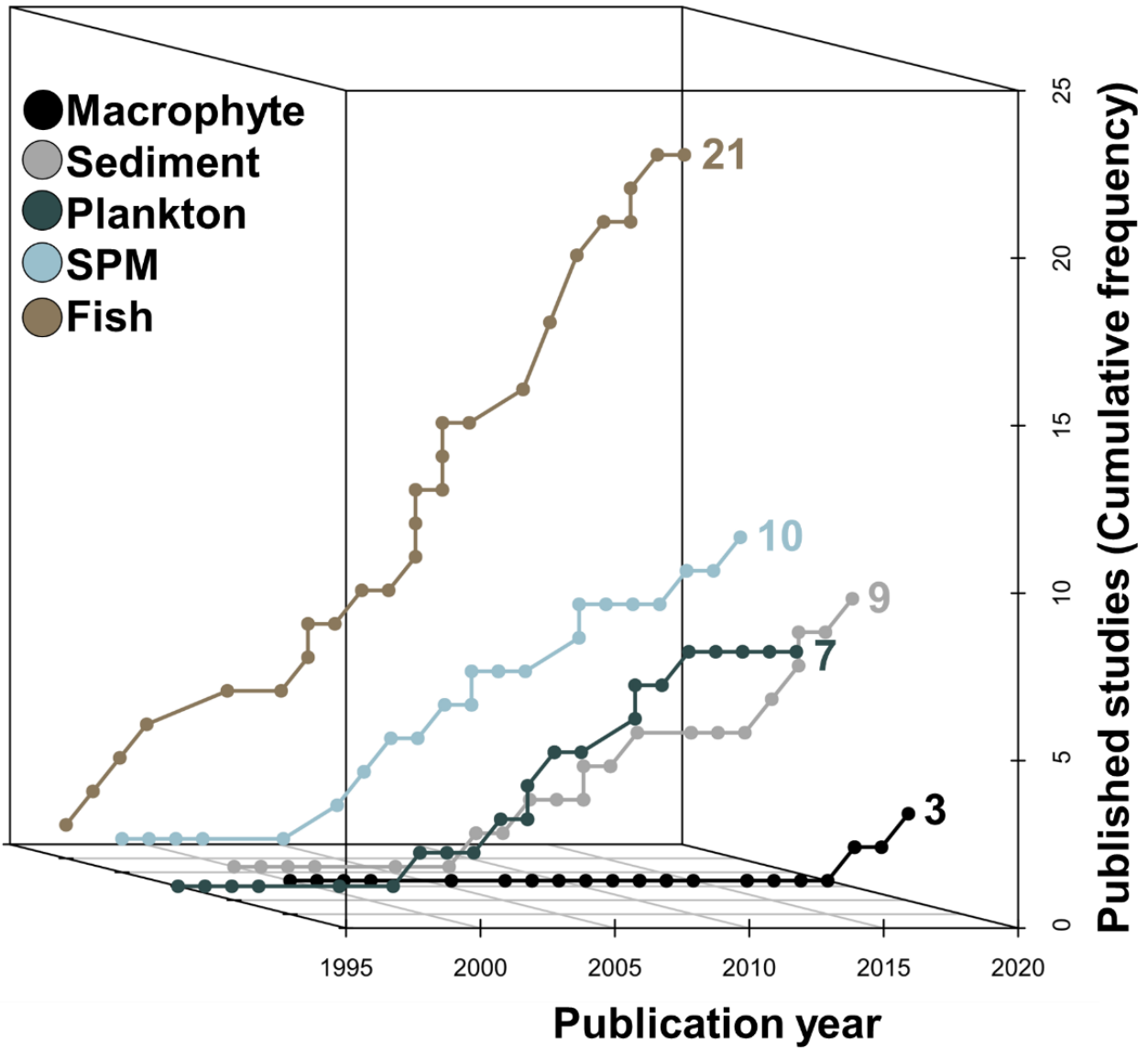
- Roulet M, Lucotte M. 1995. Geochemistry of mercury in pristine and flooded ferralitic soils of a tropical rain forest in French Guiana, South America. *Water, Air, and Soil Pollution*, 80(1-4):1079-1088.
<https://doi.org/10.1007/BF01189768>
- Ruiz-Guzmán, J.A., Marrugo-Negrete, J.L., Díez, S., 2014. Human Exposure to Mercury Through Fish Consumption: Risk Assessment of Riverside Inhabitants of the Urrá Reservoir, Colombia. *Human and Ecological Risk Assessment*, 20(5):1151-116.
<https://doi.org/10.1080/10807039.2013.862068>
- Si, Y., Zou, Y., Liu, X., Si, X., Mao, J., 2015. Mercury methylation coupled to iron reduction by dissimilatory iron-reducing bacteria. *Chemosphere* 122, 206–212.
<https://doi.org/10.1016/j.chemosphere.2014.11.054>
- Tuomola, L., Niklasson, T., Silva, E.C., Hylander, L.D., 2008. Fish mercury development in relation to abiotic characteristics and carbon sources in a six-year-old, Brazilian reservoir. *Science of The Total Environment*, 390(1):177-187.
<https://dx.doi.org/10.1016/j.scitotenv.2007.09.030>
- UPME. Unidad de planeación minero energética, 2010. Plan de expansión de referencia generación–transmisión 2010–2024. Bogotá, DC, Colombia.
- Veiga, M.M., 1996. Advisory assistance on avoidance mercury pollution from artisanal gold mining operations in Bolivar State, Venezuela. Report to UNIDO.
<https://iwlearn.net/resolveuid/795d117ae0aeb4a308c266549397a4b6>
- Veiga, M.M., 1997. Mercury in Artisanal Gold Mining in Latin America: Facts, Fantasies and Solutions. UNIDO Expert Group Meeting, Vienna.
https://unites.uqam.ca/gmf/globalmercuryforum/files/articles/marcello_veiga/veiga_1997_02.pdf
- Veiga, M.M., Hinton, J., 2001. Mercury Bioaccumulation by Aquatic Biota in Hydroelectric Reservoirs: Review and Consideration of the Mechanisms. 1st International Forum on Mercury Problem in Hydroelectric Reservoirs: The Guri Case, Bolivar State, Venezuela, Org. IAMOT/UNEG.
<https://iwlearn.net/resolveuid/06d6e05bb013d4f06198cacd3d501294>
- Venables, W.N., Ripley, B.D., 2002. *Modern Applied Statistics with S*, fourth ed. Springer, New York
<https://doi.org/10.1007/978-0-387-21706-2>.
- Verburg, P., 2014. Lack of evidence for lower mercury biomagnification by biomass dilution in more productive lakes: comment on mercury biomagnification through food webs is affected by physical and chemical characteristics of lakes. *Environmental Science & Technology*, 48(17):10524-10525.
<https://dx.doi.org/10.1021/es405415c>
- Verdon, R., Brouard, D., Demers, C., Lalumiere, R., Laperle, M., Shetagne, R., 1991. Mercury evolution (1978–1988) in fishes of the La Grande hydroelectric complex, Quebec, Canada. *Water Air & Soil Pollution*, 56(1):405-417.
<https://doi.org/10.1007/BF00342287>
- Wang, W.X., Wong, R.S.K., 2003. Bioaccumulation kinetics and exposure pathways of inorganic mercury and methylmercury in a marine fish, the sweetlips *Plectorhinchus gibbosus*. *Marine*

Ecology Progress Series, 261: 257-268.

Wasserman JC, Hacon S, Wasserman MA. 2003. Biogeochemistry of Mercury in the Amazonian Environment. *Ambio*, 32(5):336-342. <https://doi.org/10.1579/0044-7447-32.5.336>

Wiener, J.G., Krabbenhoft, D.P., Heinz, G.H., Scheuhammer, A.M., 2002. Ecotoxicology of mercury. Em: Hoffman, D.J., Rattner, B.A., Burton, G.A., Cairns, J. (Eds.), *Handbook of Ecotoxicology*. CRC Press, Boca Raton, EUA, pp. 409–463

Supplementary Material 1



Caption – Cumulative frequency of published studies on Hg cycling in South American reservoirs by environmental compartment ($N=27$). Few studies have paired data from biotic and abiotic compartments, which makes it difficult to construct multivariate predictive models.

Capítulo 3:

Total Hg and methylmercury dynamics in a river-floodplain system in the Western Amazon: influence of seasonality, organic matter, and physical and chemical parameters

→ Submetido à Revista **Science of the Total Environment** em **25/09/2018**
Qualis-Capes (Área de Biodiversidade, 2014-2016): **A2**
Fator de Impacto (2017): **4.610**
Status: **Publicado** (<https://doi.org/10.1016/j.scitotenv.2018.11.388>)

Total Hg and methylmercury dynamics in a river-floodplain system in the Western Amazon: influence of seasonality, organic matter, and physical and chemical parameters

Inacio A Pestana^{*a}, Marcelo G Almeida^a, Wanderley R Bastos^b & Cristina MM Souza^a

^aPrograma de Pós-Graduação em Ecologia e Recursos Naturais, Laboratório de Ciências Ambientais, Centro de Biociências e Biotecnologia, Universidade Estadual do Norte Fluminense Darcy Ribeiro, Av. Alberto Lamego, 2000 – Parque Califórnia – CEP: 28013-602, Campos dos Goytacazes, Rio de Janeiro, Brasil

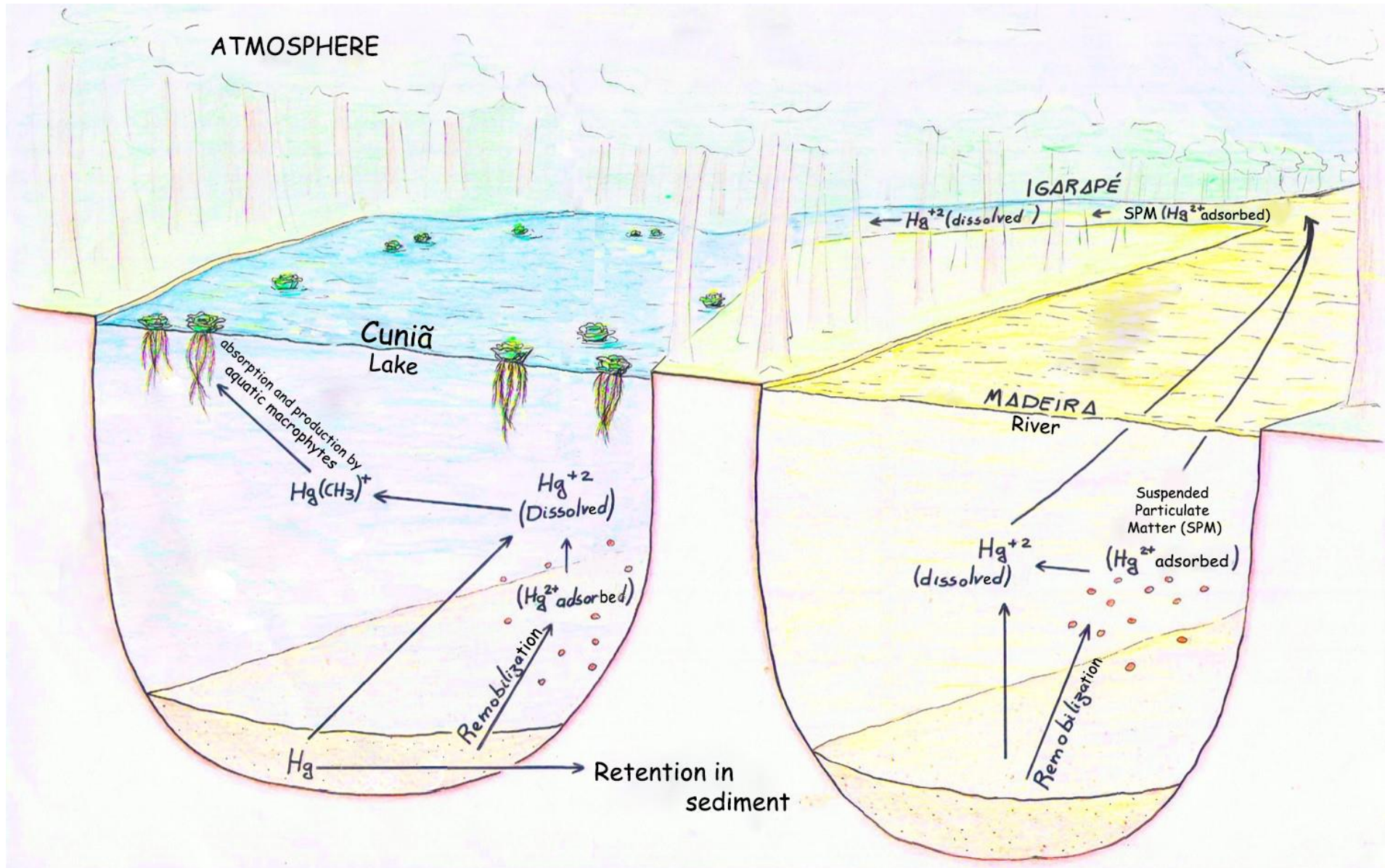
^bPrograma de Pós-Graduação em Desenvolvimento Regional e Meio Ambiente, Laboratório de Biogeoquímica Ambiental Wolfgang C. Pfeiffer, Universidade Federal de Rondônia, Av. Pres. Dutra, 2967 – Olaria – CEP: 76801-059, Porto Velho, Rondônia, Brasil

Abstract

Total mercury (Hg) and methylmercury (MeHg) circulation in a connected river-floodplain system composed of two black water (a small forest river, *igarapé*, and Cuniã Lake) and a white water body (Madeira River), located in the Madeira River Basin were evaluated during the rising-water, early and late falling-water periods. We assessed organic matter (C and N composition, (C:N)_a; and $\delta^{13}\text{C}$ isotopic signature), and physical and chemical influences (pH, dissolved O₂, electric conductivity) in relationship to Hg and MeHg concentrations. Hg and MeHg concentrations in a sediment profile and three aquatic macrophytes (*E. crassipes*, *E. azuera* and *Oryza* sp.) were measured. *Igarapé* and Cuniã Lake showed higher Hg and MeHg concentrations (115 – 709; 10 – 25 ng g⁻¹) in the suspended particulate matter compared (SPM) compared to the Madeira River (Hg: 5 – 16; MeHg: 0.2 – 0.3 ng g⁻¹), partially independent of seasonality ($p = 0.06$). Total Hg had higher affinity for the SPM (1.75 times) than for dissolved organic matter. Organic matter characteristics correlated with MeHg concentrations ($\delta^{13}\text{C}$ and (C:N)_a; $r^2 = 0.79$; $p < 0.0001$), as well as physical and chemical parameters of the water column (dissolved O₂ and pH; $r^2 = 0.80$; $p < 0.0001$), demonstrating that physical and chemical changes between the river-floodplain system affect MeHg circulation and production. The inverse correlation of MeHg and SO₄²⁻ concentrations ($r^2 = 0.73$; $p < 0.0001$) suggests the action of sulfate-reducing bacteria. Total Hg and MeHg concentrations as well as %MeHg were detected in the sediment profile (Hg: 24 – 51; MeHg: 0.6 – 3.2 ng g⁻¹; %MeHg: 1.8 – 6.2) and aquatic macrophytes (Hg: 1 – 30; MeHg: 0.3 – 7.5 ng g⁻¹; %MeHg: 1.6 – 33.7). We conclude that the highest Hg and MeHg concentrations in Cuniã Lake, compared to the Madeira River, are due to the physical and chemical differences between these environments.

Keywords: Hg; floodplain; stable isotopes; organic matter; methylation; Amazon

Graphical Abstract



1. Introduction

Alluvial floodplains, which occur widely in the Amazon region, play an important role in the Hg biogeochemical cycle (Maia et al., 2009; Maia et al., 2017; Brito et al., 2017). They exchange water with the large rivers to which they are connected to some extent all year and, specifically during the rising-water and the falling-water periods. Floodplains act as a major sink and source of water to the main rivers, which promotes physical and chemical modifications (Sioli, 1967; Bittencourt and Amadio, 2007). These modifications directly affect Hg methylation, and Hg and MeHg partitioning between the particulate and dissolved fractions of the water column (Maurice-Bourgoin et al., 2007; Maia et al., 2009).

Some floodplains form lakes characterized by high primary production, estimated at $10\text{tC hec}^{-1}\text{ year}^{-1}$, of which 73% is related to phytoplankton and aquatic macrophytes and the remaining 27% is related to the adjacent flooded forest (Junk and Furch, 1985). This creates a difference in the organic matter concentration between these lakes and the rivers to which they are connected. During the low-water period, the lower connectivity between these environments and their hydrodynamic differences partially limits the autochthonous

processes of lakes to be diluted by allochthonous entries from rivers, allowing a maximum physical and chemical parameters amplitude between these two environments (Junk, 1989; Lacerda et al., 1989; Richey et al., 2002).

Sioli (1967) classified the Amazonian water bodies into large groups based on their color, e.g. clear, white and black-water bodies. White water rivers, like Madeira and Solimões, have neutral pH and high concentrations of ions and suspended particulate matter (SPM), eroded from the Andean region. Black water rivers, like the Negro and some *igarapés* (small streams, especially those surrounding by forest), drain areas that already have very eroded soils and are characterized by high concentrations of dissolved organic carbon, low content of ions and SPM and slightly acid pH (Junk and Furch, 1985). Moreira-Turcq et al. (2003), studied the mixture of waters at the Negro and Solimões confluence (also studied by Kasper et al., 2017), verified large adsorption of the dissolved organic matter from the Negro River on the SPM present in the Solimões River. They verified that approximately 40% of the organic matter can be removed from the dissolved fraction through this process and that the SPM, now possessing organic and inorganic binding sites, easily adsorbs and transports Hg, as already reported in

the literature (Bezerra et al., 2009). Hg mobility can be influenced by: (1) the association of organic matter with the SPM that can be deposited and immobilize Hg, or (2) the formation of stable Hg complexes with organic matter in the dissolved fraction, which increases the availability of the contaminant to the biota (Bäckström et al., 2003; Hammerschmidt et al., 2004).

Given the close relationship between organic matter and Hg, several authors have used the elemental and isotopic signatures of C and N as proxies to identify the contribution of different sources of the contaminant to aquatic ecosystems (Campbell et al., 2006; Stewart et al., 2008; Cremona et al., 2009; Jara-Marini et al., 2012). These sources can be divided into five: two allochthonous sources (debris from land plants and soils); two autochthonous sources (debris from the decomposition of aquatic macrophytes and algae), and a last source formed by bacteria and fungi, whose characteristics are linked to the mixture of the first two groups (Sulzman, 2007; Martinelli et al., 2003). The isotopic signature of ^{13}C ($\delta^{13}\text{C}$) in the SPM of a black water river (Negro River) is lighter than the signature of a white-water river (Madeira River), due to the different types of soils they drain and the autotrophic – heterotrophic dynamics occurring in their

respective water columns. In the same sense, the atomic and elemental ratio between carbon and nitrogen (abbreviated by $(\text{C:N})_a$) exhibited higher values in the Negro River compared to the Madeira and Tapajós rivers, suggesting that the organic matter of black water rivers is composed of debris of vascular terrestrial plants (Hedges et al., 1986; 1994; Pinheiro et al., 2014). On the other hand, the low $(\text{C:N})_a$ ratio found in white water rivers and clear water rivers (rivers with low amounts of SPM, conductivity between 10 and 20 $\mu\text{S cm}^{-1}$, greenish waters and pH between 6 and 7; Sioli, 1967) may be a reflection of the microbial biomass, like phytoplankton and bacteria (Devol and Hedges, 2001).

Organic matter produced in floodplains by phytoplankton and aquatic macrophytes are mostly labile (i.e. low $(\text{C:N})_a$ ratio; Junk and Furch, 1985; Quay et al., 1992) and, therefore, play an important role in the formation of methylmercury (CH_3Hg^+ , abbreviated by MeHg), a toxic chemical species of Hg. Quay et al. (1992) estimated that 40% of dissolved organic carbon present in the Amazon River is produced in floodplain lakes. The decomposition of organic matter generates an acidic, anoxic and reducing environment, and under these conditions some bacteria, such as sulfate-reducing bacteria, add a methyl group to Hg (King et al., 1999; Benoit et al., 2002).

MeHg can be absorbed directly from water (by aquatic macrophytes and plankton) and in the digestive tract of other animals that feed on organisms containing MeHg (Wiener et al., 2002). Guimarães et al. (2000) reported a 30-fold higher Hg methylation potential in the periphyton associated with aquatic macrophyte roots than in the underlying sediments. In floodplains, these plants represent approximately 60% of the total carbon production of the ecosystem, functioning as an important link for MeHg transfer to the trophic chain (Mauro et al., 1999).

Hg dynamics associated with the mixture of black and white waters are best studied at a small scale, since many Amazonian systems have a connection between rivers and floodplains (Junk, 1989; Gadel et al., 2000; Bonnet et al., 2008). These smaller systems have advantages as study models, since (1) they are present throughout the Amazon region; (2) they are more accessible for field studies and, (3) because they have different connectivity levels with the main rivers during the hydrological periods of the region, they make it possible to evaluate the influence of seasonality on Hg dynamics (Sioli, 1967; Lacerda et al., 1989; SEDAM, 2012).

In this sense, the aim of this study was to evaluate total Hg and MeHg circulation in the water column of black

water (*igarapés* and Cuniã Lake) and white water bodies (Madeira River) along three hydrological periods characteristic of the region, accessing the influence of organic matter, and physical and chemical parameters differences in the Hg and MeHg associations. Our hypotheses were (1) the highest total Hg concentrations in the SPM from floodplain ecosystems (*igarapé* and Cuniã Lake) will be observed during the rising-water period, since erosion of particles from both Madeira River and the soil adjacent to the Cuniã *igarapé* is favored when the water levels of the river are high and (2) MeHg concentrations will be higher during the late falling-water period, when the influence of the Madeira River in the floodplain is smaller, due to its lower water level, and intense organic matter decomposition, generating physical and chemical conditions that favors Hg methylation.

2. Materials and Methods

2.1 Study area

Cuniã Lake (**Figure 1**) has a large and still conserved area, estimated at 180 km², representing about 1/3 of the total area of the extractive reserve of Cuniã Lake, and its water mostly comes from the Cuniã *Igarapé* (**Figure 1**), which connects the lake to the Madeira River (**Figure 1**). Other smaller *igarapés* next to sample point *Lake3* (**Figure 1**) and runoff also

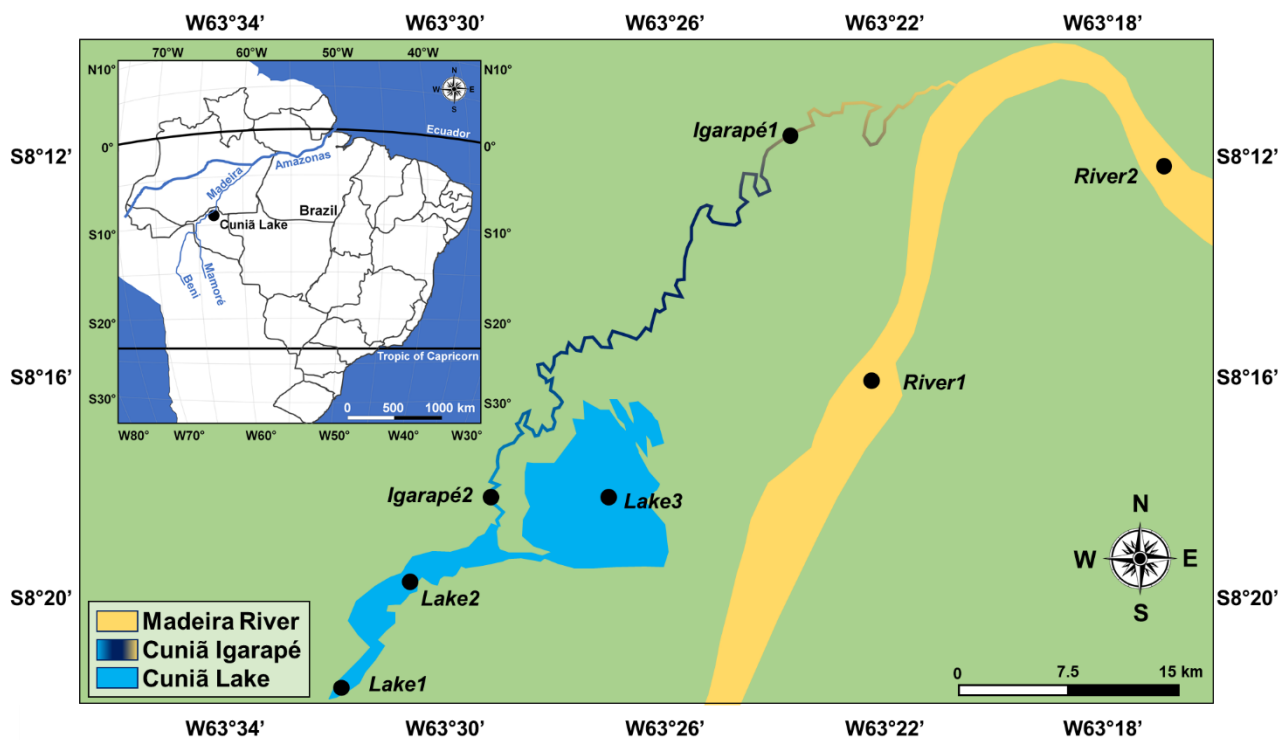


Figure 1 – Map of the river-igarapé-lake system studied and its location within Brazil (miniature). The filled circles indicate two sampling points along the Madeira River (River1, River2), two sampling points along Cuniã Igarapé (Igarapé1, Igarapé2) and three sampling points in Cuniã Lake (Lake1, Lake2, Lake3). The physical and chemical parameters are detailed in **Supplementary Material 2**. The colors illustrate the mixing of the Madeira River waters in Cuniã Igarapé with progressive sedimentation of particles along its winding path of approximately 37 km. Madeira River water flow is from south to north.

contribute as water sources to Cuniã Lake during the region's rainy season (INMET, 2018; **Supplementary Material 1**). The maximum and minimum depth recorded during the sampling campaigns was 11 and 6 meters during the rising-water and late falling-water period, respectively (**Supplementary Material 2**). The reserve is located 150 km from the city of Porto Velho in the state of Rondônia (Brazil). The geomorphology consists of alluvial plains surrounded by fluvial terraces, whose altitudes do not exceed 100 m. The area has soil types that typically occur in regions with excess water (seasonal or permanent), but with precarious drainage

and a marked O₂ deficit, which usually restricts plant growth. These soils contain excess iron hydroxide, as a consequence of the state of almost permanent reduction, which impairs the growth of species that are flood-intolerant (ICMBIO, 2008).

Igarapés are small streams typical of the Amazon region. They can connect large rivers, such as the Madeira River, with its respective floodplain and its associated lakes. Cuniã *Igarapé* is a small black water stream enclosed by forest that has a winding path of 37 km (**Figure 1**) with maximum and minimum depth of 13 and 12 meters recorded during the rising-

water and late falling-water period, respectively (**Supplementary Material 2**) and maximum width of 120 meters. During the low-water period water stagnates in the most central portion, although the connection with the Madeira River is maintained. Autochthonous production directly increases the organic matter concentration in the watercourse, promotes changes soil and sediment characteristics through the action of litter decomposition, facilitating the cation exchange processes in disaggregated particles. The environment has pH variation from 4.7 to 6.0 that promotes Hg mobility between SPM and the dissolved phase of the water column. In addition, the seasonal flood pulse of the Madeira River results in input to *igarapés* a large mass of detrital SPM (transport capacity: ~ 4.108 tSPM year⁻¹) and disaggregated particles from adjacent flooded soils of the *igarapés*, rich in biological material, carrying them to the lake (Sioli, 1967; Junk and Furch, 1985; Santos and Ribeiro, 1988; ICMBIO, 2008).

The Madeira River (**Figure 1**) was severely impacted by Hg due to gold mining activity in the 1980s, and in addition, soils have naturally high Hg concentrations (Lacerda et al., 1989; Roulet and Luccote, 1995). Hg impacts on fish and riverine population continues to be detected until the present day (Bastos et

al., 2006; Arrifano et al., 2018a; 2018b) suggesting that Hg circulation in the region is currently due mainly to natural processes that continue to create risks for the local population, specially the riverine population, as reported by Arrifano et al. (2018a; 2018b). The Madeira River is considered the second largest river of the Amazon, with 1460 km extension. This river has a drainage area of 1420000 km², annual average flow between 23000 and 31200 m³ s⁻¹ and precipitation of 1940 mm year⁻¹. Its width varies between 0.44 and 10km and its hydrochemistry is controlled by erosion from the Andean region (Sioli, 1967; Goulding, 1979; Ayres, 2004). It is classified as a white water river, with high concentration of SPM, pH close to neutral and visibility between 0.1 and 0.5 m (Sioli, 1967). The total annual discharge of the Madeira River in Porto Velho was estimated at 600 billion m³ year⁻¹ (SEDAM, 2012). The latosols can be observed in approximately 58% of the watershed (SEDAM, 2012).

2.2 Sampling

Sampling was carried out in the early falling-water, rising-water and late falling-water hydrological periods (May 2012, February 2013 and June 2013, respectively; **Supplementary Material 1**). Two sample points in the Madeira River (*Madeira1*, *Madeira2*, **Figure 1**), two sample points in the Cuniã *Igarapé*

(*Igarape1*, *Igarape2*, **Figure 1**) and three sample points in Cuniã Lake were considered (*Lake1*, *Lake2*, *Lake3*, **Figure 1**). At each point, 6 L of water was sampled, integrating the water column vertically with a Van Dorn bottle, and stored in pre-rinsed polyethylene bottles with water from the same sampled point. Before integrating the water column, its maximum depth was measured (**Supplementary Material 2**). Then, 6 L of water were sampled: 2 L just above the maximum depth, avoiding sediment resuspension, 2 L at the average depth, and 2 L in the surface layer of the water column.

A sediment profile was sampled manually from the central part of Cuniã Lake (*Lake2*; **Figure 1**) using a PVC tube during the late falling-water period (June 2013; **Supplementary Material 1**). Three species of aquatic macrophytes were also sampled during this period: *Eichornia crassipes*, *Eichornia azuera* and *Oryza* sp. Only one sample of each macrophyte was analyzed.

The physical and chemical parameters of the water column (dissolved O₂, pH, electric conductivity and temperature) were measured with digital potentiometers (Oxi 3110, pH 3110 and Cond 3110, DIGIMED, São Paulo, Brazil, respectively) during each sampling campaign and the geolocation was

registered with a GPS receiver (Trimble GeoExplorer, Model XT500, California, USA). The water column depth was measured manually with a millimeter rope (**Supplementary Material 2**), with the exception of Madeira River points, whose values were obtained from [Schwatke et al. \(2015\)](#) for the same sampling month and year as this work (**Supplementary Material 1**).

2.3 Processing of water, plant and sediment samples

Suspended particulate matter (SPM) was obtained by filtering the water samples using previously dried (by lyophilization) and weighted Whatman® GF/F filters (0.7 µm porosity) until saturation. The filtrate was acidified with HCl and kept refrigerated.

A 2 L aliquot of the filtrate (< 0.7 µm) was percolated in an organic matter solid phase extraction column (Bond Elut Plexa, Agilent, California, USA), previously activated with 6 mL of 99% methanol (Merck, Darmstadt, Germany). After percolation, elution was carried out also with 99% methanol (8 mL) to obtain a final extract (dissolved matter) for total Hg determination, besides the isotopic and elemental signature of the organic matter. It was not possible to carry out this analysis in the early falling-water period because this method was not optimized at the time.

The sampled aquatic macrophytes were separated into roots, stems, leaves, flowers and fruits (when present). All tissues were washed with ultrapure water (Milipore Mili-Q model, Integral A10, Molsheim, France) in abundance to remove the coarse material. The sediment profile (N=1) was sliced 2 by 2 cm and sieved in the < 2 mm fraction.

Filters containing SPM, aquatic macrophyte tissues and sediment samples were lyophilized (FreezeDry System, Labconco, Model 7522900, Kansas City, USA) and stored dry until chemical measurements were carried out. After lyophilization, the filters were weighted again to measure the total mass of SPM retained. The dissolved matter was dried at room temperature using a constant stream of N₂ to avoid sample contamination with aerosols.

2.4 Total Hg determination

Solubilization of lyophilized samples (0.5 g of SPM and sediment; 1 g of aquatic macrophyte tissues) followed the methodological protocol adapted from Santos et al. (2005), in the following steps: addition of HCl:HNO₃ (3, 37%:1, 65%) and KMnO₄ (5%) in a microwave oven (Mars Express, CEM, Model 907501, USA) during 25 minutes (10 min until it reached 95 °C, and 15 min with constant temperature of 95 °C and power of 1600 W). The final extract was filtered using

Whatman® 40 paper and completed to 30 mL with ultrapure water (Milipore Mili-Q model, Integral A10, Molsheim, France) in a volumetric flask. The solubilization of dissolved matter was performed in amber vials at 70 °C in a water bath using the same reagent proportions.

Total Hg determination was carried out in a mercury analyzer (QuickTrace, M-75000, CETAC, Nebraska, USA) as described by Bastos et al. (1998). Calibration was achieved using a six-point curve from 0.1 ng mL⁻¹ to 5 ng mL⁻¹ (Hg standard, Titrisol, Merck, Darmstadt, Germany). The determination coefficient (r²) acceptable for carrying out the analyzes was > 0.9996. The detection limit for SPM and sediment was 0.4 ng g⁻¹ dry weight (wt.). The detection limit for aquatic macrophyte tissues was 1 ng g⁻¹ dry wt. The recovery of sediment and SPM samples was 93% (NIST 2702) and for aquatic macrophyte samples it was 90% (NIST 1515) and the coefficient of variation between analytical triplicates was < 10%.

2.5 MeHg determination

MeHg determination in biotic (aquatic macrophyte tissues) and abiotic samples (SPM and sediment) followed the protocol described by Liang et al. (1994) and EPA 1630 (2001), respectively. Aliquots of 0.5 g (aquatic macrophyte tissues, sediment and SPM) were weighed in Teflon® tubes in which 5 mL of a 25%

KOH/methanol solution was added to extract and solubilize MeHg. These samples were kept in an oven for 6 h at 70 °C, and were shaken every hour. At the end of 6 h, the samples were allowed to rest for 48 h in the dark to avoid MeHg photodegradation.

At the end of 48 h, MeHg determination was carried out. Amber vials received 30 µL of the solubilized sample, 200 µL of a 2 mol L⁻¹ acetic acid/sodium acetate solution (CH₃COOH/CH₃COONa) and 50 µL of 1% sodium tetraethylborate (NaBEt₄) and were filled with ultrapure water (Milipore Mili-Q, model Integral A10, Molsheim, France) to 40 mL.

The determination was carried out using a gas chromatograph coupled to a cold vapor atomic fluorescence spectrometer (GC-CVAFS, MERX-M Automated Methyl Mercury Analytical System, Brooks Rand Labs, Seattle, WA, USA). Calibration was achieved using a seven-point curve from 0.5 ng mL⁻¹ to 1000 ng mL⁻¹ (MeHg standard, CH₃HgCl, Brooks Rand Labs, Washington, USA). The determination coefficient (r²) acceptable for carrying out the analyzes was > 0.999. The detection limit was 0.0017 ng g⁻¹ dry wt. and the recovery was 91±9% for biotic samples (IAEA-140) and 96±10% for abiotic samples (IAEA-356). The coefficient of variation between analytical triplicates was < 15%.

2.6 Total Fe determination

Total Fe determination in SPM samples followed the protocol described by [Pozebon et al. \(2005\)](#).

The determination was carried out using an atomic emission spectrometer (ICP-AES, Liberty Series II, Varian, Australia). Calibration was achieved using a six-point curve from 0.2 µg mL⁻¹ to 20 µg mL⁻¹ (Fe standard, Titrisol, Merck, Darmstadt, Germany). The determination coefficient (r²) acceptable for carrying out the analyzes was > 0.999. The detection limit was 0.2 µg g⁻¹ dry wt and the recovery was 93% (NIST 2702). The coefficient of variation between analytical triplicates was < 10%.

2.7 Anion determinations (PO₄³⁻, SO₄²⁻, NO₃⁻, NO₂⁻ and Cl⁻)

Aliquots (10 mL) of unfiltered water samples were placed in Teflon[®] tubes and autoclaved for 30 min at 1 atm for orthophosphate (PO₄³⁻) measurement. After autoclaving, 2 mL of a combined solution containing ascorbic acid (C₆H₈O₆), ammonium molybdate ((NH₄)₆Mo₇O₂₄), sulfuric acid (H₂SO₄) and potassium antimony tartrate (C₈H₁₀K₂O₁₅Sb₂) in the concentrations and proportions described by [Murphy and Riley \(1962\)](#) was added to each tube and the determination was carried out using a UV-visible spectrometer (UV-160A, UV-

Visible Recording Spectrophotometer, Shimadzu, Japan) at 882 nm (Murphy and Riley, 1962). Calibration was achieved using a six-point curve from 0.5 ng mL^{-1} to 100 ng mL^{-1} (orthophosphate standard, Ocean Scientific International, Hampshire, United Kingdom). The determination coefficient (r^2) acceptable for carrying out the analyzes was > 0.99 . The detection limit was estimated as three times the standard deviation of the blanks multiplied by the calibration factor, resulting in values of 0.9 ng mL^{-1} for orthophosphate. The coefficient of variation between analytical triplicates was $< 15\%$.

The nitrate (NO_3^-), nitrite (NO_2^-), sulfate (SO_4^{2-}) and chloride (Cl^-) levels were quantified using an ion chromatograph (Metrohm, Model 861, Advanced Compact IC, Switzerland), as described by Carmouze (1994). The elution base for nitrate and nitrite determination contained oxalic acid ($\text{H}_2\text{C}_2\text{O}_4$) and sodium chloride (NaCl), while for chloride and sulfate it contained calcium carbonate (Na_2CO_3) and sodium bicarbonate (NaHCO_3).

2.8 C and N elemental composition and ^{13}C isotopic signature of organic matter

The carbon and nitrogen elemental composition of organic matter was determined using 1 mg of SPM and aquatic macrophyte tissues samples placed in tin (Sn) capsules. For the

sediment, a 10 mg aliquot was used and for the dissolved matter a 100 μL aliquot was used. The determinations were carried out in an elemental analyzer (Flash 2000, Organic Elemental Analyzer, Thermo Scientific, Milan, Italy) and the atomic ratios of carbon and nitrogen (abbreviated by (C:N)_a) were calculated.

The carbon-13 isotopic ratio ($^{13}\text{C}/^{12}\text{C}$, abbreviated by $\delta^{13}\text{C}$) was determined using an interface coupled to the elemental analyzer (Conflo IV) which carries the samples to a mass spectrometer (Isotope Ratio Mass Spectrometer, IRMS, Thermo Scientific Milan, Italy). The results were expressed in relation to the Pee Dee carbonate formation (Belemnite) in parts per billion (‰), with precision of 0.1‰. The reproducibility for the same sample was 95% for all matrices (Meyers, 1994; Cloern et al., 2002; Kennedy et al., 2005).

2.9 Statistical analyses

The data were analyzed and the graphs were produced using the R software (R Core Team, 2018). The descriptive statistics used were the median and median absolute deviation (abbreviated by MAD), due to the asymmetry of most of the data. Two-way analysis of variance (two-way ANOVA) and analysis of covariance (ANCOVA) were calculated (*aov* and *lm* functions; R Core Team, 2018) and tests for multiple

comparison of means were performed *a posteriori* in both cases for the categorical variables, assuming 95% certainty (*TukeyHSD* function; R Core Team, 2018). Where necessary, a maximum likelihood function (*boxcox* function, MASS package, Venables and Ripley, 2002) was used to transform the data to meet the ANOVA and ANCOVA requirements (linearity, normality, homoscedasticity and low leverage of residuals).

The ellipses in the 2D scatter plots represent the dispersion of data to one standard deviation from the centroid of the respective variables and were calculated assuming Normal distribution of the data (*dataEllipse* function, car package, Fox and Weisberg, 2011). The overlap between the ellipse areas was calculated (*maxLikOverlap* function, SIBER package, Jackson et al., 2011) and is presented in percentage.

Linear, exponential, logarithmic and multiple regressions were calculated (*lm* function; R Core Team, 2018) and the determination coefficient (r^2), p values and the 95% confidence and prediction intervals (*predict* function, R Core Team, 2018) of the models were reported. Where necessary, a maximum likelihood function (*boxcox* function, MASS package, Venables and Ripley, 2002) was used to transform the data to meet the regression requirements (linearity, normality,

homoscedasticity and low leverage of residuals). Multiple regressions were presented through their predicted regression planes (*predict* function, R Core Team, 2018; *dcast* function, reshape2 package, Wickman, 2007), adjusted in interactive 3D graphics (*plot3d*, *surface3d*, *movie3d* functions, rgl package; Adler et al., 2018).

3. Results

3.1 Physical and chemical parameters of the water column

Significant effects of the relative distance from the floodplain points to the Madeira River and of the hydrological periods (ANCOVA without interaction) were detected in the values of the physical and chemical parameters, with the exception of temperature, which presented constant values among the sampled points and hydrological periods (**Figure 2 and Supplementary Material 2**).

Spatially, dissolved O₂ ($r^2 = 0.25$; $p = 0.005$), electrical conductivity ($r^2 = 0.85$; $p < 0.000001$) and pH ($r^2 = 0.53$; $p = 0.000001$) presented exponential decrease of their values with increasing distance from the Madeira River toward the floodplain lake (**Figure 2**).

Seasonally, pH and dissolved O₂ values were significantly higher during the late falling-water period when compared to

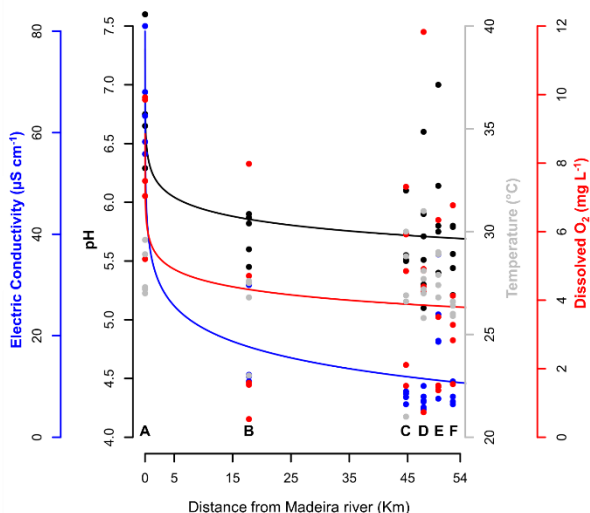


Figure 2 – Variation of the physical and chemical parameters with increasing distance from the Madeira River. **(A)** River1 and River2; **(B)** Igarapé1; **(C)** Igarapé2; **(D)** Lake2; **(E)** Lake1; **(F)** Lake3 sample points (**Figure 1**). Logarithmic regressions explain the process satisfactorily for **pH** ($r^2 = 0.53$; $p = 0.000001$; $Y = -0.1479\ln(X) + 6.2814$), **electrical conductivity** ($r^2 = 0.86$; $p < 0.000001$; $Y = -6.352\ln(X) + 36.091$) and **dissolved O₂** ($r^2 = 0.24$; $p = 0.005$; $Y = -0.4642\ln(X) + 5.6492$). The **temperature** did not show variations with increasing distance from the Madeira River ($r^2 = 0.02$, $p = 0.35$) and had median \pm MAD of 27.2 \pm 1.0.

the rising-water period ($p = 0.018$ and $p = 0.0002$, respectively; **Supplementary Material 2**) and early falling-water period ($p = 0.0001$ and $p = 0.00002$, respectively; **Supplementary Material 2**). Electrical conductivity values were marginally higher during the rising-water period when compared to the late falling-water period ($p = 0.04$; **Supplementary Material 2**).

3.2 Suspended particulate matter

3.2.1 Total Hg

A significant effect of the sampled ecosystems (river, *igarapé* and lake) on

total Hg concentrations in SPM (Two-Way AONVA; $p = 0.000001$; **Figure 3A**) as well as a marginally significant interaction of seasonality with the sampled ecosystems were detected (Two-Way AONVA; $p = 0.04$; **Figure 3A**).

Total Hg concentrations in the SPM were not different between the lake and *igarapé* in any of the evaluated hydrological periods (**Figure 3A**). On the other hand, significant differences were observed in total Hg concentrations in the SPM between the river and the *igarapé*-lake system in all the hydrological periods (**Figure 3A**).

Increasing total Hg concentrations in the SPM towards the floodplain ecosystems (river < *igarapé* = lake) were observed during the rising-water and early falling-water periods (**Figure 3A**). The highest total Hg concentrations were observed in the lake during the rising-water period (709.2 ± 367.7 , **Figure 3A**) and the lowest were observed in the river during the early falling-water period (5.4 ± 2.7 , **Figure 3A**).

3.2.2 MeHg

Sampled ecosystems (river, *igarapé* and lake) had different MeHg concentrations associated with SPM (**Figure 3B**; Two-Way ANOVA: $p < 0.0001$). No significant direct effects of seasonality or interaction between

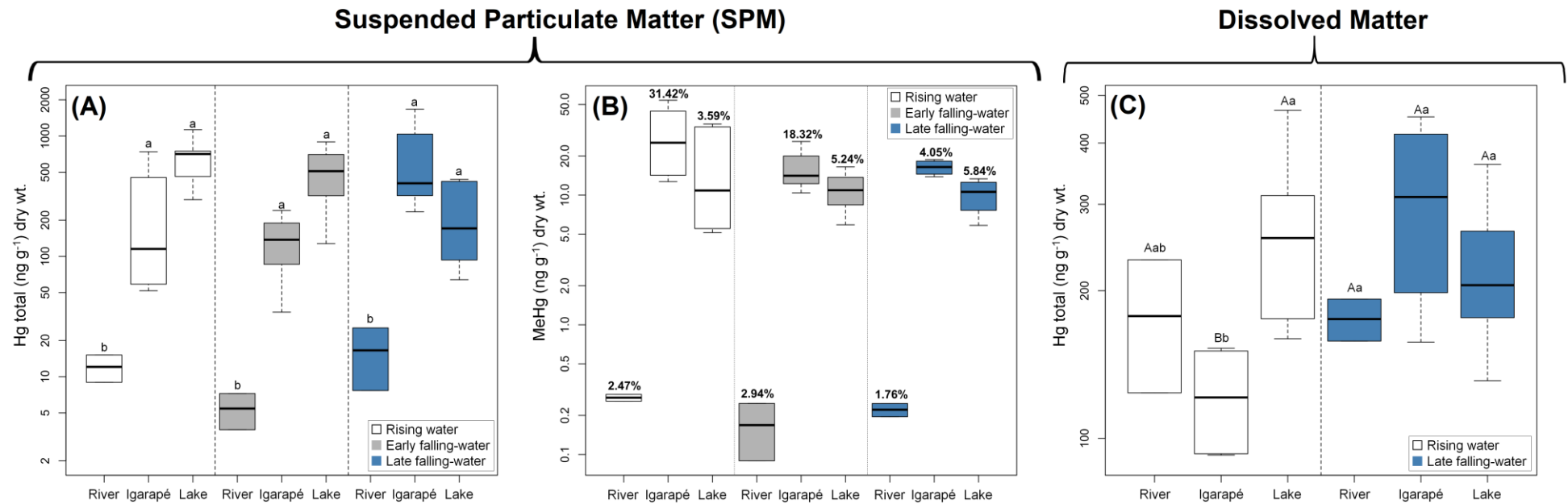


Figure 3 (A) – Total Hg concentrations in SPM in the river-*igarapé*-lake system for each hydrological period sampled. Lowercase letters identify the differences ($p < 0.05$) between ecosystems within the same hydrological period. **(B)** – MeHg concentrations in SPM in the river-*igarapé*-lake system for each hydrological period sampled. No significant direct effects of seasonality or interaction between seasonality and sampled ecosystems were detected ($p = 0.29$ and $p = 0.96$, respectively). Significant differences were observed in MeHg concentrations in the SPM between the river and the *igarapé*-lake system in all hydrological periods evaluated ($p < 0.000001$). %MeHg (MeHg/total Hg ratio) is indicated for each ecosystem and hydrological period. **(C)** – Total Hg concentrations in dissolved matter in the river-*igarapé*-lake system for each hydrological period sampled. Lowercase letters identify the differences ($p < 0.05$) between ecosystems within the same hydrological period while uppercase letters differentiate ($p < 0.05$) the hydrological periods within the same ecosystem. The distances between the y-axis values were log-transformed to optimize the data visualization in all panels.

seasonality and sampled ecosystems were detected (Two-Way ANOVA: $p = 0.29$ and $p = 0.96$, respectively).

MeHg concentrations in the SPM was different between the lake and the *igarapé* in each hydrological period evaluated ($p = 0.06$; **Figure 3B**). In addition, MeHg concentrations in the SPM were different between the river and the *igarapé*-lake system in all hydrological periods evaluated ($p < 0.000001$; **Figure 3B**).

3.2.3 $\delta^{13}\text{C}$ signature and (C:N)_a ratio of organic matter

The $\delta^{13}\text{C}$ isotopic signature and the (C:N)_a ratio of the organic matter associated with the SPM overlapped between the *igarapé* and the lake while they could be used to differentiate the *igarapé*-lake system from the river (**Figure 4A**). The overlap between the *igarapé* and the lake represented 88% of all the isotopic and elemental area covered by the *igarapé* and 43% of all the isotopic and elemental area covered by the lake (**Figure 4A**).

The $\delta^{13}\text{C}$ signature of the organic matter associated with the SPM from the river had higher values (heavier isotopic signature, i.e., higher ^{13}C content related to ^{12}C content), while smaller values (lighter isotopic signature, i.e., lower ^{13}C content related to ^{12}C content) were

observed in the *igarapé*-lake system (**Figure 4A**). The (C:N)_a ratio presented slightly smaller values in the river compared to the *igarapé*-lake system (**Figure 4A**).

3.2.4 MeHg and total Hg associations with geochemical supports

MeHg concentrations in the SPM were associated with the (C:N)_a ratio and the $\delta^{13}\text{C}$ of organic matter also in the SPM (**Figure 5**). Through multivariate regression ($r^2 = 0.79$; $p < 0.0001$) it is possible to predict higher MeHg concentrations in SPM with higher organic matter degradation (higher (C:N)_a ratio values) and lighter isotopic signature (lower $\delta^{13}\text{C}$ values) of organic matter (**Figure 5**).

MeHg concentrations in the SPM were associated with the oxygenation level of the water column and its acidity (**Figure 6A**). Through multivariate regression ($r^2 = 0.80$; $p < 0.0001$) it was possible to predict higher MeHg concentrations in SPM with lower the oxygenation (lower dissolved O₂ values) and higher acidity (lower pH values) of the water column (**Figure 6A**).

MeHg concentrations in SPM were also associated with the SO₄²⁻ concentrations in the water column (**Figure 7A; Supplementary Material 3**). Through exponential regression ($r^2 = 0.73$; $p < 0.0001$) it was possible to predict

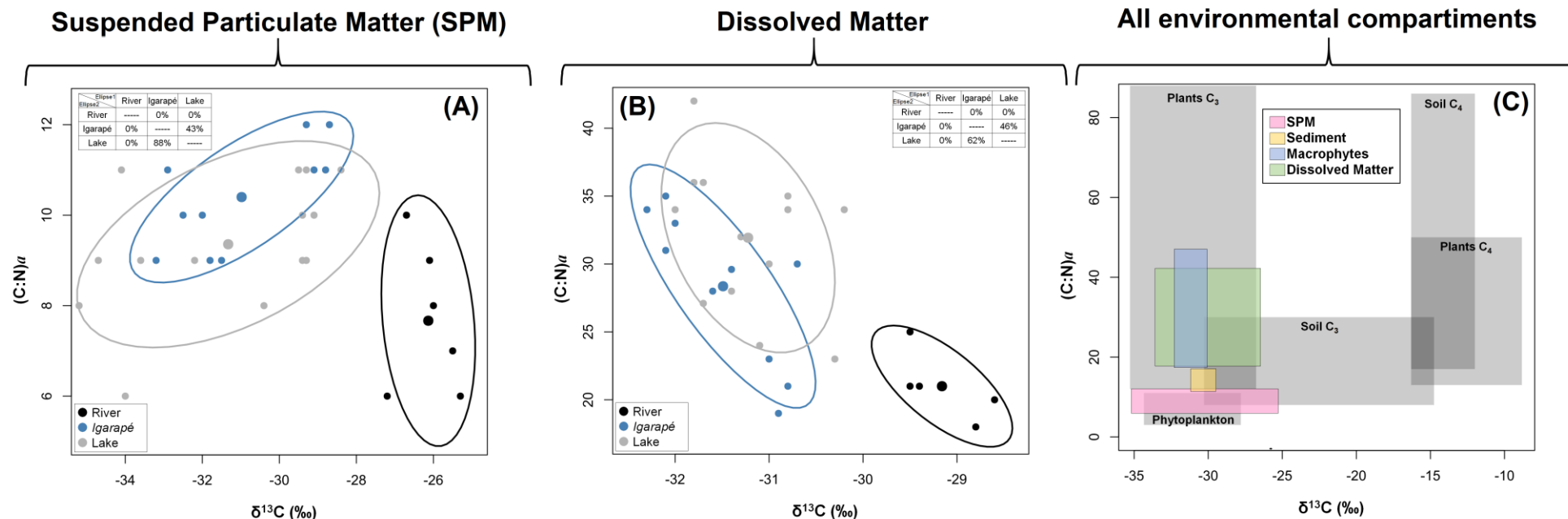


Figure 4 (A) – Carbon and nitrogen elemental composition ((C:N)_a ratio) and carbon-13 ($\delta^{13}\text{C}$) isotopic signature in the SPM for the three evaluated ecosystems. The internal table represents the percentage of isotopic area overlapped between Ellipse 1 and Ellipse 2, in relation to Ellipse 1 area. The ellipses were constructed considering distance of one standard deviation from the centroids of the respective variables. **(B)** Carbon and nitrogen elemental composition ((C:N)_a ratio) and carbon-13 ($\delta^{13}\text{C}$) isotopic signature in the dissolved matter for the three evaluated ecosystems. **(C)** Carbon and nitrogen elemental composition ((C:N)_a ratio) and carbon-13 ($\delta^{13}\text{C}$) isotopic signature reported for the Amazon region (light grey, no borders; [Hedges et al., 1986](#); [Meyers, 1994](#); [Martinelli et al., 2003](#); [Kim et al., 2012](#)). The isotopic and elemental area determined for each of the environmental compartments from this study is represented superimposed (in color, with borders).

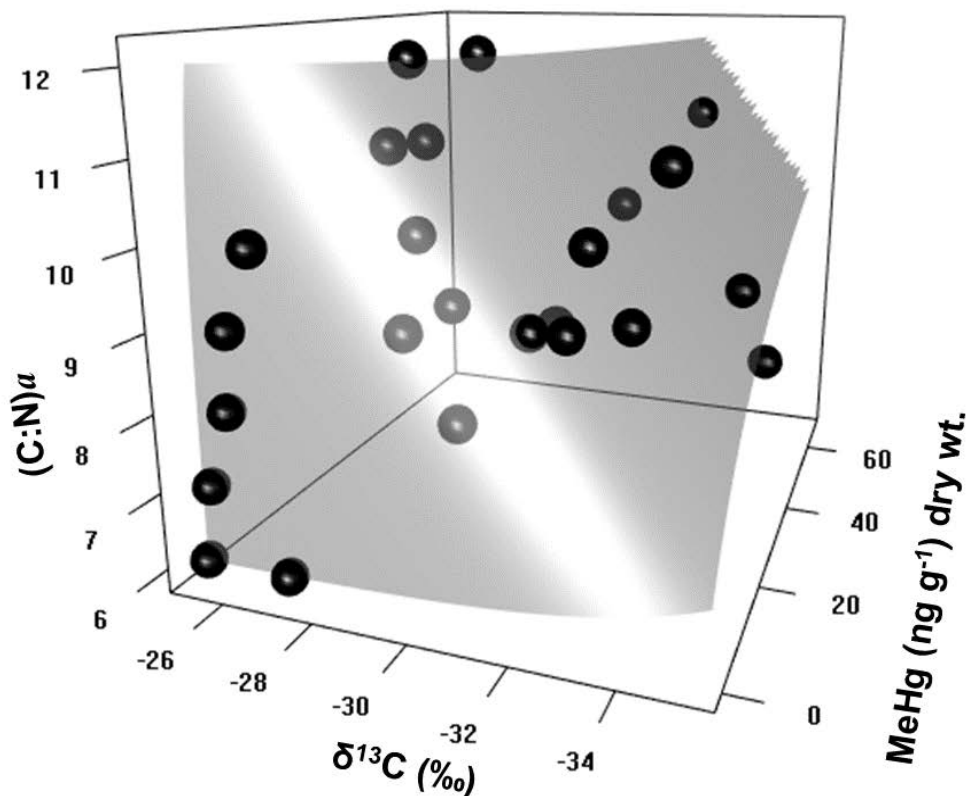


Figure 5 – Multivariate regression of MeHg concentration in the SPM with the carbon and nitrogen elemental composition ((C: N)_a ratio) and carbon-13 ($\delta^{13}\text{C}$) isotopic signature also in SPM. The regression plane is represented by the transparent gray form and was constructed with the following equation: $Z = e^{-0.4130X + 0.5861Y - 16.1855}$ ($r^2 = 0.79$; $p = 0.00000001$). If you are unable to view this graph interactively, [click here](#).

higher MeHg concentrations with lower the SO_4^{2-} concentrations in the water column (**Figure 7A**).

Total Hg concentrations in SPM were associated with total Fe concentrations also in SPM (**Figure 7B**). Through quadratic regression ($r^2 = 0.57$; $p < 0.0001$) it was possible to predict higher total Hg concentrations in SPM with higher Fe concentrations up to a limit of $50 \mu\text{g g}^{-1}$ dry wt. After this limit, a decrease in total Hg concentrations in the SPM with

increasing Fe concentrations was observed.

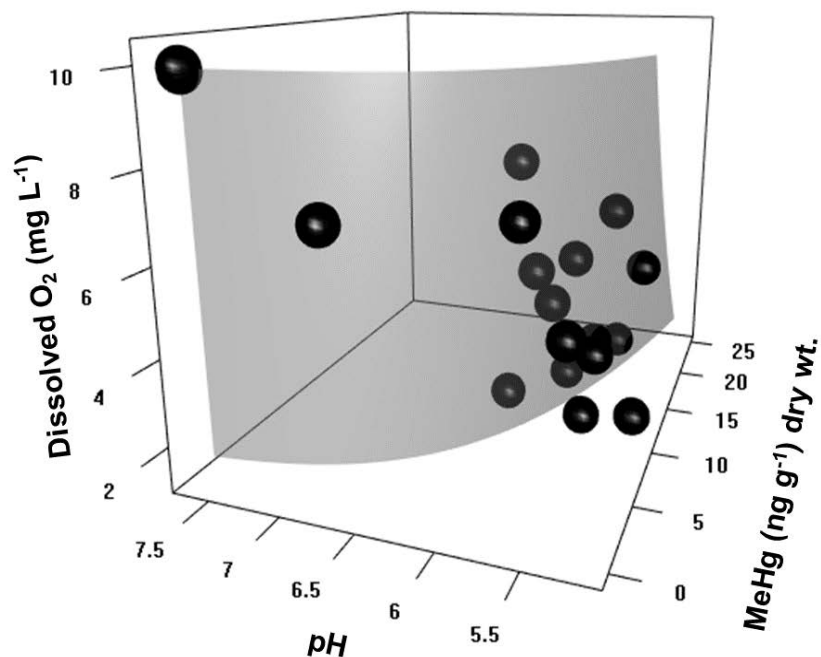
3.3 Dissolved matter

3.3.1 Total Hg

A marginally significant effect of the interaction of sampled ecosystems (river, *igarapé* and lake) and seasonality on total Hg concentrations in the dissolved matter was detected (**Figure 3C**; Two-Way ANOVA: $p = 0.02$).

^aThis is an interactive graph. Click to activate the animation. Adobe Acrobat Reader® and Adobe Flash Player® are required for viewing and can be obtained for free [here](#) and [here](#).

(A)



(B)

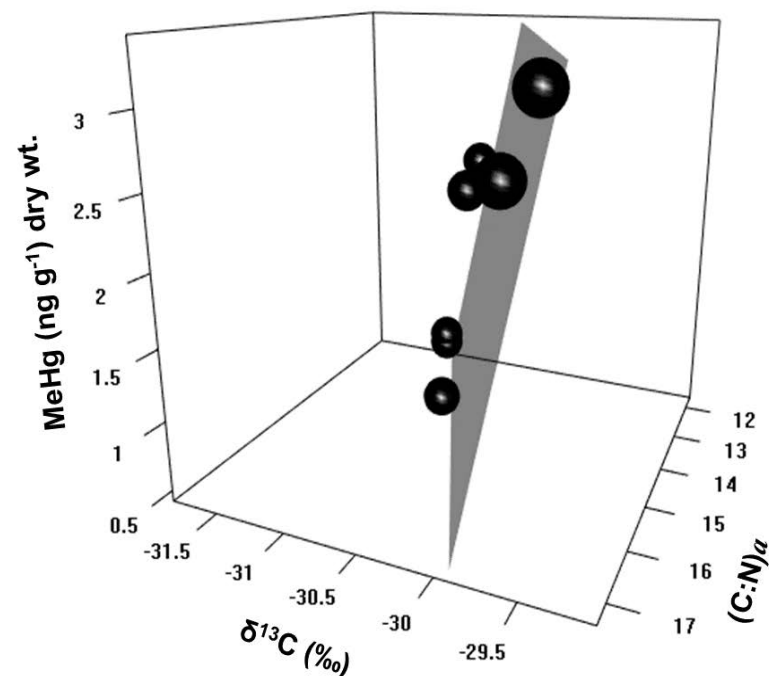


Figure 6 – (A) Multivariate regression of MeHg concentration in the SPM with water column oxygenation (dissolved O₂) and its acidity (pH). The regression plane is represented by the transparent gray form and was constructed with the following equation: $Z = e^{-1.6392X - 0.0771Y + 11.8969}$ ($r^2 = 0.80$; $p = 0.000001$). If you are unable to view this graph interactively, [click here](#). (B) Multivariate regression of MeHg concentration in the sediment profile with the carbon and nitrogen elemental composition ((C:N)_a ratio) and carbon-13 (δ¹³C) isotopic signature. The regression plane is represented by the transparent gray form and was constructed with the following equation: $Z = 4.67X - 0.95Y + 157.52$ ($r^2 = 0.93$; $p = 0.004$). If you are unable to view this graph interactively, [click here](#).

^aThis is an interactive graph. Click to activate the animation. Adobe Acrobat Reader® and Adobe Flash Player® are required for viewing and can be obtained for free [here](#) and [here](#).

The only seasonal difference detected in total Hg concentrations in dissolved matter, although marginally significant, was in the *igarapé* ($p = 0.03$), with lower values in the rising-water period (121.2 ± 41.7 ; **Figure 3C**) compared to the late falling-water period (310.5 ± 158.0 ; **Figure 3C**).

Spatially, total Hg concentrations in the dissolved matter from the *igarapé* were significantly lower (121.2 ± 41.7 ; **Figure 3C**) than those observed in the lake during the rising-water period (256.1 ± 101.7 ; **Figure 3C**; $p = 0.03$).

3.3.2 $\delta^{13}\text{C}$ signature and (C:N)_a ratio of organic matter

The $\delta^{13}\text{C}$ isotopic signature and the (C:N)_a ratio of the organic matter associated with the dissolved matter were overlapped between the *igarapé* and the lake, while they did allow for differentiation of the *igarapé*-lake system from the river (**Figure 4B**). The overlap between the *igarapé* and the lake represented 62% of all the isotopic and elemental area covered by the *igarapé* and 46% of all the isotopic and elemental area covered by the lake (**Figure 4B**).

The $\delta^{13}\text{C}$ signature of the organic matter associated with the dissolved matter in the river presented higher values (heavier isotopic signature), while smaller values (lighter isotopic signature) were

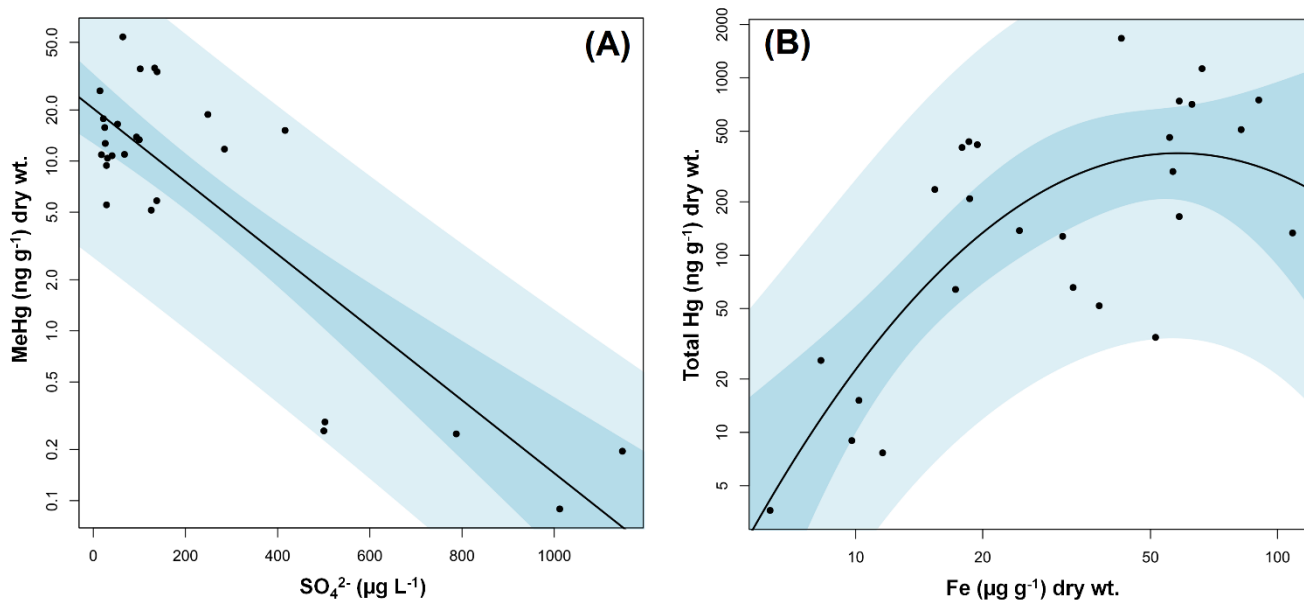


Figure 7 – **(A)** Exponential regression between MeHg concentration in the SPM and SO_4^{2-} concentration in the water column. The regression is indicated by the black solid line and was constructed using the following equation: $Y = 20.38903X^{-0.004945}$ ($r^2 = 0.73$; $p = 0.00000001$). The light blue shaded area represents the prediction interval of the model while the dark blue shaded area represents the confidence interval of the model, both calculated with 95% certainty. The distances between the y-axis values were log-transformed to optimize the data visualization. **(B)** – Quadratic regression between total Hg total and total Fe concentration in the SPM. The regression is indicated by the black solid line and was constructed using the following equation: $\ln(Y) = -0.9057X^2 + 7.3611X - 9.0281$ ($r^2 = 0.57$; $p = 0.00000001$). The distances between the y-axis values were log-transformed to optimize the data visualization.

observed in the *igarapé-lake* system (**Figure 4B**). The (C:N)_a ratio presented slightly smaller values in the river compared to the *igarapé-lake* system (**Figure 4B**).

3.4 Sediment profile

3.4.1 Total Hg and MeHg

Total Hg and MeHg concentrations increased with depth (**Supplementary Material 4**). The lowest total Hg concentration was observed in the surface layer (0 cm; 24.6 ng g⁻¹) while the highest was observed at the greatest depth (12 cm; 51.9 ng g⁻¹; **Supplementary Material 4**).

The lowest MeHg concentration was observed in the first 4 cm (0.6 ng g⁻¹; **Supplementary Material 4**) while the highest concentration was observed at the greatest depth (12 cm; 3.2 ng g⁻¹; **Supplementary Material 4**). The lowest %MeHg was also observed in subsurface (4 cm, 1.8%; **Supplementary Material 4**) while the highest %MeHg was determined at the greatest depth (12 cm; 6.2%; **Supplementary Material 4**).

3.4.2 MeHg associations with geochemical supports

MeHg concentrations in the sediment were associated with the (C:N)_a ratio and the δ¹³C of organic matter also in the sediment (**Figure 6B**). Through

multivariate regression ($r^2 = 0.93$; $p = 0.004$) it was possible to predict higher MeHg concentrations in the sediment profile with higher degradation of organic matter (higher (C:N)_a values) and heavier isotopic signature (higher δ¹³C values; **Figure 6B**).

3.5 Aquatic macrophytes

3.5.1 Total Hg and MeHg

The highest %MeHg were observed in the roots among all aquatic macrophyte tissues evaluated (%MeHg: 20.9 – 33.7; **Figure 8**). The highest MeHg concentrations observed in *E. azuera* and *E. crassipes* were in the roots (7.5 and 6.3 ng g⁻¹, respectively), while *Oryza* sp. showed higher MeHg concentrations in leaves (0.9 ng g⁻¹). The highest total Hg concentrations observed in *E. azuera* and

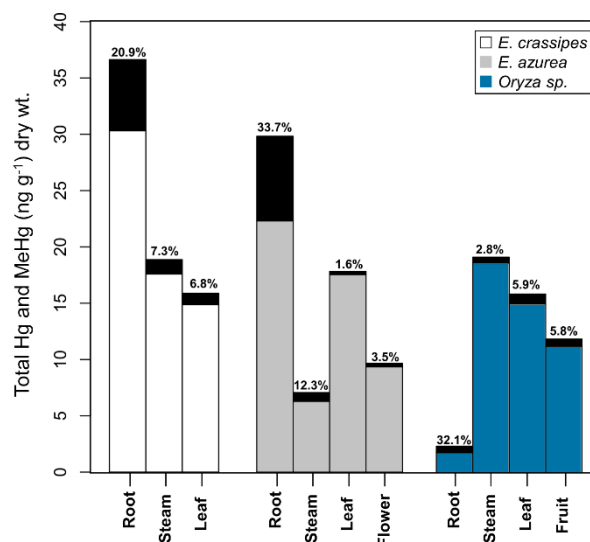


Figure 8 – Total Hg concentration (white, gray and blue bars) and MeHg concentration (black bars) in the aquatic macrophyte tissues (N=1) sampled during the late falling-water period. The %MeHg (MeHg / total Hg ratio) is indicated for each aquatic macrophyte tissue sample

E. crassipes were in the roots (30.3 and 22.3 ng g⁻¹, respectively), while *Oryza* sp. showed higher MeHg concentrations in stems (18.6 ng g⁻¹).

MeHg concentration ratios between leaves and roots of macrophytes *E. crassipes*, *E. azuera* and *Oryzasp.* were 0.16, 0.04 and 1.6, respectively. For total Hg, the ratios were 0.49, 0.78 and 8.41, respectively.

3.5.2 $\delta^{13}\text{C}$ signature and (C:N)_a ratio of organic matter

The $\delta^{13}\text{C}$ signature and (C:N)_a ratio of the macrophyte tissues were within the range described for plants with C₃ metabolism previously analyzed in the Amazon region (**Figure 4C**). Comparatively, the $\delta^{13}\text{C}$ signature of the dissolved matter had a broader distribution than that from aquatic macrophytes overlapping with signatures of Amazonian soils under the influence of plants with C₃ metabolism (**Figure 4C**). The coverage of SPM $\delta^{13}\text{C}$ signature was similar to dissolved matter, although with (C:N)_a ratios typically from phytoplankton reported for the Amazon region (**Figure 4C**). The sediment showed (C:N)_a ratios with intermediate values between SPM and the area covered by aquatic macrophytes and dissolved matter (**Figure 4C**).

4. Discussion

4.1 The physical and chemical parameters transition from Madeira River to Cuniã *igarapé*-lake system

The pH and dissolved O₂ decreased with increasing distance from the Madeira River in relation to the floodplain (**Figure 2**), due to: (1) decreasing O₂ physical diffusion to the water column, considering the transition from a lotic and turbulent flow to a lentic one; and (2) organic matter leaching from adjacent forest soils to the *igarapé*-lake aquatic system (Roulet et al., 1999; 2001; Maia et al., 2009) that increases biochemical O₂ demand for decomposition and generates acidity and anoxia as a result (Aprile and Darwich, 2013). All these changes are, in the first instance, a consequence of the water type change (Sioli, 1967) from the Madeira River (white water) to the *igarapé*-lake system (black water). The higher (C:N)_a ratio observed in the *igarapé*-lake system compared to the river indicates higher organic matter degradation (**Figures 4A and 4B**). Moreover, the (C:N)_a ratio and $\delta^{13}\text{C}$ of the dissolved matter covers Amazonian soils under the influence of plants with C₃ metabolism (**Figure 4C**).

The decreasing electrical conductivity observed for the same spatial context (**Figure 2**) is related to three aspects. First is the progressive SPM sedimentation along the river-lake transect

(**Supplementary Material 5**; [Sioli, 1967](#); [Aprile and Darwich, 2013](#)): the SPM transported by the Madeira River is essentially mineral ([Gibbs, 1967](#)), able to adsorb ions and to promote their co-precipitation. Hydrodynamically, the winding *igarapé* course (**Figure 1**) promotes the sedimentation of particles ([Santos and Ribeiro, 1988](#); **Supplementary Material 5**). Second, organic matter leaching from adjacent forest soils (**Figure 4C**) enhances the complexation of the available ions ([Bezerra et al., 2009](#)). Finally, the aquatic macrophytes present along the river-lake transect (personal observation) act as geochemical barriers, absorbing the ions from the water column ([Aprile and Darwich, 2013](#)).

Seasonally, the highest dissolved O₂ concentrations observed in the late falling-water period compared to the other periods may reflect (1) higher photosynthetic activity in this period and phytoplankton growth, which saturates the water column with O₂, although the SPM concentration was higher in the late falling-water period in the *igarapé*-lake system compared to the other hydrological periods evaluated (**Supplementary Material 5**; $p < 0.05$), which, in turn, may have restricted partially the light penetration in the water column; (2) higher O₂ exchange with the atmosphere due to

higher water column surface/volume ratio that, in turn, is due to lower water column depth during the late falling-water period (**Supplementary Material 2**); (3) lower microbial activity that decreases the biochemical oxygen demand. Indeed, the $\delta^{13}\text{C}$ signature is lighter in the *igarapé*-lake system (**Figures 4A and 4B**) compared to the river and with (C:N)_a ratios typically from phytoplankton reported for the Amazon region (**Figure 4C**). [Caraballo et al. \(2014\)](#) also observed a more oxygenated water column during the falling-water period, studying a floodplain under the influence of the Negro and Solimões rivers, highlighting the daily variation in oxygenation, with peaks in the epilimnion between 10:00 a.m. and 3:00 p.m. precisely when the measurements of this study were made. On the other hand, [Brito et al. \(2017\)](#), studying a floodplain under the influence of the Solimões River, observed a more oxygenated and homogenized water column during the low-water period compared to the rising-water and high-water period.

4.2 Spatial-temporal dynamics of total Hg in SPM and dissolved matter

The highest total Hg concentrations observed in the lake during the rising-water period (**Figure 3A**) reflect the drag of particles caused by the entrance of river water into the *igarapé*-lake system as well as its progressive sedimentation towards

the lake (**Supplementary Material 5**): the association of low SPM loadings with high Hg concentrations (**Supplementary Material 5; Figure 3A**) indicates that coarse and heavier particles (with low adsorption area) settle along the *igarapé* path while fine and lighter particles (with high adsorption area) remain suspended in the water column. The particles in the water column are a mixture of those from the Madeira river and those from adjacent soils of the *igarapé*-lake system ([Aprile and Darwich, 2013](#)). The contrasting isotopic signature between the *igarapé*-lake system and the river shows that the organic matter present in the water column of from adjacent soils of the *igarapé*-lake system (**Figures 4A and 4B**) while the mineral particles are mostly from the Madeira River (**Supplementary Material 5**). In addition, total Hg and total Fe association in SPM (**Figure 7B**) suggest that the binding sites of the mineral fraction are close to saturation, which characterizes efficient Hg transport, as also reported by [Maia et al. \(2009; 2017\)](#) for the particulate fraction of the water column. In this analysis, total Fe concentrations act as a proxy for Fe-oxyhydroxides, which have a layer of organic matter on their surface that enhances the SPM affinity for Hg ([Feyte et al., 2010](#)).

In the hydrodynamic context, the lake acts as the final sedimentation site of these particles that explains the higher total Hg concentrations in this environment during the rising-water period. This pattern has also been reported by other authors that have studied a river-floodplain system in the Amazon ([Roulet et al., 1999](#); [Maia et al., 2009](#); [Brito et al., 2017](#); [Maia et al., 2017](#); **Supplementary Material 6**).

The transition from the rising-water to the initial falling-water period did not promote any change in the total Hg concentration pattern in the river-*igarapé*-lake system (**Figure 3A**). On the other hand, the transition from the initial falling-water to the late falling-water period promoted marginally significant effects on the total Hg concentration between the lake and the *igarapé* that showed higher total Hg concentrations compared to the former (**Figure 3A**). The similar depth between the *igarapé* and lake in this period (**Supplementary Material 2**) facilitates the horizontal homogenization of the water column between these two environments that may explain this change. This seasonal change in Hg concentrations between the lake and the channel that connects it to its main river was also observed by [Brito et al. \(2017\)](#) in the low water period, compared to the rising-water and high-water periods.

This seasonal change between the rising-water and the late falling-water period can be observed more clearly in the dissolved matter (**Figure 3C**) that showed a 2.5-fold increase of the total Hg concentration in the *igarapé* compared to the lake. The dissolved matter has more horizontal mobility between water masses when compared to the SPM, since smaller and lighter particles undergo lower gravity driven sedimentation. This higher mobility is reflected in the decreasing overlap of isotopic and elemental signatures of the *igarapé*-lake system between the SPM and dissolved matter of 24% (**Figures 4A and 4B**). On the other hand, the dissolved matter is less efficient in Hg adsorption and transport per unit of dry mass, presenting concentrations 1.75-fold lower compared to SPM.

4.3 Methylation in the water column of the river-*igarapé*-lake system

MeHg concentration pattern in the river-*igarapé*-lake system did not show differences among the hydrological periods evaluated (**Figure 3B**). On the other hand, other authors (Kasper et al., 2014; Brito et al., 2017) have observed higher MeHg concentrations during the rising-water and high-water periods (**Supplementary Material 6**), since a deeper water column is more susceptible to developing anoxic hypolimnion that promotes Hg methylation. In this study, the

water level variation was not significant among the hydrological periods sampled (**Supplementary Materials 1 and 2**) and can explain the similarity of MeHg concentrations.

The slightly higher MeHg concentrations in the SPM observed in the *igarapé* in all hydrological periods sampled suggest higher methylation rates in this environment compared to the lake (**Figure 3B**). Brito et al. (2017), studying a floodplain connected to the Solimões River, also observed higher MeHg concentrations in the channel that connects the floodplain to the main river, but only in the low-water period, compared to the rising-water and high-water periods (**Supplementary Material 6**). In this study, however, the distance between Cuniã Lake and the Madeira River is approximately 37 km (**Figure 1**), which limits the seasonal influence of the main river on the lake and may explain the similar MeHg concentrations in the SPM among hydrological periods (**Figure 3B**).

Higher %MeHg in the *igarapé* compared to the lake are reflected in the organic matter elemental composition that had slightly higher (C:N)_a ratios in the *igarapé* compared to the lake, indicating more degraded organic matter. This association between MeHg production and the (C:N)_a ratios can be directly visualized in the multiple regression model

(**Figure 5**), which shows an exponential increase in the MeHg concentration with the increase of (C:N)_a ratio. In addition, the association of higher MeHg concentrations with lighter $\delta^{13}\text{C}$ values suggests that organic matter derived from phytoplankton (**Figure 4C**) is better at promoting the methylation process than that derived from adjacent soils to the *igarapé*-lake system.

Several authors have reported that sulfate-reducing bacteria are capable of Hg methylation (King et al., 1999; Benoit et al., 2002; Muresan et al., 2008). Indeed, higher MeHg concentrations in SPM were associated with lower SO_4^{2-} concentrations in the water column (**Figure 7A**). The increase of MeHg concentrations with decreasing SO_4^{2-} concentrations suggests the consumption of these anions by the sulfate-reducing bacteria for organic matter decomposition, together with the Hg methylation.

In addition to organic matter elemental and isotopic signature, the physical and chemical parameters variables also showed associations with MeHg concentrations (**Figure 6A**). The low oxygenation and higher acidity, generated by organic matter decomposition, were exponentially associated with high MeHg concentrations (**Figure 6A**). This relationship between water column oxygenation and MeHg

concentrations has also been observed by other authors in Amazonian ecosystems (Muresan et al., 2008; Almeida, 2012; Kasper et al., 2014; Brito et al., 2017).

4.4 Hg deposition and methylation in the sediment profile

The increase of total Hg and MeHg concentrations in the sediment profile with increasing depth reinforces the depositional character that the lake has in the river-*igarapé*-lake system (**Supplementary Material 4**). This, along with the low depth of the water column during the sampling (**Supplementary Material 2**), also suggests that there is high sediment remobilization in its upper layers which, in turn, might be (1) driven by wind or (2) associated with the seasonal flood pulse of the Madeira River (Junk and Furch, 1985). Bastos et al. (2006) and Almeida et al. (2014), analyzing the surface sediment of several lakes adjacent to the Madeira River (**Supplementary Material 6**), observed higher total Hg concentrations in Cuniã Lake (98.13 ± 19.50), compared to the other eight sampled lakes. These higher Hg concentrations may be associated with greater distance from the lake to the Madeira River compared to the other sampled lakes, which makes it a more efficient sedimentation and retention environment.

Increasing MeHg concentration and %MeHg with depth indicate higher methylation rates in lower sediment layers. This is due to the higher anoxia found in these layers, which favors the methylation process (Mauro et al., 1999). The multiple regression model indicated an increase in MeHg concentrations with increasing (C:N)_a ratio values, due to the decomposition that happens in this compartment (Figure 6B). In the same model, increasing MeHg concentrations were associated with heavier $\delta^{13}\text{C}$ values, that indicates that the organic matter deposited in the sediments mostly comes from the adjacent soils to the *igarapé*-lake system (Figure 4C), which nourishes dense vegetation and arboreal trees (personal observation) with C₃ photosynthetic metabolism.

4.5 Influence of the aquatic macrophyte biotype on the total Hg and MeHg accumulation and translocation

The highest %MeHg was observed in the aquatic macrophyte roots (Figure 8), a microenvironment that shelters a variety of microorganisms that use the organic matter retained from the water column and exudated by these plants in anaerobic respiration, generating anoxia and acidity, which promotes Hg methylation (Mauro et al., 1999).

The aquatic macrophytes *E. crassipes* and *E. azurea* that are floating

and rooted biotypes, respectively, showed high total Hg and MeHg concentrations in their roots compared to *Oryza* sp., which also is a rooted biotype. On the other hand, *Oryza* sp. was the only sampled aquatic macrophyte in which total Hg and MeHg ratios between leaf and root were higher than 1, suggesting efficient translocation of these chemical species to the aerial component of the plant. This suggests that Hg translocation may be more associated with plant species than with biotype. In addition, as aquatic macrophytes harbor diverse fauna (Sánchez-Botero et al., 2003; Aprile and Darwich et al., 2013) and can be consumed by them, they can act in the Hg trophic transfer to the aquatic food chain. The detection of Hg and MeHg in ingestible tissues such as the fruit of *Oryza* sp. and structures frequently accessed by floral visitors like the flowers of *E. azurea* illustrate this phenomenon.

5. Conclusion

Typical floodplain ecosystems, represented in this study by the *igarapé* and Cuniã Lake, had higher total Hg and MeHg concentrations in the water column (SPM and dissolved material), partially independent of seasonality, compared to the Madeira River, to which they are connected. The distance between the Madeira River and Cuniã Lake plays an important role in the Hg and MeHg

circulation, due to process that occur along the 37 km of the Cuniã *igarapé*. Total Hg showed higher affinity for the SPM than for the dissolved matter, indicating more efficient transport by the former.

In the *igarapé*-lake system, the elemental and isotopic composition of the organic matter were useful to predict MeHg concentrations, as well as the oxygenation and acidity measured in the water column, showing that physical and chemical changes between the river-floodplain system affect MeHg circulation and production. The inverse relationship between MeHg and SO_4^{2-} suggests the action of sulfate-reducing bacteria in this process. Total Hg and MeHg concentrations as well as %MeHg found in the sediment profile and aquatic macrophyte tissues demonstrated Hg and MeHg transfer along the trophic chain.

6. Acknowledgments

We thank the Laboratório de Biogeoquímica Ambiental Wolfgang C. Pfeifferat Universidade Federal de Rondônia for the field logistics and MeHg measurements, as well as the Laboratório de Ciências Ambientais of Universidade Estadual do Norte Fluminense Darcy Ribeiro for elemental composition and isotopic signature determinations. Wanderley R. Bastos received support from the Conselho Nacional de Desenvolvimento Científico e Tecnológico

for studies about Hg circulation in Amazonian ecosystems (CNPq-Universal-11, No. 476560/2011-0). Cristina MM Souza received support from Fundação de Amparo à Pesquisa do Estado do Rio de Janeiro for the purchase of the reagents used in some of the chemical analyses of this work (FAPERJ; C-26/111.368/2012). This study was also financed in part by Coordenação de Aperfeiçoamento de Pessoa de Nível Superior – Brazil (CAPES) – Finance Code 001. We also thank the reviewers for significantly improving the quality and accuracy of this paper through the valuable comments.

7. References

- Adler D, Murdoch D, Nenadic O, Urbanek S, Chen M, Gebhardt A, Bolker B, Csardi G, Strzelecki A, Senger A, Eddelbuettel D. 2018. RGL - 3D visualization device system for R using OpenGL. <https://r-forge.r-project.org/projects/rgl/>
- Almeida R. 2012. Estudo da origem, mobilização e organificação do mercúrio no reservatório da UHE – Samuel, RO. Tese de Doutorado, Universidade Federal do Rio de Janeiro, Centro de Ciências da Saúde Instituto de Biofísica Carlos Chagas Filho, Rio de Janeiro, 117p.
- Almeida R, Bernardi JVE, Oliveira RC, Carvalho DP, Manzatto AG, Lacerda LD, Bastos WR. 2014. Flood pulse and spatial dynamics of mercury in sediments in Puruzinho lake, Brazilian Amazon. *Acta Amazonica*, 44(1):99-106. <http://dx.doi.org/10.1590/S0044-59672014000100010>

- Aprile F, Darwich AJ. 2013. Nutrients and water-forest interactions in an Amazon floodplain lake: an ecological approach. *Acta Liminologica Brasiliensia* 25(2):169-182.
<http://dx.doi.org/10.1590/S2179-975X2013000200008>
- Arrifano, G.P.F., Del Carmen Rodriguez Martin-Doimeadios, R., Jiménez-Moreno, M., Augusto-Oliveira, M., Rogério Souza-Monteiro, J., Paraense, R., Rodrigues Machado, C., Farina, M., Macchi, B., do Nascimento, J.L.M., Crespo-Lopez, M.E., 2018a. Assessing mercury intoxication in isolated/remote populations: Increased S100B mRNA in blood in exposed riverine inhabitants of the Amazon. *NeuroToxicology* 68, 151–158.
<https://doi.org/10.1016/j.neuro.2018.07.018>
- Arrifano, G.P.F., Martín-Doimeadios, R.C.R., Jiménez-Moreno, M., Fernández-Trujillo, S., Augusto-Oliveira, M., Souza-Monteiro, J.R., Macchi, B.M., Alvarez-Leite, J.I., do Nascimento, J.L.M., Amador, M.T., Santos, S., Ribeiro-dos-Santos, Â., Silva-Pereira, L.C., Oriá, R.B., Crespo-Lopez, M.E., 2018b. Genetic Susceptibility to Neurodegeneration in Amazon: Apolipoprotein E Genotyping in Vulnerable Populations Exposed to Mercury. *Frontiers in Genetics* 9, 1–12.
<https://doi.org/10.3389/fgene.2018.00285>
- Aryes GA. 2004. Distribuição do Mercúrio nas Águas Superficiais do rio Madeira. Dissertação de mestrado em Geociências – Geoquímica Ambiental (PPG-GEO). Universidade Federal Fluminense. 69 pp. (in Portuguese)
- Bäckström M, Darío M, Karlsson S, Allard B. 2003. Effects of a fulvic acid on the adsorption of mercury and cadmium on goethite. *Science of The Total Environment*, 304(1-3): 257–268.
[https://doi.org/10.1016/S0048-9697\(02\)00573-9](https://doi.org/10.1016/S0048-9697(02)00573-9)
- Bastos WR, Gomes JPO, Oliveira RC, Almeida R, Nascimento EL, Bernardi JVE, Lacerda LD, Silveira EG, Pfeiffer WC. 2006. Mercury in the environment and riverside population in the Madeira River Basin, Amazon, Brazil. *Science of The Total Environment*, 1(1):334-351.
<https://doi.org/10.1016/j.scitotenv.2005.09.048>
- Bastos WR, Malm O, Pfeiffer WR, Clearly D. 1998. Establishment and analytical quality control of laboratories for Hg determination in biological and geological samples in the Amazon, Brazil. *Ciência e Cultura*. 50(4): 255-260.
- Benoit JM, Gilmour CC, Heyes A, Mason RP, Miller CL. 2002. Geochemical and biological controls over mercury production and degradation in aquatic systems. *Biogeochemistry of Environmentally Important Trace Elements. ACS Symposium Series* 835, 262–297.
<https://dx.doi.org/10.1021/bk-2003-0835.ch019>
- Bezerra PSS, Takiyama LR, Bezerra CWB. 2009. Complexation of metal ions by dissolved organic matter: modeling and application to real system. *Acta Amazonica*, 39(3):639-648.
<http://dx.doi.org/10.1590/S0044-59672009000300019>
- Bittencourt MM, Amadio SA. 2007. Proposta para identificação rápida dos períodos hidrológicos em áreas de várzea do rio Solimões-Amazonas nas proximidades de Manaus. *Acta Amazonica*, 37(2):303-308.

<http://dx.doi.org/10.1590/S0044-59672007000200019>

- Bonnet MP, Barroux G, Martinez JM, Seyler F, Moreira Turcq P, Cochonneau G, Melack J, Boaventura G, Maurice-Bourgoin L, Leon JG, Roux E, Calmant S, Kosuth P, Guyot JL, Seyler P. 2008. Floodplain hydrology in an Amazon floodplain lake (Lago Grande de Curuaí). *Journal of Hydrology*, 349(1-2):18–30.
<https://doi.org/10.1016/j.jhydrol.2007.10.055>
- Brito BC, Forsberg BR, Kasper D, Amaral JHF, Vasconcelos MRR, Sousa OP, Cunha FAG, Bastos WR. 2017. The influence of inundation and lake morphometry on the dynamics of mercury in the water and plankton in an Amazon floodplain lake. *Hydrobiologia*, 790(1):35-48.
<https://doi.org/10.1007/s10750-016-3017-y>
- Campbell L, Hecky RE, Dixon DG, Chapman LJ. 2006. Food web structure and mercury transfer in two contrasting Ugandan highland crater lakes (East Africa). *African Journal of Ecology*, 44(3):337–346.
<https://doi.org/10.1111/j.1365-2028.2006.00582.x>
- Caraballo P, Forsberg BR, Almeida FF, Leite RG. 2014. Diel patterns of temperature, conductivity and dissolved oxygen in an Amazon floodplain lake: description of a *friagem* phenomenon. *Acta Limnologica Brasiliensia*, 26(3):318-331.
<http://dx.doi.org/10.1590/S2179-975X2014000300011>
- Carmouze JP. 1994. O Metabolismo dos Ecossistemas Aquáticos: Fundamentos Teóricos, Métodos de Estudo e Análises Químicas. Editora Edgard Blücher, São Paulo. 254p. (in Portuguese)
- Cloern JE, Canuel EA, Harris D. 2002. Stable carbon and nitrogen isotopes composition of aquatic and terrestrial plants of the San Francisco Bay estuarine system. *Limnology and Oceanography*, 47(3):713–729.
<https://doi.org/10.4319/lo.2002.47.3.0713>
- Cremona F, Hamelin S, Planas D, Lucotte M. 2009. Sources of organic matter and methylmercury in littoral macroinvertebrates: a stable isotope approach. *Biogeochemistry*, 94(1):81-94.
<https://doi.org/10.1007/s10533-009-9309-9>
- Devol AH, Hedges JI. 2001. Organic matter and nutrients in the mainstem Amazon River. In *The Biogeochemistry of the Amazon Basin* (eds. M. E. McClain, R. L. Victoria and J. E. Richey). Oxford University Press, Oxford, pp. 275–306.
- EPA. US Environmental Protection Agency 1630. 2001. Methylmercury in water by distillation, aqueous ethylation, purge and trap, and CVAFS. EPA 821-R-01-020.
- Feyte S, Tessier A, Gobeil C, Cossa D. 2010. In situ adsorption of mercury, methylmercury and other elements by iron oxyhydroxides and organic matter in lake sediments. *Applied Geochemistry*, 25(7):984-995.
<https://doi.org/10.1016/j.apgeochem.2010.04.005>
- Fox J, Weisberg S. 2011. An {R} Companion to Applied Regression, Second Edition. Thousand Oaks CA: Sage. URL: <http://socserv.socsci.mcmaster.ca/jfox/Books/Companion>
- Gadel F, Serve L, Benedetti M, Cunha LCD, Blazi JL. 2000. Biogeochemical characteristics of organic matter in the particulate and colloidal fractions

- downstream of the rio Negro and Solimoes rivers confluence. *Agronomie EDP Sciences*, 20(5):477-490. <https://doi.org/10.1051/agro:2000143>
- Gibbs RJ. 1967. The Geochemistry of the Amazon River System: Part I. The Factors that Control the Salinity and the Composition and Concentration of the Suspended Solids. *GSA Bulletin*, 78(10):1203-1232. [https://dx.doi.org/10.1130/0016-7606\(1967\)78\[1203:TGOTAR\]2.0.CO;2](https://dx.doi.org/10.1130/0016-7606(1967)78[1203:TGOTAR]2.0.CO;2)
- Goulding M. 1979. *Ecologia de pesca no rio Madeira*. Manaus. CNPq/INPA, 172p.
- Guimarães JR, Meili M, Mauro JB, Hylander LD, de Castro e Silva E, Roulet M, de Lemos R. 2000. Mercury net methylation in five tropical flood plain regions of Brazil: high in the root zone of floating macrophyte mats but low in surface sediments and flooded soils. *The Science of the Total Environment*, 261(1-3):99-107. [https://doi.org/10.1016/S0048-9697\(00\)00628-8](https://doi.org/10.1016/S0048-9697(00)00628-8)
- Hammerschmidt CR, Fitzgerald WF, Lamborg CH, Balcom PH, Visscher PT. 2004. Biogeochemistry of methylmercury in sediments of Long Island Sound. *Marine Chemistry*, 90(1-4):31-52. <https://doi.org/10.1016/j.marchem.2004.02.024>
- Hedges JI, Cowie GL, Richey JE, Quay PD, Benner R, Strom M, Forsberg BR. 1994. Origins and processing of organic matter in the Amazon River as indicated by carbohydrates and amino acids. *Limnology and Oceanography*, 39(4):743-761. <https://doi.org/10.4319/lo.1994.39.4.0743>
- Hedges JI, Ertel JR, Quay PD, Grootes PM, Richey JE, Devol AH, Farwell GW, Schmidt FW, Salati E. 1986. Organic carbon-14 in the Amazon River system. *Science* 231(4742):1129-1131. <https://doi.org/10.1126/science.231.4742.1129>
- ICMBIO. Instituto Chico Mendes de Conservação da Biodiversidade. 2008. Relatório Parametrizado - Unidade de Conservação, Unidade de Conservação: Reserva Extrativista Lago do Cuniã. Acessível em: <http://sistemas.mma.gov.br/cnuc/index.php?ido=relatorioparametrizado.exibeRelatorioandrelatorioPadrao=trueandidUc=233> (in Portuguese)
- INMET. Instituto Nacional de Meteorologia. 2018. Estação Meteorológica Automática de Porto Velho (A925). Disponível em: http://www.inmet.gov.br/portal/index.php?r=home/pageandpage=rede_estacoes_auto_graf (in Portuguese)
- Jackson AL, Parnell AC, Inger R, Bearhop S. 2011. Comparing isotopic niche widths among and within communities: SIBER - Stable Isotope Bayesian Ellipses in R. *Journal of Animal Ecology*, 80(3):595-602. <http://dx.doi.org/10.1111/j.1365-2656.2011.01806.x>
- Jara-Marini ME, Soto-Jiménez MF, Páez-Osuna F. 2012. Mercury Transfer in a Subtropical Coastal Lagoon Food Web (SE Gulf of California) Under Two Contrasting Climatic Conditions. *Environmental Toxicology*, 27(9):526-536. <https://doi.org/10.1002/tox.20670>
- Junk WJ, Furch K. 1985. The physical and chemical properties of Amazonian waters and their relationships with the biota. In: *Key Environments Amazonia*. Pergamon Press, Oxford, p. 3-17.

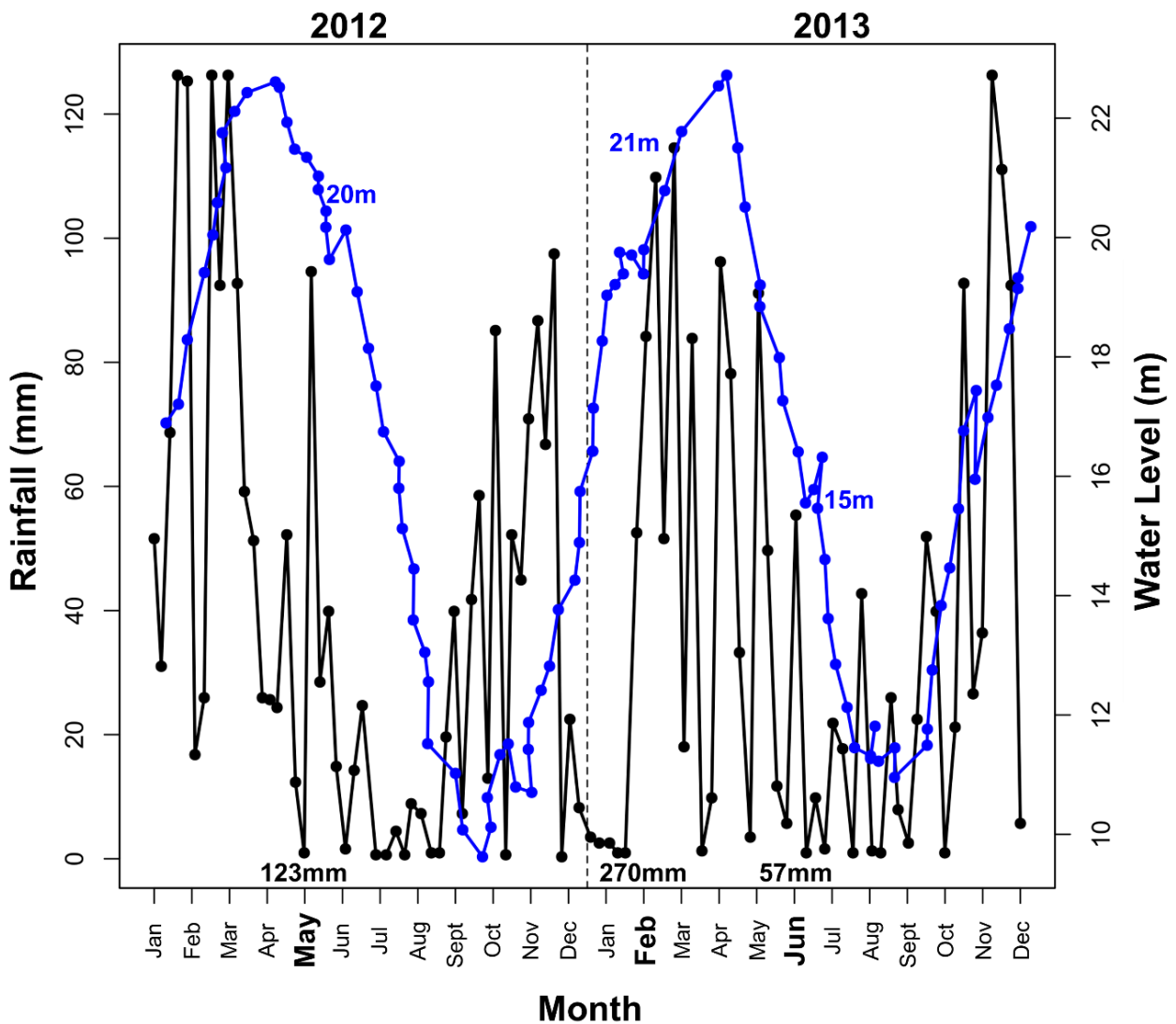
- Junk WJ. 1989. The use of Amazonian floodplains under an ecological perspective. *Interciência*, 14(6):317–22.
- Kasper D, Forsberg BR, Amaral JHF, Leitão RP, Py-Daniel SS, Bastos WR, Malm O. 2014. Reservoir Stratification Affects Methylmercury Levels in River Water, Plankton, and Fish Downstream from Balbina Hydroelectric Dam, Amazonas, Brazil. *Environmental Science and Technology*, 48(2):1032–1040. <https://dx.doi.org/0.1021/es4042644>
- Kasper D, Forsberg BR, Amaral JHF, Py-Daniel SS, Bastos WR, Malm O. 2017. Methylmercury Modulation in Amazon Rivers Linked to Basin Characteristics and Seasonal Flood-Pulse. *Environmental Science and Technology*, 52(24):14182-141191. <https://doi.org/10.1021/acs.est.7b04374>
- Kennedy P, Kennedy H, Papadimitriou S. 2005. The effect of acidification on the determination of organic carbon, total nitrogen and their stable isotopic composition in algae and marine sediment. *Rapid Communication in Mass Spectrometry*, 19(8):1063-1068. <https://doi.org/10.1002/rcm.1889>
- Kim JH, Zell C, Moreira-Turcq P, Pérez MAP, Abril G, Mortillaro JM, Weijers JWH, Meziane T, Sinninghe Damsté JS. 2012. Tracing soil organic carbon in the lower Amazon River and its tributaries using GDGT distributions and bulk organic matter properties. *Geochimica et Cosmochimica Acta*, 90(1):163–180. <https://doi.org/10.1016/j.gca.2012.05.014>
- King JK, Saunders FM, Lee RF, Jahnke RA. 1999. Coupling mercury methylation rates to sulfate reduction rates in marine sediments. *Environmental Toxicology and Chemistry*, 18(7):1362–1369. <https://dx.doi.org/10.1002/etc.5620180704>
- Lacerda LD, Pfeiffer WC, Ott AT, Silveira EG. 1989. Mercury Contamination in the Madeira River, Amazon-Hg Inputs to the Environment. *Biotropica*, 21(1):91-93. <https://doi.org/10.2307/2388449>
- Liang L, Bloom NS, Horvat M. 1994. Simultaneous determination of mercury speciation in biological materials by GC/CVAFS after ethylation and room-temperature precollection. *Clinical Chemistry*, 40(4):602-607. <http://clinchem.aaccjnls.org/content/40/4/602>
- Maia PD, Maurice L, Tessier E, Amouroux D, Cossa D, Moreira-Turcq P, Etcheber H. 2017. Role of the floodplain lakes in the methylmercury distribution and exchanges with the Amazon River, Brazil. *Journal of Environmental Sciences*, 68:24-40. <https://doi.org/10.1016/j.jes.2018.02.005>
- Maia PD, Maurice L, Tessier E, Amouroux D, Cossa D, Pérez M, Moreira-Turcq P, Rhéault I. 2009. Mercury distribution and exchanges between the Amazon River and connected floodplain lakes. *Science of the Total Environment*, 407: 6073–6084. <https://doi.org/10.1016/j.scitotenv.2009.08.015>
- Martinelli LA, Victoria RL, de Camargo PB, de Cassia Piccolo M, Mertes L, Richey JE, Devol AH, Forsberg BR. 2003. Inland variability of carbon–nitrogen concentrations and $\delta^{13}\text{C}$ in Amazon floodplain (várzea) vegetation and sediment. *Hydrological Processes*, 17(7):1419–1430. <https://doi.org/10.1002/hyp.1293>

- Maurice-Bourgoin L, Bonnet MP, Martinez JM, Kosuth P, Cochonneau G, Moreira-Turcq P, Guyot JL, Vauchel P, Filizola N, Seyler P. 2007. Temporal dynamics of water and sediment exchanges between the Curuaí floodplain and the Amazon River main stream, Brazil. *Journal of Hydrology*, 335(1):140–156. <https://doi.org/10.1016/j.jhydrol.2006.11.023>
- Mauro JBN, Guimarães JRD, Melamed R. 1999. Mercury methylation in tropical macrophyte: influence of abiotic parameters. *Applied Organometallic Chemistry*, 13(9):631–636. [https://doi.org/10.1002/\(SICI\)1099-0739\(199909\)13:9<631::AID-AOC905>3.0.CO;2-E](https://doi.org/10.1002/(SICI)1099-0739(199909)13:9<631::AID-AOC905>3.0.CO;2-E)
- Meyers PA. 1994. Preservation of elemental and isotopic source identification of sedimentary organic matter. *Chemical Geology*, 114(3-4):289-302. [https://doi.org/10.1016/0009-2541\(94\)90059-0](https://doi.org/10.1016/0009-2541(94)90059-0)
- Moreira-Turcq PF, Seyler P, Guyot JL, Etcheber H. 2003. Characteristics of organic matter in the mixing zone of the Rio Negro and Rio Solimões of the Amazon River. *Hydrological Processes*, 17(7):1393-1404. <https://doi.org/10.1002/hyp.1291>
- Muresan B, Cossa D, Richard S, Dominique Y. 2008. Methylmercury sources in a tropical artificial reservoir. *Applied Geochemistry*, 23(5): 1101-1126. <https://dx.doi.org/10.1016/j.apgeochem.2007.11.006>
- Murphy J, Riley JP. 1962. A modified single solution method for the determination of phosphate in natural waters. *Analytica Chimica Acta*, 27:31-36. [https://doi.org/10.1016/S0003-2670\(00\)88444-5](https://doi.org/10.1016/S0003-2670(00)88444-5)
- Pinheiro GMS, Poitrasson F, Sondag F, Cochonneau G, Vieira LC. 2014. Contrasting iron isotopic compositions in river suspended particulate matter: the Negro and the Amazon annual river cycles. *Earth and Planetary Science Letters*, 394:168-178. <http://dx.doi.org/10.1016/j.epsl.2014.03.006>
- Pozebon D, Lima EC, Maia SM, Fachel JMG. 2005. Heavy metals contribution of non-aqueous fluids used in offshore oil drilling. *Fuel*, 84(1):53-61. <https://doi.org/10.1016/j.fuel.2004.08.002>
- Quay PD, Wilbur DO, Richey JE, Hedges JI, Devol AH, Victoria R. 1992. Carbon cycling in the Amazon river: implication from the ¹³C compositions of particles and solutes. *Limnology and Oceanography*, 37(4):857–871. <https://doi.org/10.4319/lo.1992.37.4.0857>
- R Core Team. 2018. R: A language and environment for statistical computing. R Foundation for Statistical Computing, Vienna, Austria. URL <https://www.R-project.org/>.
- Richey JE, Melack JM, Aufdenkampe AK, Ballester VM, Hess LL. 2002. Outgassing from Amazonian rivers and wetlands as a large tropical source of atmospheric CO₂. *Nature*, 416:617–620. <https://doi.org/10.1038/416617a>
- Roulet M, Lucotte M. 1995. Geochemistry of mercury in pristine and flooded ferralitic soils of a tropical rain forest in French Guiana, South America. *Water, Air, and Soil Pollution*, 80(1-4):1079-1088. <https://doi.org/10.1007/BF01189768>

- Roulet M, Lucotte M, Farella N, Serique G, Coelho H, Sousa Passos CJ, Silva EJ, Andrade PS, Mergler D, Guimarães JRD, Amorim M. 1999. Effects of recent human colonization on the presence of mercury in Amazonian ecosystems. *Water, Air, Soil Pollution* 112(3-4): 297–313. <https://doi.org/10.1023/A:1005073432015>
- Roulet M, Guimarães JRD, Lucotte M. 2001. Methylmercury Production and Accumulation in Sediments and Soils of an Amazonian Floodplain – Effect of Seasonal Inundation. *Water, Air, and Soil Pollution*, 128(1-2):41-60. <https://doi.org/10.1023/A:1010379103335>
- Sánchez-Botero JI, Farias ML, Piedade MT, Garcez DS. 2003. Ictiofauna associada às macrófitas aquáticas *Eichhornia azurea* (SW.) Kunth. e *Eichhornia crassipes* (Mart.) Solms. no lago Camaleão, Amazônia Central, Brasil. *Acta Scientiarum Biological Sciences*, 25(2):369-375. <http://dx.doi.org/10.4025/actascibiols.ci.v25i2.2026>
- Santos EJ, Herrmann AB, Frescura VLA, Curtius AJ. 2005. Simultaneous determination of As, Hg, Sb, Se and Sn in sediments by slurry sampling axial view inductively coupled plasma optical emission spectrometry using on-line chemical vapor generation with internal standardization. *Journal of Analytical Atomic Spectrometry*, 20(6):538-543. <https://dx.doi.org/10.1039/B502964C>
- Santos UM, Ribeiro MNG. 1988. A hidroquímica do rio Solimões - Amazonas. *Acta Amazonica*, 18(3-4):145-172. <http://dx.doi.org/10.1590/1809-43921988183172>
- Schwatke C, Dettmering D, Bosch W, Seitz F. 2015. DAHITI – an innovative approach for estimating water level time series over inland waters using multi-mission satellite altimetry. *Hydrology and Earth System Sciences*, 19(1):4345-4364. <https://doi.org/10.5194/hess-19-4345-2015>
- SEDAM. Secretaria do Estado do Desenvolvimento Ambiental. 2012. Boletim Climatológico de Rondônia, Porto Velho, 22p (in Portuguese).
- Sioli H. Studies in Amazonian Waters. 1967. In: Atas do simpósio sobre a biota amazônica, Vol. 3, pp. 9-50. Conselho Nacional de Pesquisas, Rio de Janeiro (in Portuguese).
- Stewart AR, Saiki MK, Kuwabara JS, Apers CN, Marvin-DiPasquale M, Krabbenhoft DP. 2008. Influence of plankton mercury dynamics and trophic pathways on mercury concentrations of top predator fish of a mining-impacted reservoir. *Canadian Journal of Fisheries and Aquatic Sciences*, 65(11):2351–2366. <https://doi.org/10.1139/F08-140>
- Sulzman EW. 2007. Stable isotope chemistry and measurement: a primer. In: Michener RH, Lajtha K. *Stable isotopes in ecology and environmental science*, 2nd edition. Blackwell Publishing, p. 1-21
- Venables WN, Ripley BD. 2002. *Modern Applied Statistics with S*. Fourth Edition. Springer, New York. <https://doi.org/10.1007/978-0-387-21706-2>
- Wickham H. 2007. Reshaping Data with the reshape Package. *Journal of Statistical Software*, 21(12):1-20. <http://dx.doi.org/10.18637/jss.v021.i12>

Wiener, J.G., Krabbenhoft, D.P., Heinz, G.H., Scheuhammer, A.M., 2002. Ecotoxicology of mercury. In: Hoffman, D.J., Rattner, B.A., Burton, G.A., Cairns, J. (Eds.), Handbook of Ecotoxicology. CRC Press, Boca Raton, EUA, pp. 409–463.

Supplementary Material 1



Caption – Rainfall (INMET, 2018) and water level (Schwatke et al., 2015) for the Madeira River during the years that this study was conducted. The sampled months are highlighted in bold on the x-axis and represent the early falling-water (May 2012), rising-water (February 2013) and late falling-water (June 2013) periods. The Madeira River water during the sampled periods is shown in blue, while the accumulated rainfall for the sampled periods is highlighted in black on the graph.

Supplementary Material 2 – Physical and chemical parameters of sampled points (**Figure 1**). The centrality and dispersion of data (median \pm median absolute deviations, MAD) were calculated for each variable in each hydrological period. Upper and lowercase letters represent statistical differences among hydrological periods for each median calculated, considering 95% certainty.

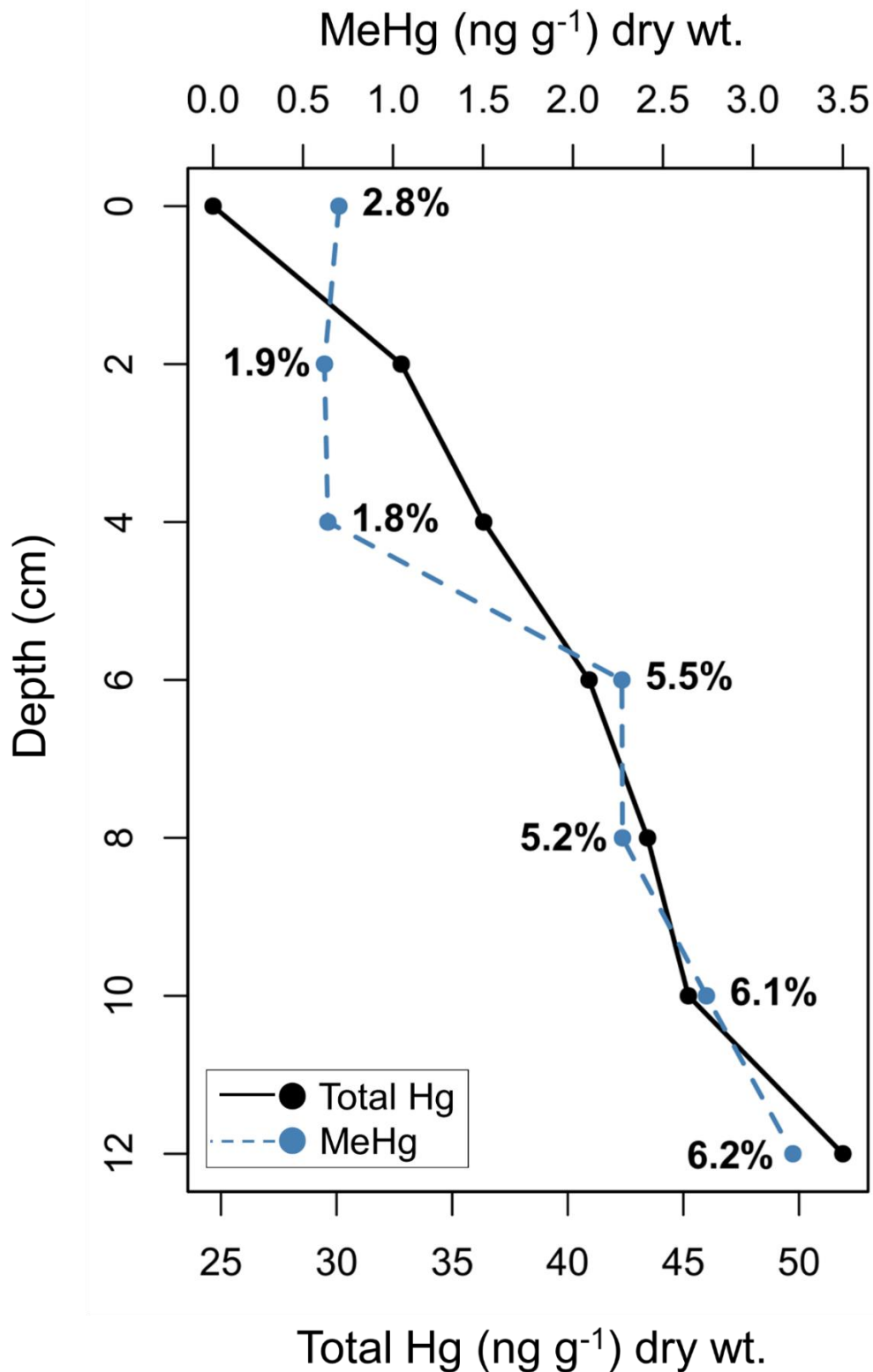
Hydrological Period	Sample Point	Depth (m)	Temperature (°C)	pH	Electric Conductivity ($\mu\text{S cm}^{-1}$)	Dissolved O ₂ (mg L ⁻¹)
Rising-water (February 2013)	River1	21	29.6	6.7	68.0	7.5
	River2	21	28.9	6.6	81.0	7.0
	Igarapé1	13	28.4	5.6	9.0	3.5
	Igarapé2	12	27.5	5.8	30.0	1.6
	Lake1	8	26.5	5.5	9.5	3.0
	Lake2	8	27.9	5.6	7.5	4.5
	Lake3	11	28.4	5.9	27.5	1.4
	Median \pm MAD		27.8 \pm 1.5 ^a	5.7 \pm 0.3 ^b	15.0 \pm 11.1 ^a	3.0 \pm 2.3 ^b
Early falling- water (May 2012)	River1	20	27.2	6.3	63.3	5.2
	River2	20	27.2	6.3	63.3	5.2
	Igarapé1	12	26.6	5.5	6.5	1.5
	Igarapé2	12	26.8	5.4	11.0	0.5
	Lake1	9	25.9	5.2	10.9	1.5
	Lake2	9	27.4	5.4	8.0	2.6
	Lake3	9	27.2	5.3	7.6	1.5
	Median \pm MAD		26.8 \pm 0.6 ^a	5.4 \pm 0.2 ^b	10.1 \pm 3.7 ^{ab}	1.5 \pm 1.1 ^b
Late falling-water (June 2013)	River1	15	27.3	7.6	58.2	9.9
	River2	15	27.0	7.6	55.8	9.8
	Igarapé1	9	28.8	5.8	8.2	6.6
	Igarapé2	9	23.0	5.6	12.1	6.3
	Lake1	10	26.0	5.8	6.7	5.4
	Lake2	10	31.0	6.6	6.3	8.4
	Lake3	6	26.8	6.3	21.5	4.9
	Median \pm MAD		27.0 \pm 1.5 ^a	5.9 \pm 0.4 ^a	10.3 \pm 5.3 ^b	6.5 \pm 2.6 ^a

Supplementary Material 3

Caption – Major anions concentrations determined in the river-*igarapé*-lake system for all hydrological periods sampled.

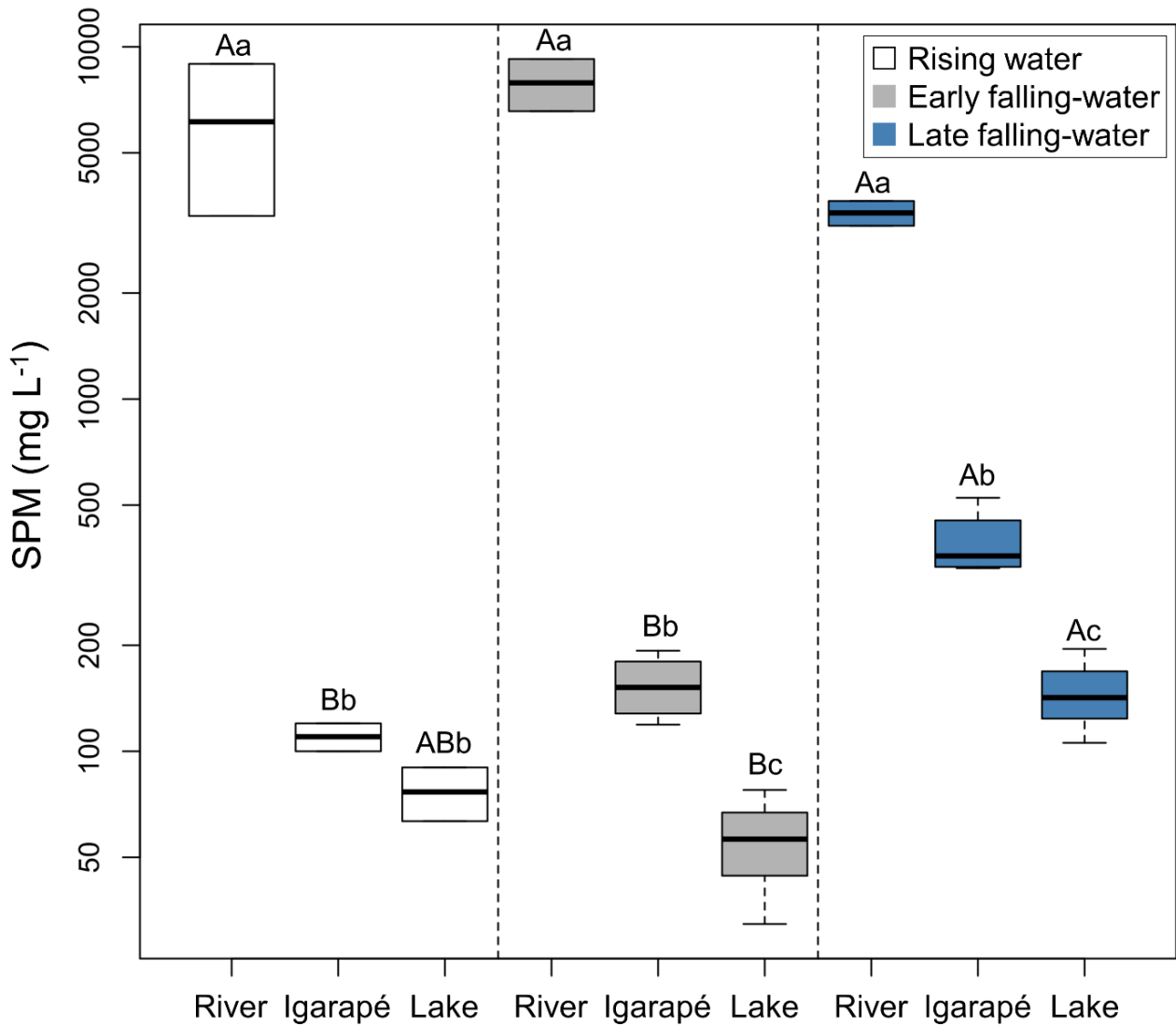
Hydrological Period	Site	Cl ⁻ (mg L ⁻¹)	NO ₂ ⁻ (µg L ⁻¹)	NO ₃ ⁻ (µg L ⁻¹)	SO ₄ ²⁻ (µg L ⁻¹)	PO ₄ ³⁻ (µg L ⁻¹)
Rising-water	River	113.3 ± 100.3	0.1 ± 0.1	186.0 ± 0.7	967.7 ± 254.8	2.0 ± 1.3
	Igarape	39.1 ± 7.1	0.6 ± 1.0	367.7 ± 404.7	195.1 ± 175.1	19.0 ± 35.0
	Lake	45.8 ± 30.4	0.7 ± 1.1	285.7 ± 213.8	123.6 ± 93.7	1.2 ± 0.2
Early falling-water	River	48.3 ± 4.4	0.6	112.1	501.4 ± 1.7	7.4 ± 11.1
	Igarape	32.5 ± 7.6	0.1 ± 0.1	19.9 ± 6.0	54.3 ± 36.6	8.6 ± 12.2
	Lake	60.6 ± 37.5	0.1 ± 0.1	180.1 ± 238.6	89.2 ± 49.3	4.8 ± 1.7
Late falling-water	River	101.5	0.1	779.3 ± 339.8	1011.9	67.0 ± 93.8
	Igarape	24.9 ± 1.3	0.1 ± 0.2	1093.2 ± 874.3	22.7 ± 11.5	4.1 ± 3.5
	Lake	216.7 ± 166.9	0.1 ± 0.1	523.8 ± 670.3	87.7 ± 116.2	70.4

Supplementary Material 4



Caption –Total Hg and MeHg concentrations along a sediment profile sampled in the central part of Cuniã Lake (*Lake2*; **Figure 1**) during the late falling-water period. The %MeHg (MeHg/total Hg ratio) is indicated for each depth, next to the MeHg concentrations.

Supplementary Material 5



Caption – SPM concentrations in the river-*igarapé*-lake system for each hydrological period sampled. Lowercase letters identify the differences ($p < 0.05$) between ecosystems within the same hydrological period while uppercase letters differentiate ($p < 0.05$) the hydrological periods within the same ecosystem. The distances between the y-axis values were log-transformed to optimize the data visualization.

Supplementary Material 6 – Studies of floodplain-river systems in the Amazon region and their concentrations of Hg chemical species

Environmental compartment	Site	Hydrological Period/Lake name	Total Hg (ng g ⁻¹) dry wt.	MeHg (ng g ⁻¹) dry wt.	%MeHg	Reference
Sediment	Floodplain Lake (Tapajós River)	Enseada Grande	214.5 ± 31.8	0.3 ± 0.3	0.2 ± 0.1	Roulet et al. 2001
	Floodplain Lake (Amazon River)	Curuai	125.1 ± 43.4	0.3 ± 0.1	0.2 ± 0.1	Maia et al. 2017
	Floodplain Lake (Madeira River)	Puruzinho	60.3 ± 17.6			Almeida et al. 2014
	Floodplain Lake (Madeira River)	Cuniã	98.1 ± 19.5			Bastos et al. 2006
	Floodplain Lake (Madeira River)	Puruzinho	53.0 ± 9.0			Bastos et al. 2006
Suspended Particulate Matter	River (Solimões)	Rising-water	458.2	1.1	0.2	
		High water	84.3	0.8	0.9	
		Low water	95.5	0.4	0.4	
	<i>Igarapé</i>	Rising-water	248.9	2.5	1.0	
		High water	128.9	1.9	1.5	Brito et al. 2017^a
		Low water	100.0	2.5	2.5	
	Floodplain Lake (Solimões River)	Rising-water	233.8 ± 48.0	2.4 ± 1.2	1.0	
		High water	219.3 ± 33.9	8.1 ± 1.8	3.7	
		Low water	66.7 ± 9.5	2.3 ± 0.5	3.5	
	River (Solimões)	High water	-----	0.6	-----	
		Early Falling-water	-----	1.0	-----	
		Late Falling-water	-----	1.5	-----	Kasper et al. 2017^b
		Low water	-----	1.9	-----	
		High water	-----	0.1	-----	
		Low water	-----	1.1	-----	
River (Negro)	High water	-----	0.1	-----		
River (Amazon)	Low water	-----	1.1	-----		
	Rising-water	212.0 ± 95.9	1.0 ± 0.7	0.5		
	High water	56.6	1.5	2.6		
Floodplain Lake (Amazon River)	Low water	26.1	-----	-----		
	Rising-water	214.8 ± 264.6	1.2 ± 0.7	0.6	Maia et al. 2017	
	High water	558.0 ± 490.0	3.1 ± 2.0	0.5		
	Low water	115.7 ± 132.6	0.3 ± 0.3	0.2		

^aData transformed to mass basis based on the mean SPM load reported by the authors ([Kasper et al., 2017](#)) for each environment.

^bData transformed to a mass basis based on the mean SPM load reported by the authors ([Brito et al. 2017](#); Solimões River), and the mean SPM load reported by [Pinheiro et al. \(2014\)](#) (Negro River) for each hydrological period.

2. Discussão Geral

As concentrações de MeHg determinadas no MPS coletado no reservatório da Hidrelétrica de Samuel apresentaram diferenças mais marcadas entre os períodos hidrológicos coletados (**Figura 4, Capítulo 1**) quando comparadas com aquelas determinadas no MPS coletado no sistema *igarapé-lago Cuniã* (**Figura 4, Capítulo 3**). Isso pode estar relacionado com os períodos hidrológicos amostrados em cada um dos ecossistemas: no reservatório de Samuel os períodos hidrológicos amostrados (águas altas, vazante e águas baixas) abrangeram melhor a amplitude de variação do ciclo de inundação dos rios amazônicos quando comparado com aqueles amostrados no sistema *igarapé-lago Cuniã* (enchente, vazante inicial e vazante tardia). Associado a isso, a similaridade da profundidade da coluna d'água nos pontos do igaraé e lago Cuniã (**Tabela 1, Capítulo 3**) e a distância ao rio Madeira de aproximadamente 37 km (**Figura 1, Capítulo 3**) podem ter contribuído para a limitar os efeitos da sazonalidade sobre as concentrações de MeHg no MPS.

Outra diferença no funcionamento desses ecossistemas foi percebida nas associações do MeHg com a razão atômica de carbono e nitrogênio (razão (C:N)_a) da matéria orgânica no MPS. No reservatório de Samuel, foi possível predizer maiores concentrações de MeHg quanto maior fosse a razão (C:N)_a (**Figura 7, Capítulo 1**) enquanto que no sistema *igarapé-lago Cuniã* essa associação foi inversa (maiores concentrações de MeHg associadas à menores valores da razão (C:N)_a (**Figura 6, Capítulo 3**). Isso indica que o MeHg no MPS coletado no reservatório de Samuel está associado a uma matéria orgânica mais degradada, provavelmente oriunda da lixiviação dos solos de floresta adjacentes, quando comparado com o MPS coletado no sistema *igarapé-lago Cuniã*, que apresenta uma contribuição mais expressiva da produção autóctone associada ao fitoplâncton.

O perfil sedimentar coletado no reservatório de Samuel apresentou maiores concentrações de MeHg nas camadas superficiais do sedimento (**Figura 5, Capítulo 1**) enquanto que naquele coletado no lago Cuniã foi observado um aumento marcado na concentração de MeHg com a profundidade (**Figura 12, Capítulo 3**). Isso pode sugerir que o lago Cuniã é um ambiente de sedimentação mais eficiente que o reservatório de Samuel ou, sinergicamente a isso, que o controle artificial da hidrodinâmica do reservatório de Samuel afeta a sedimentação de partículas naquele ambiente.

Por outro lado, a assinatura isotópica e elementar da matéria orgânica do lago Cuniã (**Figura 15, Capítulo 3**) e do reservatório de Samuel (**Figura 8, Pestana et al., 2016**) indicam que a principal fonte de Hg para ambos os ecossistemas são os solos da região.

3. Considerações Finais

A circulação de Hg nos ecossistemas aquáticos amazônicos artificiais (**Capítulos 1 e 2**) e naturais (**Capítulo 3**) está intimamente associada à dinâmica da matéria orgânica nesses ambientes (**Capítulos 1 e 3**). O estado de degradação da matéria orgânica (**Capítulos 1 e 3**) e os parâmetros físico-químicos da coluna d'água (**Capítulos 2 e 3**) são peças-chave para a compreensão do processo de metilação de Hg nesses ecossistemas que, uma vez transformado em MeHg, pode se biomagnificar ao longo da cadeia trófica (**Capítulo 2**).

As macrófitas aquáticas (**Capítulos 1 e 3**), a coluna d'água (**Capítulos 1, 2 e 3**) e o sedimento (**Capítulos 1 e 3**) são compartimentos do ecossistema capazes de metilar o Hg e, por isso, podem ser utilizados como indicadores em estudos de monitoramento em ambientes naturais e artificiais.

O manejo preventivo de ecossistemas artificiais deve ser realizado para evitar o acúmulo progressivo de Hg e MeHg em itens consumidos pela população, como os peixes (**Capítulo 2**). Algumas estratégias podem auxiliar grandemente na diminuição do impacto da construção de hidrelétricas no acúmulo de Hg nos compartimentos do ecossistema. Por exemplo, a remoção da vegetação nativa antes da inundação de uma área terrestre diminui o conteúdo de matéria orgânica lábil dos solos e, com isso, também a taxa de metilação de Hg nos sedimentos. Em hidrelétricas já construídas, pode-se promover a aeração do sedimento de fundo para diminuir a abundância de bactérias sulfato-redutoras e, com isso, as taxas de metilação do Hg, embora seja logisticamente desafiador promover esse tipo de estratégia em reservatórios com grandes áreas.

Em ecossistemas naturais (**Capítulo 3**), por outro lado, ações de divulgação científica devem ser realizadas para avisar os moradores locais do risco do uso da água de lagos em atividades de agricultura ou mesmo do consumo direto de peixes ou outros organismos em determinadas épocas do ano em que a concentração de MeHg é elevada nesses compartimentos.

Como sugestão para estudos futuros, o fracionamento da coluna d'água através de técnicas de ultrafiltração em ambientes amazônicos naturais e artificiais pode incrementar ainda mais a literatura com as características da matéria orgânica carregada pela coluna d'água e ajudar no entendimento de fontes ainda mais específicas de Hg para o ecossistema aquático.

4. Referências

- Almeida R. 2012. Estudo da Origem, Mobilização e Organificação do Mercúrio no Reservatório da UHE-Samuel, RO. Tese de Doutorado. Instituto de Biofísica Carlos Chagas Filho UFRJ/IBCCF, Rio de Janeiro. 117p.
- Bernoux M, Carvalho MCS, Volkoff B, Cerri CC. 2002. Brazil's soil carbon stocks. *Soil Science Society of America Journal*, 66(3):888-896. <https://doi.org/10.2136/sssaj2002.8880>
- Castello L, Macedo MN. 2016. Large-scale degradation of the Amazon freshwater ecosystem. *Global Change Biology*, 22(3):990–1007. <https://dx.doi.org/10.1111/gcb.13173>
- Couto. 2004. *Limnologia Aplicada*. Universidade Federal Rural do Rio de Janeiro. <http://www.ufrj.br/institutos/it/de/acidentes/dam.htm>
- Dorea J, Barbosa A, Ferrari I, Souza J. 2010. Mercury in hair and in fish consumed by Riparian women of the Rio Negro, Amazon, Brazil. *International Journal of Environmental Health Research*, 13(3):239-248. <https://doi.org/10.1080/0960312031000122398>
- EPA. U.S. Environmental Protection Agency. 2016. National Lakes Assessment 2012: A Collaborative Survey of Lakes in the United States. <https://www.epa.gov/national-aquatic-resource-surveys/national-lakes-assessment-2012-report>
- Fadini PS, Jardim WF. 2001. Is the Negro River Basin (Amazon) impacted by naturally occurring mercury? *Science of The Total Environment*, 275(1-3):71-82. [https://doi.org/10.1016/S0048-9697\(00\)00855-X](https://doi.org/10.1016/S0048-9697(00)00855-X)
- Fleming EJ, Mack EE, Green PG, Nelson DC. 2006. Mercury methylation from unexpected sources: molybdate-inhibited freshwater sediments and an iron-reducing bacterium. *Applied Environmental Microbiology*, 72(1):457-464. <http://dx.doi.org/10.1128/AEM.72.1.457-464.2006>
- Guallar, E., Sanz-Gallardo, M.I., van't Veer, P., Bode, P., Aro, A., Gomez-Aracena, J., Kark, J.D., Riemersma, R.A., Martin-Moreno, J.M., Kok, F.J., 2002. Mercury, Fish Oils, and the Risk of Myocardial Infarction. *The New England Journal of Medicine*, 347(23):1747-1754. <https://dx.doi.org/10.1056/NEJMoa020157>
- Guimarães JRD, Meili IM, Hylander LD, Silva EC, Roulet M, Mauro JBN, Lemos RA. 2000. Mercury net methylation in five tropical floodplain regions of Brazil: high in the root zone of floating macrophyte mats but low in surface sediments and flooded soils. *The Science of the Total Environment*, 261(1-3):99-107. [https://doi.org/10.1016/S0048-9697\(00\)00628-8](https://doi.org/10.1016/S0048-9697(00)00628-8)
- Hylander, L.D., Gröhn, J., Tropp, M., Vikström, A., Wolpher, H., Silva, E.C., Meili, M., Oliveira, L.J., 2006. Fish mercury increase in Lago Manso, a new hydroelectric reservoir in tropical Brazil. *Journal of Environmental Management*, 81(2):155-166. <https://dx.doi.org/10.1016/j.jenvman.2005.09.025>

- IEA. International Energy Agency. 2014. Electric power consumption (kWh per capita). <https://data.worldbank.org/indicator/eg.use.elec.kh.pc>
- Jackson TA. 1991. Biological and Environmental Control of Mercury Accumulation by Fish in Lakes and Reservoirs of Northern Manitoba, Canada. *Canadian Journal of Fisheries and Aquatic Sciences*, 48(12):2449–2470. <https://dx.doi.org/10.1139/f91-287>
- Johnson M. 2003. Case Study: Mercury Contamination in the Amazon. Reducing soil erosion may provide a lasting solution. International Development Research Centre. <https://idl-bnc-idrc.dspacedirect.org/handle/10625/52893>
- Junk WJ, Furch K. 1985. The physical and chemical properties of Amazonian waters and their relationships with the biota. In: Prance GT, Lovejoy TE, editors. *Key environments Amazonia*. New York, Pergamon, p. 3-17.
- Junk WJ. 1989. The use of Amazonian floodplains under an ecological perspective. *Interciência*, 14(6):317–322.
- King JK, Saunders FM, Lee RF, Jahnke RA. 1999. Coupling mercury methylation rates to sulfate reduction rates in marine sediments. *Environmental Toxicology Chemistry*, 18(7):1362–1369. <https://dx.doi.org/10.1002/etc.5620180704>
- Lacerda LD, Malm O. 2008. Mercury contamination in aquatic ecosystems: an analysis of the critical areas. *Estudos Avançados*, 22(63): 173-190. <http://dx.doi.org/10.1590/S0103-40142008000200011>
- Lacerda LD, Pfeiffer WC, Ott AT. 1989. Mercury contamination in the Madeira River, Amazon: Mercury inputs to the environment. *Biotropica*, 21(1):91-93. <https://doi.org/10.2307/2388449>
- Lacerda LD, Salomons W. 1998. Mercury from gold and silver mining. A chemical time bomb? Springer-Verlag Berlin Heidelberg. 147pp. <https://doi.org/10.1007/978-3-642-58793-1>
- Lechler PJ, Miller JR, Lacerda LD, Vinson D, Bozongo J-C, Lyons WB, Warwick JJ. 2000. Elevated mercury concentrations in soils, sediments, water, and fish of the Madeira River basin, Brazilian Amazon: a function of natural enrichments? *Science of The Total Environment*, 260(1-3):87-96. [https://doi.org/10.1016/S0048-9697\(00\)00543-X](https://doi.org/10.1016/S0048-9697(00)00543-X)
- Maia PD, Maurice L, Tessier E, Amouroux D, Cossa D, Moreira-Turcq P, Etcheber H. 2017. Role of the floodplain lakes in the methylmercury distribution and exchanges with the Amazon River, Brazil. *Journal of Environmental Sciences*, 68:24-40. <https://doi.org/10.1016/j.jes.2018.02.005>
- Maia PD, Maurice L, Tessier E, Amouroux D, Cossa D, Pérez M, Moreira-Turcq P, Rhéault I. 2009. Mercury distribution and exchanges between the Amazon River and connected floodplain lakes. *Science of the Total Environment*, 407: 6073–6084. <https://doi.org/10.1016/j.scitotenv.2009.08.015>

- Malm O, Pfeiffer WC, Souza CMM, Reuther R. 1990. Mercury pollution due to gold mining in the Madeira river Basin, Amazon/Brazil. *Ambio*, 19(1):11-15.
- Malm O. 1998. Gold Mining as a Source of Mercury Exposure in the Brazilian Amazon. *Environmental Research*, 77(2):73-78. <https://doi.org/10.1006/enrs.1998.3828>
- Mauro JBM, Guimarães JRD, Melamed R. 1999. Aguapé agrava contaminação por mercúrio. *Ciência Hoje*, 25(150):68-71
- Montgomery S, Lucotte M, Pichet P, Mucci A. 1995. Total dissolved mercury in the water column of several natural and artificial aquatic systems of Northern Quebec (Canada). *Canadian Journal of Fisheries and Aquatic Sciences*, 52(11):2483–2492. <https://doi.org/10.1139/f95-839>
- Myers GJ, Davidson PW, Weiss B. 2004. Methyl mercury exposure and poisoning at Niigata, Japan. *Seychelles Medical and Dental Journal*, 7(1):132-133.
- Nriagu JO, Pfeiffer WC, Malm O, Souza CMM, Mierle G. 1992. Mercury pollution in Brazil. *Nature*, 356:389. <https://doi.org/10.1038/356389a0>
- Parks JM, Johns A, Podar M, Bridou R, Hurt RA Jr, Smith SD, Tomanicek SJ, Qian Y, Brown SD, Brandt CC, Palumbo AV, Smith JC, Wall JD, Elias DA, Liang L. 2013. The Genetic Basis for Bacterial Mercury Methylation. *Science*, 339(6125):1332-1335. <https://doi.org/10.1126/science.1230667>
- Pestana IA, Bastos WR, Almeida MG, Carvalho DP de, Resende CER, Souza, CMM. 2016. Spatial-temporal dynamics and sources of total Hg in a hydroelectric reservoir in the Western Amazon, Brazil. *Environmental Science and Pollution Research*, 23(10):9640-9648. <https://doi.org/10.1007/s11356-016-6185-4>
- Pfeiffer WC, Lacerda LD. 1988. Mercury inputs into the Amazon region, Brazil. *Environmental Technology Letters*, 9(4):325-330. <https://doi.org/10.1080/09593338809384573>
- Porvari P. 1995. Mercury levels of fish in Tucuruí hydroelectric reservoir and in River Mojú in Amazonia, in the state of Pará, Brazil. *Science of The Total Environment*, 175(2):109-117. [https://dx.doi.org/10.1016/0048-9697\(95\)04907-X](https://dx.doi.org/10.1016/0048-9697(95)04907-X)
- Rice DC, Schoeny R, Mahaffey K. 2003. Methods and Rationale for Derivation of a Reference Dose for Methylmercury by the U.S. EPA. *Risk Analysis: An International Journal*, 23(1):107-115. <https://dx.doi.org/10.1111/1539-6924.00294>
- Roulet M, Lucotte M. 1995. Geochemistry of mercury in pristine and flooded ferralitic soils of a tropical rain forest in French Guiana, South America. *Water, Air, and Soil Pollution*, 80(1-4):1079-1088. <https://doi.org/10.1007/BF01189768>
- Sioli H. *Studies in Amazonian Waters*. 1967. In: Atas do simpósio sobre a biota amazônica, Vol. 3, pp. 9-50. Conselho Nacional de Pesquisas, Rio de Janeiro.
- Straškraba M, Tundisi JG. 2000. Diretrizes para o gerenciamento de lagos: Gerenciamento da qualidade de água de represas. Oficina de textos, São Paulo, 300 pp.

- Tollefson J. 2011. A struggle for power. *Nature*, 479:160-161. <https://dx.doi.org/10.1038/479160a>
- Wasserman JC, Hacon S, Wasserman MA. 2003. Biogeochemistry of Mercury in the Amazonian Environment. *Ambio*, 32(5):336-342. <https://doi.org/10.1579/0044-7447-32.5.336>
- WHO. World Health Organization & International Programme on Chemical Safety. 1990. Methylmercury / published under the joint sponsorship of the United Nations Environment Programme, the International Labour Organisation, and the World Health Organization. <http://www.who.int/iris/handle/10665/38082>
- Wiener JG, Krabbenhoft DP, Heinz GH, Scheuhammer AM. 2002. Ecotoxicology of mercury. Em: Hoffman, D.J., Rattner, B.A., Burton, G.A., Cairns, J. (Eds.), *Handbook of Ecotoxicology*. CRC Press, Boca Raton, EUA, pp. 409–463.